

## Genesis and rates of fluid flow at the Mercator mud volcano, Gulf of Cadiz

M. HAECKEL<sup>1</sup>, C. BERNDT<sup>2</sup>, V. LIEBETRAU<sup>1</sup>, P. LINKE<sup>1</sup>,  
A. REITZ<sup>1</sup>, J. SCHÖNFELD<sup>1</sup> AND H. VANNESTE<sup>2</sup>

<sup>1</sup>IFM-GEOMAR, Kiel, Germany (mhaeckel@ifm-geomar.de;  
areitz@ifm-geomar.de; vlietbrau@ifm-geomar.de;  
jschoenfeld@ifm-geomar.de; plinke@ifm-geomar.de)

<sup>2</sup>NOC, Southampton, UK (cbe@noc.soton.ac.uk;  
hlaev105@soton.ac.uk)

Mud volcanism is a widespread phenomenon in the Gulf of Cadiz (GoC) and provides a window into deep structural and diagenetic processes [1]. Sediment pore fluids from the Mercator mud volcano (MMV), located in the El Arraiche mud volcano field offshore Morocco, are extremely enriched in chloride reaching up to 5.3 M (thus, exceeding normal seawater values by a factor of 9). Na/Cl ratios are close to 1 suggesting halite dissolution by the ascending fluid. This is corroborated by 3D seismic data that shows an active anticline below the eastern flank of the MMV, which can only be explained by a rising salt diapir. Additionally, the fluids are highly enriched in Li and B indicating a deep fluid source from mineral dewatering reactions at elevated temperatures (>100 °C). A deep fluid source is also supported by a radiogenic <sup>87</sup>Sr/<sup>86</sup>Sr porewater signal of 0.7106 as well as the morphology of quartz and gypsum crystals transported within the ascending mud matrix. These crystals are probably of Triassic origin. Hence, the geochemical and the 3D seismic data suggest that the Triassic salt province 500 km further south on the Moroccan Margin might extend further north than previously known and that halokinesis has to be considered as a driving force for mud volcanism in the GoC.

Finally, a 1-D transport-reaction model has been applied to constrain the fluid advection rates. The numerical simulations of conservative porewater compounds Cl, Li, and B reveal upward fluid flow rates of ~6 cm/a at the top of the MMV, gradually decreasing to 0.3 cm/a towards the rim. In addition, a CTD mounted onto a video sled system provided bottom water salinity and temperature information (about 2 m above the seafloor) from tracks crossing the MMV. In combination with the numerical porewater analysis, this unique spatial data set allows to constrain the overall budgets for the release of water, methane, and other porewater constituents as well as the heat flow of the MMV.

### References

- [1] Hensen C., Nuzzo M., Hornibrook E., Pinheiro L.M., Bock B., Magalhaes V.H. and Brückmann W., (2007), *Geochim. Cosmochim. Acta* **71**, 1232-1248.

## Arsenic mineralogy in high-As wastes at historic gold mine sites, New Zealand

L. HAFFERT AND D. CRAW

Geology Department, University of Otago, PO Box 56,  
Dunedin, New Zealand

The studied mine processing sites are part of the Phoenix Mine and the Blackwater Mine, which are historic gold mines hosted within the Otago schist and Greenland Group schist, respectively. The processing of arsenopyrite ore produced very arsenic rich residues (up to 40 wt% As) and no rehabilitation was undertaken after mine closure at either mine. Thus, the studied sites possess suitable conditions for the study of the physical and chemical characteristics of secondary arsenic minerals, especially with respect to time. At the Blackwater Mines all arsenic was originally present as arsenolite (arsenic trioxide polymorph, As<sup>III</sup>), which is a by-product of arsenopyrite roasting. At the Phoenix Battery, where roasting did not take place, arsenopyrite was the original arsenic phase. High dissolved arsenic concentrations derived from the processing residues are temporarily immobilized by the formation of hydrated iron arsenates in the downstream environment. At the Blackwater Mine the hydrated iron arsenate is in the form of scorodite (FeAsO<sub>4</sub>·2H<sub>2</sub>O), whereas at the Phoenix Battery it is in the form of kankite (FeAsO<sub>4</sub>·3.5 H<sub>2</sub>O). In the past the precipitation of hydrated iron arsenates, especially scorodite, has been mainly associated with acidic environments. The studied mine sites are, however, excellent examples for iron arsenate precipitation in a geological setting with high neutralizing capacity and predominant circum-neutral pH. The stability of the hydrated arsenates depends on dissolved arsenic concentrations and is, therefore, controlled by the solubility and availability of the original As phase. In addition, the stability of As is further enhanced by the inherent morphology of the hydrated iron arsenates which precipitates as an interstitial cement, thereby creating an impermeable surface crust and preventing further dissolution of underlying arsenic minerals.

## Application of *in situ* cosmogenic nuclide analysis to landform evolution in (palaeo)-periglacial south-west Britain

J.H. HÄGG<sup>1</sup>, M.A. SUMMERFIELD<sup>1</sup>, C. SCHNABEL<sup>2</sup>,  
W.M. PHILLIPS<sup>3</sup> AND S. FREEMAN<sup>2</sup>

<sup>1</sup>Institute of Geography, School of Geosciences, University of Edinburgh, UK (j.hagg@ed.ac.uk)

<sup>2</sup>Scottish Universities Environmental Research Centre, East Kilbride, UK

<sup>3</sup>Idaho Geological Survey, University of Idaho, Moscow, ID, USA

Located beyond the southern limit of glaciation in Britain, the upland granitic terrain of Dartmoor, south-west England, has been exposed to long intervals of intense periglacial activity during the Pleistocene. This region has been significant in debates about appropriate models of long-term landscape change, most notably two-phase versus single-phase models of landform evolution, and the development of tors (Linton, 1955; Palmer & Nielsen, 1962). However, given the previous lack of quantitative techniques capable of constraining denudation and specific process rates, and thereby testing developmental models, for these features there remains much uncertainty in the interpretation of the classic landforms of the region. Here we present the results of research utilising *in-situ* cosmogenic nuclides to evaluate geomorphological processes and report on three key aspects of landform development: (1) the formation of tors and models of outcrop emergence in non-glaciated regions; (2) the development of regolith and boulderfields under periglacial conditions; and (3) catchment-averaged denudation rates derived from alluvial sediments. This variety of landforms and scale of investigation facilitates an integrated approach to the understanding of catchment-scale erosional dynamics. In addition, the complex nature of landform development that is evident in the area provides challenges to the application of *in-situ* cosmogenic nuclides and highlights both the potential and limitations of the technique.

### References

- Linton D.L., (1955), *Geographical Journal*, **121**, 470-487  
Palmer J.A. and Nielsen R.A., (1962), *Proc. of the Yorkshire Geol. Soc.*, **33**, 315-339

## Origin of tungsten mineralization in the quartzdioritic unit of the Boroujerd Granitoid Complex (Western Iran) using geochemical evidences

M. HAGHNAZAR, D. ESMAEILI AND M.V. VALIZADEH

School of Geology, University College of Science, University of Tehran, Iran (haghnazar@khayam.ut.ac.ir; esmaili@khayam.ut.ac.ir; mvalizad@chamran.ut.ac.ir)

Boroujerd Granitoid Complex of the Sanandaj-Sirjan Zone consists of three main units: granodiorite, quartzdiorite and monzogranite. In Nezamabad area (SE of this complex), quartzdioritic unit has been cut by various quartz-tourmaline veins having NW-SE trending. Tungsten mineralization (scheelite) accompanying by arsenopyrite, pyrite, pyrrhotite, chalcopyrite, sphalerite, malachite, azurite and quartz and tourmaline as gangue are generally associated with the veins.

The geochemical signature of this unit is compared with the well known W-bearing and W-barren granites (Lemann *et al.*, 1994; Srivastava and Sinha, 1997; Singh and Singh, 2001) in order to investigate their relationship with tungsten mineralization in the area.

The host quartzdioritic unit of the quartz-tourmaline veins is mostly depleted in silica (52-63%), total alkalis (4.6%), Rb (94 ppm), Nb (10 ppm), W (6 ppm) and Sn (3 ppm) with low DI and enriched in CaO (6.11%), MgO (4.16%), FeO (4.19%), MnO (0.14%), Sr (285 ppm) and Ba (359 ppm). Compared with the W-barren granites, the K/Rb (211) and Ba/Rb (4) ratios of this granitoid are also higher than its Rb/Sr ratio (0.34). All these geochemical evidences as well as I-type characteristics of the quartzdiorite unit (Ahmadi-Khalaji *et al.*, 2007) indicate that the unit behaves as a barren granite.

On the other hand, geochemical investigation on the metamorphosed sedimentary rocks (hornfels and spotted schist) existing in contact with the quartzdioritic unit demonstrates that the W-bearing fluid originated from the dehydration of the metamorphosed sedimentary rocks and it mixing with granitic fluids.

The quartzdioritic unit is a W-barren granite of a low differentiated magma and has no significant role in tungsten mineralization. In contrary, metamorphic rocks fluids can be considered as the main source for tungsten mineralization rather than granitic fluids.

### References

- Ahmadi-Khalaji A., Esmaily D., Valizadeh M.V. and Rahimpour-bobab H., (2007), *JAES* **29** 859-877.  
Lehmann B., Jungyusuk N., Khositant S., Höhndorf A. and Kuroda Y., (1994), *J of Southeast Asian Earth Sciences* **10** 51-63.  
Singh S.K. and Singh S., (2001), *Gondwana Research* **4** 487-795.  
Srivastava P.K. and Sinha A.K., (1997), *J of Geochemical Exploration* **60** 173-184.

## Reaction textures of allanite in metagranitoids: A sub-micrometer insight in REE-mobility

A. HAHN<sup>1</sup>, G. FRANZ<sup>2</sup> AND D. RHEDE<sup>1</sup>

<sup>1</sup>GeoForschungsZentrum Potsdam, Section 4.1 and 4.2, 14473 Potsdam, Germany (ahahn@gfz-potsdam.de; rhede@gfz-potsdam.de)

<sup>2</sup>TU Berlin, Fachgebiet Mineralogie-Petrologie, 13355 Berlin, Germany (gerhard.franz@tu-berlin.de)

Various reaction textures of accessory allanite in an orthogneiss from the Tauern Window (Austria), which experienced metamorphism (max. 500-550°C, 1.0 GPa; Selverstone 1993), and extensive metasomatism have been investigated by high-resolution BSE images (JEOL Hyperprobe JXA-8500 F, field-emission cathode).

Euhedral to anhedral ( $\varnothing$  150 - 500  $\mu\text{m}$ ), partly zoned allanite crystals have corona-type textures with polycrystalline (REE+Y)-poor epidote/clinozoisite rims (type 1). Variable deformation stages resulted in regularly to sigmoid or irregularly shaped rims of 20 - 200  $\mu\text{m}$  thickness. Anhedral titanite crystals (15  $\mu\text{m}$ ) mark the core-rim boundary along the epidote/clinozoisite site of the paragenesis. Micropores within allanite (type 2), partly filled with Th- or REE-silicates, are part of the core-rim zonation (relatively REE+Y+Th-rich to -poor) or scattered over allanite. Th-silicates on grain boundaries of newly formed (REE+Y)-poor epidote/clinozoisite (polycrystalline epidote/ clinozoisite rim of allanite) indicate decomposition and reprecipitation of that phase. Patchy aggregates of allanite and REE-poor epidote with intermediate compositions, changing in an irregular pattern on the  $\mu\text{m}$  and sub- $\mu\text{m}$  scale, are the dominant feature in the intensely deformed orthogneiss (type 3). In addition to these well-known textures up to 1  $\mu\text{m}$  wide mineral-filled channels within elongate textures (max. 80  $\mu\text{m}$ ) in an allanite of type (3) were found (type 4). The zoned channels pass perpendicular through the internal textures, which are orientated parallel and perpendicular to the long axis of the allanite and connect (REE+Y+Th)-poor with relatively (REE+Y+Th)-enriched parts of the unzoned crystals.

In a preliminary interpretation texture (1) was formed in late- to postmagmatic stage in the protolith, textures (2, 3, 4) indicate a simultaneous fluid-assisted decomposition of allanite and growth of (REE+Y)-poor epidote/clinozoisite in an open system during metamorphism. The Th-silicate on grain boundaries within the epidote/clinozoisite rims of allanite and sub-micrometer wide channels within allanite possibly indicate multistage grain boundary diffusion and a gradually changing composition of the fluid phase during the breakdown process.

### References

Selverstone J. (1993), *Schweiz. Mineral. Petrograph. Mitt.* **73**, 229-239.

## The bulk chemical composition of the upper Martian crust

B. C. HAHN AND S. M. MCLENNAN

Department of Geosciences, Stony Brook University, Stony Brook, NY 11794-2100 (bhahn@mantle.geo.sunysb.edu; Scott.McLennan@sunysb.edu)

There is strong evidence that the Martian surface has been extensively chemically homogenized over time due to broad-scale impact gardening, an apparent lack of plate tectonic fractionation and evolution, long-term global eolian processes, and periodic fluvial transport. Despite wide geographic separation, soil chemistry from landing site analyses (MER, Pathfinder, and Viking) are remarkably similar with most variation attributed to the addition of some local rock components - strongly implying that the unconsolidated fraction of the Martian surface has been reasonably well-homogenized. Gamma-Ray Spectrometer (GRS) elemental abundance maps agree well with surface analyses and, with some notable exceptions, global GRS elemental abundance maps reveal less broad-scale chemical variation compared to the terrestrial or lunar surfaces.

Therefore, it has been suggested that the chemical composition of averaged Martian soil analyses reflect the bulk chemical composition of the Martian surface from which they are derived - much in the same way terrestrial sedimentary chemistry can be used as a proxy for the bulk terrestrial upper crust. Weathering, sedimentary transport, and deposition naturally sample a wide array of source rocks with the resultant chemistry being an efficient mixture of source terrains.

With carefully screened MER APXS data, we develop an estimate of major and trace element crustal chemistry based upon MER soil averages. GRS global chemical averages for certain elements are used to corroborate compositions calculated from the soil data and in some cases GRS global averages for a particular element are assumed to represent the bulk upper crust. Where applicable, SNC chemistry and canonical cosmochemical relationships are also incorporated into the bulk determination.

## Petrogenesis of meta-peridotites in the Takab area, NW Iran

R. HAJIALIOGHLI<sup>1</sup>, M. MOAZZEN<sup>1</sup>, A. JAHANGIRI<sup>1</sup>,  
G. DROOP<sup>2</sup>, R. BOUSQUET<sup>3</sup> AND R. OBERHÄNSLI<sup>3</sup>

<sup>1</sup>Department of Geology, University of Tabriz, 51664 Tabriz, Iran (r\_hajialioghli@yahoo.co.uk)

<sup>2</sup>School of Earth, Atmospheric and Environmental Sciences, University of Manchester, Oxford Road, Manchester, M13 9PL, UK

<sup>3</sup>Institut für Geowissenschaften, Universität Potsdam, Postfach 601553, D-14415 Potsdam, Germany

The Takab meta-ultramafic rocks of north western Iran crop out in association with a variety of metamorphic rocks including mafic granulites, amphibolites, calc-silicates, granitic gneisses and pelitic schists. The protoliths of the Takab meta-peridotites were mainly harzburgite and dunite with subordinate lherzolite. All peridotite varieties contain primary Cr,Al-spinel. The peridotites were modified by metasomatism under low-grade conditions and later amphibolite-facies metamorphism, the thermal peak of which occurred at temperature of 410-530°C, corresponding to an orogenic setting.

Chemical compositions of the porphyroclastic olivine, pyroxene and spinel in the investigated meta-peridotites give temperature of 1000-1200°C; clinopyroxene barometry yields a pressure of 24±2.7kbar, corresponding to a depth of ca. 72km.

The results are consistent with oceanic lithospheric upper mantle origin (i.e. in an ophiolitic setting) of the meta-ultramafic rocks in the Takab area. Similarities in the stratigraphy, lithology and age data (relative and isotopic ages) of the protoliths of the Takab complex and equivalent units from the Central Iran Zone suggest that the Takab complex has a Neoproterozoic-Early Cambrian age and experienced the Pan-African orogeny. The strips of the ultramafic rock in the study area are remnants of the Proto-Tethyan oceanic lithosphere.

## Li isotope fractionation in the subducted slab – A case study from the Raspas complex, Ecuador

RALF HALAMA<sup>1</sup>, TIMM JOHN<sup>2</sup>, VOLKER SCHENK<sup>1</sup>,  
WILLIAM F. McDONOUGH<sup>3</sup> AND ROBERTA L. RUDNICK<sup>3</sup>

<sup>1</sup>Institut für Geowissenschaften & SFB 574, Universität Kiel, 24118 Kiel, Germany (rh@min.uni-kiel.de)

<sup>2</sup>Physics of Geological Processes, University of Oslo, 0316 Oslo, Norway (timm.john@fys.uio.no)

<sup>3</sup>Department of Geology, University of Maryland, College Park, MD, 20742, USA

Lithium isotopes are a potentially powerful geochemical tracer of subducted material due to significant isotopic fractionation on the Earth's surface and the fluid-mobile behaviour of Li. To improve our ability to track recycled Li in the mantle, and to understand the transfer of Li from the slab through the mantle wedge to the volcanic arc, it is important to constrain the Li isotopic composition of subducted material and the isotopic changes that may occur during the subduction process.

Here, we report results from a detailed geochemical and Li isotope study on the now exhumed part of a subducted slab from the Raspas complex (Ecuador), which comprises serpentinites, eclogites, blueschists and high-pressure metapelites. Eclogites show MORB-like trace element signatures and are LREE-depleted. They are characterized by a light Li isotopic composition with  $\delta^7\text{Li}$  ranging from 0 to -13. These values are considerably lower than those of fresh and altered MORB ( $\delta^7\text{Li} = +3$  to  $+14$ ; Chan *et al.*, 1992), but they overlap with those of Alpine eclogites (Zack *et al.*, 2003). In contrast, blueschists and metapelites, as well as the serpentinites that are interpreted to represent the mantle portion of the subducted slab, have Li isotopic compositions in between the eclogites and MORB. A negative correlation between  $\delta^7\text{Li}$  and Li/Dy for the eclogites suggests that influx of Li from an external source may have been responsible for decrease in  $\delta^7\text{Li}$  in the eclogites. Moreover, the elevated Li concentrations in some of the eclogites (up to 94 ppm) are difficult to reconcile with Li loss during dehydration alone. Although none of the associated lithologies is particularly rich in Li, eclogite-facies fluids that may contain up to 438 ppm Li (Svensen *et al.*, 2001) could provide a suitable source of Li. These results suggest that fluid-assisted kinetic isotope fractionation (Teng *et al.*, 2006) may have played a role in causing the light Li isotope composition of the eclogites, as also suggested by Marschall *et al.* (2007).

### References

- Chan, L.-H., *et al.*, 1992, *EPSL* **108**, 151-160.  
Zack, T., *et al.*, 2003, *EPSL* **208**, 279-290  
Svensen, H., *et al.*, 2001, *J. met. Geol.* **19**, 165-178.  
Teng, F.-Z., *et al.*, 2006, *EPSL* **243**, 701-710.  
Marschall, H., *et al.*, 2007, *This volume*

## The Pb isotope evolution of Arctic Ocean intermediate water over the past 16 million years

B.A. HALEY<sup>1</sup>, M. FRANK<sup>1</sup>, R. SPIELHAGEN<sup>1,2</sup> AND J. FIETZKE<sup>1</sup>

<sup>1</sup>IFM-GEOMAR, Leibniz Institute of Marine Sciences at the University of Kiel, Germany, bhaley@ifm-geomar.de

<sup>2</sup>Academy of Sciences, Humanities and Literature, Mainz, Germany

We present the first record of the dissolved Pb isotope composition of Arctic intermediate water of the past 16 Myr. The data were obtained from leaches of sediments of IODP Leg 302 (“ACEX”) drill-cores and from a piston-core (PS2185), both located near the North Pole on the Lomonosov Ridge (~1200m water depth). Both the leaches and bulk dissolutions of the same sediments show similar Pb isotope compositions in the “Neogene” (>1 Ma) and in the “Pleistocene” (<1 Ma) sediments, although the median values differ slightly between the two sections (e.g. <sup>206</sup>Pb/<sup>204</sup>Pb ~18.5 in the “Neogene” versus ~18.6 in the “Pleistocene”). These central Arctic isotope signatures are much less radiogenic compared with N. Atlantic records, and, although similar trends between these two basins are observable for the Pleistocene, they differed significantly during the Neogene.

From these observations and comparisons in Pb-Pb isotope space, we argue that the source of dissolved Pb in Arctic intermediate waters has primarily been derived locally from exchange with sinking ice transported sediment particles. These sediments originated from the Eurasian shelves and have continuously been carried to the North Pole region via the Transpolar Drift for the past 16 Ma.

On short millennial time scales of the Quaternary our Arctic records reflect isotopic changes in the Siberian continental sources of Pb. The most likely process driving these changes was incongruent weathering and soil formation during interglacial periods. These soils were a reservoir of relatively unradiogenic Pb, which was eroded and supplied to the Arctic ocean as an early “pulse” at interglacial-glacial transitions. Our central Arctic Pb isotope record only shows a significant glacial-interglacial cyclicity for the past ~1 Ma. On the longer Myr timescales of the Neogene, the Pb isotope data do not indicate very pronounced variations and do, for example, not show any major changes during the ~2.7 Ma intensification of Northern Hemispheric Glaciation, as observed for dissolved records in the N. Atlantic. The long term variability will be discussed in terms of relatively small changes in the continental input sources (i.e., Siberia vs. Northern Canada/Greenland).

## <sup>86</sup>Sr/<sup>88</sup>Sr ratio by ICP-MS-MC as a new tracer of terrestrial geochemical processes

L. HALICZ<sup>1</sup>, I. SEGAL<sup>1</sup>, N. FRUCHTER<sup>2</sup>, B. LAZAR<sup>2</sup> AND M. STEIN<sup>1</sup>

<sup>1</sup>Geological Survey of Israel, 30 Malkhe Israel St., Jerusalem (ludwik@gsi.gov.il; motis@vms.huji.ac.il; irena.segal@gsi.gov.il)

<sup>2</sup>Institute of Earth Sciences, The Hebrew University of Jerusalem (boaz.lazar@huji.ac.il; noaf01@pob.huji.ac.il)

This study shows that the stable isotopic composition of strontium (the <sup>86</sup>Sr/<sup>88</sup>Sr ratio expressed as δ<sup>86</sup>Sr values) in sedimentary rocks may vary significantly. The rocks were analyzed by MC-ICP-MS “Nu Plasma” (fitted with Aridus sample introduction system). Five Faraday collectors were used for measurement of following isotopes: <sup>83</sup>Kr (as monitor of <sup>86</sup>Kr interference from the argon gas, where <sup>86</sup>Kr=1.52·<sup>83</sup>Kr), <sup>85</sup>Rb (to correct for <sup>87</sup>Rb interference) and three strontium isotopes (<sup>86</sup>Sr, <sup>87</sup>Sr, <sup>88</sup>Sr). Each measurement comprised three blocks, each block consisting of 28 measurements of 10 seconds integration time. The zero reference points were reset simultaneously for all measured masses by deflecting the potential of the electrostatic analyzer before each block measurement. The optimum Sr concentration was 0.1-0.2 mg·L<sup>-1</sup>, giving sensitivity of ~5-7 V·ppm<sup>-1</sup>.

All rocks that originated in the marine environment: corals (*porites lutea* and *acropora* from the Gulf of Aqaba); Cretaceous limestone (Judea Mt.); Pliocene epigenetic dolomite (Dead Sea rift margins) as well as lacustrine evaporitic aragonite (Dead Sea) yielded uniform δ<sup>86</sup>Sr value (-0.28±0.07 ‰) within the 1σ error of Red Sea and Atlantic seawater (-0.35±0.04 ‰). On the other hand, secondary materials (products of chemical weathering) from the terrestrial environment of the Judea Mt. such as speleothem calcite and terra rossa soil (airborne dust particles residual rock material) both yielded significantly higher δ<sup>86</sup>Sr value (0.17±0.03 ‰). It should be noted that both groups are distinctly different from the SRM987 standard that has by definition a value of 0 ‰. It appears that strontium isotopes are fractionated within the terrestrial environment by geochemical processes such as chemical weathering and genesis of soils and hence <sup>88</sup>Sr/<sup>86</sup>Sr ratio may be developed as a tracer for these processes.

## Growth of the Earth's core

A.N. HALLIDAY<sup>1</sup>, R.B. GEORG<sup>1</sup>, T.L. GROVE<sup>2</sup>,  
D.-C. LEE<sup>3</sup>, A. MARKOWSKI<sup>4</sup>, G. QUITTÉ<sup>5</sup>,  
E.A. SCHAUBLE<sup>6</sup>, S.J. SINGLETARY<sup>7</sup> AND  
H.M. WILLIAMS<sup>1</sup>

<sup>1</sup>Earth Sciences, Oxford University (alexh@earth.ox.ac.uk)

<sup>2</sup>Earth, Atmos. & Planet. Sci., MIT

<sup>3</sup>Earth Sciences, Academia Sinica, Taipei

<sup>4</sup>Earth Sciences, ETH Zürich

<sup>5</sup>Laboratoire des Sciences de la Terre, ENS Lyon

<sup>6</sup>Earth and Space Sciences, UCLA

<sup>7</sup>Natural Sciences, Fayetteville State University

Hafnium-tungsten chronometry provides evidence that some magmatic iron meteorite parent bodies formed relatively small cores within a million years of the start of the solar system. Similar timescales can be inferred from martian meteorites and ureilites. There is some evidence that the degree of siderophile element depletion, possibly reflecting relative core size, increased over the first 10<sup>7</sup> years on Mars and the angrite parent body. How the Earth's core started is less clear and some assume more efficient core growth under reducing conditions. The Si isotopic compositions of mantle-derived silicate rocks from the Earth and Moon are heavy relative to those from Mars and Vesta which in turn are identical to those of chondrites. A likely explanation for this is Si isotopic fractionation during high pressure and high temperature metal segregation. On this basis Si is one of the light elements in the Earth's core. There is a hint of an analogous effect for oxygen. However, the heterogeneity within the circumstellar disk renders this interpretation less certain. Similarly, slightly heavy Fe in the bulk silicate Earth may reflect high pressure core formation in the presence of perovskite. The Moon does not have a high pressure core yet lunar basalts display O, Si and Fe isotopic compositions similar to those found on Earth. This can be reconciled with giant impact simulations provided there was efficient mixing between the silicate Earth and the protolunar disk as recently proposed (Pahlevan and Stevenson 2005). This being the case the Moon represents an important new archive for the composition of the early silicate Earth and demonstrates that Si and possibly O were already light elements in the core before the Giant Impact.

### Reference

Pahlevan K. and Stevenson D.J. (2005) The oxygen isotope similarity between the Earth and Moon – source region or formation process? *LPSC XXXVI*, 2382.

## Molecular and isotopic study of acidic metabolites in the deep biosphere employing petroleum reservoirs as natural bioreactors

C. HALLMANN<sup>1</sup>, K. GRICE<sup>1</sup> AND L. SCHWARK<sup>2</sup>

<sup>1</sup>Isotope and Molecular Biogeochemistry Group, Curtin University, Perth, Western Australia

(C.Hallmann@curtin.edu.au, K.Grice@curtin.edu.au)

<sup>2</sup>Institute of Geology, University of Cologne, Germany  
(Lorenz.Schwark@uni-koeln.de)

Being systems that support a biologically active environment, petroleum reservoirs can be used as naturally occurring analogues to bioreactors in view of studying the anaerobic catabolism and metabolism of an extremophile deep-subsurface biosphere. Although living cells have been identified in deep sub-seafloor sediments (Schippers *et al.*, 2004), cell organic matter is not preserved well in the aqueous environment. The hydrophobic oil matrix of petroleum reservoirs, in contrast, can act as an accumulator of *in-situ* produced metabolites and cell-wall lipids.

This presentation will examine the molecular distribution and stable carbon isotopic variation between carboxylic acids and their non-carboxylated hydrocarbon counterparts in oils that were biologically degraded to various extents and recovered from different non-communicating compartments of a reservoir. Oils were fractionated into compound classes and further analysed by gas chromatography (GC) and mass spectrometry (MS), as well as isotope ratio monitoring (irm)GC-MS.

The lack of microbial petroleum degradation in reservoirs that were ever heated >80°C suggests that microbes have been present in the sediments since their deposition and possibly survive by the release of volatile organic acids from dispersed sedimentary organic matter (Wellsbury *et al.*, 1997). Significant migration and recolonization of microbes in the subsurface does not appear to take place. The escape into the deep could be an ancestral evolutionary survival strategy that allows microbes to maintain their viability for extremely long periods, to the expense of pushing the physicochemical limits of life. Understanding the evolution of earth's early biosphere is therefore closely related to understanding the biochemical adaptation of life to extreme environments, which can only be studied in present-day analogues, one of which are deep anaerobic petroleum reservoirs. This study focusses on the structural and isotopic analysis of carboxylic acids as indicators of deep biosphere processes.

### References

Schippers, A., Neretin, L., Kallmeyer, J., Ferdelman, T., Cragg, B., Parkes, J., and Jørgensen, B. (2005) *Nature* **433**, 861-864.  
Wellsbury, P., Goodman, K., Barth, T., Cragg, B., Barnes, S., and Parkes, J. (1997) *Nature* **388**, 573-576.

## Li diffusion and isotopic fractionation in olivines crystals

CEDRIC HAMELIN<sup>1</sup>, MARC CHAUSSIDON<sup>2</sup>,  
JEAN-ALIX BARRAT<sup>1</sup>, PIERRE BECK<sup>3</sup> AND  
MARCEL BOHN<sup>4</sup>

<sup>1</sup>CNRS UMR 6538, U.B.O.-I.U.E.M., place Nicolas Copernic,  
29280 Plouzané Cedex, France

(cedric.hamelin@sdt.univ-brest.fr; barrat@univ-brest.fr]

<sup>2</sup>CRPG-CNRS UPR 2300, 15 rue Notre-Dame des Pauvres,  
54501 Vandoeuvre-les-Nancy Cedex, France  
(chocho@crpg.cnrs-nancy.fr)

<sup>3</sup>Geophysical Laboratory, Carnegie Institution of Washington,  
5251 Broad Branch Road NW, DC 20015-1305  
Washington, USA (pbeck@ciw.edu)

<sup>4</sup>CNRS UMR 6538, IFREMER, BP70, 29280 Plouzané,  
France (bohn@ifremer.fr)

In order to constrain the behavior of lithium isotopes in crystals during magma cooling, the study of a fresh pillow-lava with large olivine crystals has been undertaken. An ion-microprobe was used to measure lithium abundances and isotopic compositions both in olivine phenocrysts and in the pillow rim glass. Profiles in  $\delta^7\text{Li}$  conducted through olivines show very different patterns correlated with their cooling history. Olivines embedded in the pillow rim glass display no variation in Li abundance ( $[\text{Li}] = 1.2 \mu\text{g.g}^{-1}$ ) and isotopic composition ( $\delta^7\text{Li} = +6 \text{‰}$ ). However, a large Li isotopic zoning is found from crystal cores ( $\delta^7\text{Li} = +6 \text{‰}$ ,  $[\text{Li}] = 1.1 \mu\text{g.g}^{-1}$ ) to rims ( $\delta^7\text{Li} = -11 \text{‰}$ ,  $[\text{Li}] = 1.4 \mu\text{g.g}^{-1}$ ) for olivines set in microcrystalline groundmass. The cores of large olivine phenocrysts are equilibrated with the pillow rim glass ( $\delta^7\text{Li} = +6 \text{‰}$ ,  $[\text{Li}] = 3.4 \mu\text{g.g}^{-1}$ ).

Recently, detailed investigation of the Li isotopic composition of large phenocrysts in various magmatic environments demonstrated that microscale  $\delta^7\text{Li}$  variations were due to fractionation of lithium isotopes during late stage chemical diffusion (Barrat *et al.*, 2005; Beck *et al.*, 2006; Jeffcoate *et al.*, 2006). In our case, the diffusion-induced Li isotopes fractionation is the only process able to explain such diverse zoning in olivines from one single pillow lava. Our study brings new constraints on the Li fractionation during the diffusion process and suggests that the pristine  $\delta^7\text{Li}$  values can be completely erased in small phenocrysts, even in the case of rapidly cooled volcanics. The use of Li isotopes in crystals for tracking mantle heterogeneities should be taken with extreme caution.

### References

- Barrat J.A., Chaussidon M., Bohn M., Gillet P., Gopel C., and Lesourd M., (2005), *Geochimica et Cosmochimica Acta* **69**, 5597-5609.  
Beck P., Chaussidon M., Barrat J.A., Gillet P., and Bohn M., (2006), *Geochimica et Cosmochimica Acta* **70**, 4813-4825.  
Jeffcoate A.B., Elliott T., Kasemann S.A., Ionov D., Cooper K., and Brooker R., (2007), *Geochimica et Cosmochimica Acta* **71**, 202-218.

## $\delta^7\text{Li}$ systematics of mantle xenoliths from Kilbourne Hole: Unraveling metasomatic & diffusional processes

S.J. HAMMOND<sup>1,2</sup>, I.J. PARKINSON<sup>1</sup>, R.H. JAMES<sup>1</sup>,  
N.W. ROGERS<sup>1</sup> AND J. HARVEY<sup>3</sup>

<sup>1</sup>Dept. of Earth Sciences, The Open University, Walton Hall,  
Milton Keynes, MK7 6AA, UK.

(s.hammond@open.ac.uk)

<sup>2</sup>Dept. of Earth Science and Eng., Imperial College London,  
South Kensington Campus, London, SW7 2AZ, UK.

<sup>3</sup>Boston University TIMS Facility, Department of Earth  
Sciences, 675 Commonwealth Avenue, Boston, MA  
02215, USA.

We present a detailed Li isotopic study of spinel-peridotites from Kilbourne Hole, New Mexico, including whole rock and hand picked mineral separate  $\delta^7\text{Li}$  data (measured by MC-ICP-MS) and in-situ  $\delta^7\text{Li}$  data measured by ion microprobe. From this detailed approach the effects of mantle metasomatism and diffusion can be unravelled.

The xenolith suite can be divided into those which are in textural equilibrium, and those which have interacted with the host lava. Whole rock values for the sample suite range from +4.5 ‰ to -2.9 ‰. Of the samples which are in textural equilibrium, mineral separates reveal that olivine, orthopyroxene, and clinopyroxene are all in isotopic equilibrium, and grains analysed by ion microprobe are homogeneous in both Li and  $\delta^7\text{Li}$  across grains, with the exception of the outer 50  $\mu\text{m}$  in some clinopyroxene grains. The two lightest  $\delta^7\text{Li}$  are found in equilibrated LREE enriched harzburgites, which is consistent with these samples having completely equilibrated with a melt with a slightly negative  $\delta^7\text{Li}$  (-3 ‰), possibly from a garnet pyroxenite/eclogite source (although partial equilibration with a heavy  $\delta^7\text{Li}$  melt can also explain these data).

Kilbourne Hole peridotite xenoliths have rapid transit times (~0.2 days), which is long enough to produce the Li isotope perturbation observed in the clinopyroxene grains by more rapid diffusion of  $^6\text{Li}$  compared to  $^7\text{Li}$  from the host lava.

The extent of clinopyroxene reaction correlates with a decrease in whole rock  $\delta^7\text{Li}$ , which can be explained by reaction driven diffusion with the host lava. Li diffusion in clinopyroxene is at least ten times faster than in olivine [1], and so interactions between peridotite and melt produce clinopyroxene with lighter  $\delta^7\text{Li}$  than co-existing mineral phases. Clinopyroxene data that have very light  $\delta^7\text{Li}$  values (e.g. [2]) have been used to argue a very light  $\delta^7\text{Li}$  component in the mantle. However, without evidence of Li isotopic equilibrium, the existence of such a component must be treated with caution.

### References

- [1] Parkinson *et al.*, (2007), *Earth. Planet. Sci. Lett.* doi:10.1016/j.epsl.2007.03.023  
[2] Nishio *et al.*, (2004), *Earth. Planet. Sci. Lett.* **217** 245-261.

## Diagnosis of pollution state of the coasts in the vicinity of an oil terminal : Bioremediation effect

R. HAMOUDA, N. OUERTANI AND H. BÉLAYOUNI

Faculté des Sciences de Tunis, Département de Géologie,  
Laboratoire de Géochimie organique,  
(hamoudarym@yahoo.fr)

Coastal marine environments near the oil harbour installations can be the object of a chronic oil pollution coming from purging water of the storage tanks of oil, as well as water coming from ballast operations of tankers. In the oil terminal of the south of Tunisia, this water is collected in tanks before their discharge in a natural lagoon which communicates with the Mediterranean Sea. This lagoon is periodically flooded by sea water (tide phenomena). The objective of this work is the diagnosis of the pollution state of the lagoon. This study is based on the analysis of the COT and the technics of liquid and gas chromatography.

Analysis of TOC and TH (total hydrocarbon) in surface sediments of the lagoon permit to note that:

-TH varies between 200 and 4020 ppm.

positive correlation calculated between the TOC and TH, attest of the homogeneity of the organic matter contained in the sediments

-% of saturated hydrocarbons vary between 6 and 12% and are classic of an organic matter inherited from original biomass;

-The organic matter presents a mixed origin terrestrial and marine. N-alkane distribution is bimodal: first mode characterized by n-alkanes from C21 to C33 with a CPI of 2,1 characterising organic matter from waxe plants, the second mode is centred on n-alkanes from C17 to C20 without odd to even prevalence and characterizes a marine organic matter. Presence of UCM with a hump developed under all the range of n-alkanes attest of an important microbial activity in sediments.

Surface sediments of the lagoon seems not to be contaminated by water coming from the systems of water treatment of oil residues. These results show the role of these lagunar systems to manage and eliminate pollution :bioremediation effect.

### References

- Aksu A.E., Abrajano T., Mudie P.J., et Yaşar D. (1999). *Marine Geology* **153**, 303–318.
- Colombo, J.C., E. Pelletier, C. Brochu, and M. Khalil. (1989). *Environ. Sci. Technol.* **23**:888-894.
- Jaffé R., Mead R., Hernandez M. E., Peralba M. C. et DiGuida O.A. (2001) *Org. Geochem.*, **32**. 507-526
- Burns K.A. et Knap A.H. (1989) *Mar. Pollut. Bull* **20**, 391-398.
- Miranda A.C.M.L., Loureiro M.R.B., Cardoso J.N. (1999) *Org. Geochem.* **30**. 1027-1038
- Chaineau C.H., Morel J.L. and Oudot J. (1995): *Environ. Sci. Technol.* **29**, 1615–1621.

## Weathering processes in karst river, southwest China: Implication from riverine sulphur and strontium isotope

GUILIN HAN<sup>1</sup>, ZHIFANG XU<sup>2</sup> AND YANG TANG<sup>1,3</sup>

<sup>1</sup>The State Key Laboratory of Environmental Geochemistry, Institute of Geochemistry, Chinese Academy of Sciences, Guiyang 550002, China (hanguilin@vip.skleg.cn)

<sup>2</sup>The Institute of Geology and Geophysics, Chinese Academy of Sciences, P.O.Box 9825, Beijing 100029, China

<sup>3</sup>Graduate School of Chinese Academy of Sciences, Beijing 100039, China

Geochemistry of river waters draining karst terrain in SW China has been studied in order to characterize the hydrogeochemistry of the rivers, to determine natural chemical and physical weathering rates in typical areas and anthropogenic contaminants. The studied area is impacted by serious sulphuric acid rain because of coal-mining and combustion and coal-formation strata in Guizhou Province. Another aim of the work is to study the effect of sulphuric acid on the carbonate weathering.

### Results and Discussions

Water samples of karst river water from the Guizhou province (Wujiang River and Yuanjiang River) in karst-dominated regions were analyzed for dissolved major element concentrations ( $\text{HCO}_3^-$ ,  $\text{NO}_3^-$ ,  $\text{SO}_4^{2-}$ ,  $\text{Cl}^-$ ,  $\text{Ca}^{2+}$ ,  $\text{Mg}^{2+}$ ,  $\text{K}^{2+}$ ,  $\text{Na}^+$ ),  $\text{Sr}^{2+}$  and  $^{87}\text{Sr}/^{86}\text{Sr}$  and  $\delta^{34}\text{S}$  of dissolved sulfate ( $\delta^{34}\text{S}_{\text{SO}_4}$ ) in summer. The waters of the Wujiang River have high  $\text{Sr}^{2+}$  concentrations and lower  $^{87}\text{Sr}/^{86}\text{Sr}$  ratios (0.7074-0.7115), while those of Qingshuijiang River, one of two major tributaries of the Yuanjiang River system, show higher Sr isotopic ratios (0.7088-0.7155) and low Sr concentrations. Weathering rates of silicates and carbonates were determined from major element mass balance with Sr isotope.

The sulfur isotopic compositions ( $\delta^{34}\text{S}$ ) in Wujiang River catchments range from -7.70‰ to 13.06‰ and have higher  $\text{SO}_4^{2-}$  concentrations, which are inferred to be mainly derived from anthropogenic emissions and/or the oxidation of sulfide minerals in the coal-containing strata in the studied area. Samples from Yuanjiang River, which is dominated by clastic rocks, have relative enrich  $\delta^{34}\text{S}$  (-4.81‰ to 4.13‰) and lower  $\text{SO}_4^{2-}$  concentrations, which appears to result from solution of gypsum and rainwater  $\text{SO}_4^{2-}$ . The carbonate weathering of sulfuric acid may become an important  $\text{CO}_2$  source to atmosphere and can counteract the  $\text{CO}_2$  consumption by silicate weathering, so the presence of sulfuric acid should be seriously considered to calculated  $\text{CO}_2$  budget in this kind of area.

### Acknowledgements

This work was funded by the National Natural Science Foundation of China (Grant no: 40673010, 40503017).

## Source origin of the ultrapotassic lavas from the Leucite Hills, Wyoming: Hf isotope constraints

BARRY B HANAN<sup>1</sup>, JANNE BLICHERT-TOFT<sup>2</sup>,  
RICHARD H. KINGSLEY<sup>3</sup> AND JEAN-GUY SCHILLING<sup>3</sup>

<sup>1</sup>San Diego State University, San Diego, CA 92182-1020,  
USA (Barry.Hanan@sdsu.edu)

<sup>2</sup>Ecole Normale Supérieure de Lyon, 69364 Lyon Cedex 7,  
France (jblicher@ens-lyon.fr)

<sup>3</sup>University of Rhode Island, Narragansett, Rhode Island  
02882, USA (kingsley@gso.uri.edu, jgs@gso.uri.edu)

The Leucite Hills of SW Wyoming consist of 22 volcanic outcrops that occur over an area of ~ 2,500 km<sup>2</sup>. The lavas consist of 3 types of lamproite, basic to ultramafic madupite (M), and more silicic wyomingite and orendite (W/O), characterized by phlogopite phenocrysts in a groundmass of leucite, diopside, apatite, ±sanidine, ±glass. Volcanism spanned 3.0-0.89 Ma. 84% of the <0.7 km<sup>3</sup> of magma was erupted between 0.94 and 0.89 Ma. The lamproites cross-cut the NE flank of the Late Cretaceous Rock Springs Uplift and are underlain by the Archean Wyoming craton, stabilized at 3.2-2.5 Ga. The Wyoming subcontinental lithospheric mantle (SCLM) was enriched metasomatically >1.0 Ga by ancient subduction of carbonate-bearing sediments.

Previous radiogenic isotope studies indicate that M, and W/O have distinct Nd isotopic compositions, but overlap in Pb and Sr isotope space. In general, M is more radiogenic in Pb and Nd, but less in Sr than W/O. New Hf isotope ranges are similar, but the M are more radiogenic on average. εHf ranges from -13.1 to -15.9 for M and from -13.5 to -17.1 for W/O. In the εNd-εHf diagram the M fall about the mantle array with ΔεHf varying from -4.0 to +1.1. In contrast, W/O plots above the mantle array, at more negative εNd, with ΔεHf varying from -0.8 to +5.7. The isotopic character of the M and W/O require discrete mantle sources.

Outstanding questions are: (1) what caused the sources to melt; and (2) are the sources located in the SCLM or in the asthenosphere? A possible solution involves delamination of dense eclogitized SCLM. Delamination and sinking of the heterogeneous SCLM could cause asthenosphere to rise, melt, and heat and interact with the lithosphere. Sinking delaminated SCML may devolatilize, contributing to further melting of the asthenosphere, and/or sinking material. In this model, the M forms first, followed by the W/O. The positive ΔεHf of the W/O suggests that its mantle source was previously depleted and contained residual garnet and/or was recently metasomatized by carbonate-rich fluid. This could have taken place a few million years prior to the formation of the lavas, perhaps during the eruption of the M lavas.

### References

- Elkins-Tanton, L.T. (2007) *J Geophys Res* **112**, 13p.  
Bizimis, M. *et al.* (2003) *Contrib Mineral Petrol* **145**, 281-300  
Lange, R.A. *et al.* (2000) *Earth Planet Sci Lett* **174**, 329-40.  
Mirnejad, H. and K. Bell (2006) *J Petrol* **47**, 2463-2489.  
Vollmer *et al.* (1984) *Contrib Mineral Petrol* **87**, 359-368.

## Geochemistry of post-shield lavas from paired Loa- and Kea-trend Hawaiian volcanoes

DIANE HANANO<sup>1</sup>, DOMINIQUE WEIS<sup>1</sup>, SARAH ACIEGO<sup>2</sup>,  
JAMES S. SCOATES<sup>1</sup> AND DONALD J. DEPAOLO<sup>2</sup>

<sup>1</sup>PCIGR, Dept. of Earth and Ocean Sciences, Univ. of British  
Columbia, 6339 Stores Road, Vancouver, BC, V6T 1Z4,  
Canada (dhanano@eos.ubc.ca)

<sup>2</sup>Center for Isotope Geochemistry, Earth and Planetary  
Science, Univ. of California, Berkeley, CA, 94720, USA

Late-stage lavas formed by small degrees of melting can be used as high-resolution tracers of source components and heterogeneities in the Hawaiian mantle plume. This study presents high-precision isotopic ratios (Sr, Nd, Hf, Pb) and trace element concentrations of late- and post-shield lavas from four Hawaiian volcanoes: Mauna Kea and Kohala on the Kea-trend and their counterparts Hualalai and Mahukona on the Loa-trend.

Mauna Kea and Hualalai demonstrate a systematic shift to distinctly less radiogenic Pb and Sr isotopic compositions as they evolve from the shield to post-shield stage. Post-shield lavas from both volcanoes deviate from the mixing trends (Sr-Pb, Nd-Pb, Hf-Pb) defined by Hawaiian shield-stage lavas, reflecting involvement of a more depleted source component similar to that sampled by rejuvenated lavas from other Hawaiian volcanoes. Interaction with oceanic crust and lithosphere (low <sup>87</sup>Sr/<sup>86</sup>Sr, high <sup>206</sup>Pb/<sup>204</sup>Pb) beneath Hawaii cannot explain the observed compositions of Hualalai post-shield lavas, which have some of the least radiogenic Pb isotopic compositions (<sup>206</sup>Pb/<sup>204</sup>Pb = 17.888-18.011) of recent Hawaiian volcanoes. In contrast, Kohala and Mahukona become more radiogenic with respect to Pb during the waning stages of volcanism. Post-shield lavas from these volcanoes remain within the Loa-Kea mixing hyperbola, but are shifted to more depleted Sr, Nd, and Hf isotopic compositions.

Despite their contrasting Pb isotope systematics, post-shield lavas from all four volcanoes preserve the striking Loa-Kea Pb bilateral asymmetry inferred for the Hawaiian plume over the past ~1.5 Myr [1]. However, post-shield lavas and tholeiites from Kohala form a Pb-Pb linear array that crosses the Loa-Kea isotopic division. The sampling of Loa-type heterogeneities has been observed at other Kea-trend volcanoes [e.g. 2] and may be related to structure within the plume conduit. The coupled isotopic systematics of both volcanic pairs indicates the successive sampling of isotopically distinct material intrinsic to the Hawaiian plume. The enriched trace element signatures of the post-shield lavas ((La/Yb)<sub>N</sub> = 6.0-16.3) further suggests that this material is not related to MORB. The isotopic similarities between the post-shield and rejuvenated lavas imply continuity of these heterogeneities on a million year timescale and have implications for models of Hawaiian plume structure.

### References

- [1] Abouchami *et al.*, (2005), *Nature* **434**, 851-856.  
[2] Marske *et al.*, (2007), *EPSL*, in press.

## Time scales of intracratonic orogeny

MARTIN HAND

Continental Evolution Research Group, School of Earth and Environmental Sciences University of Adelaide, SA, Australia

Intracratonic orogeny represents an intriguing endmember of the tectonic spectrum in that deformation is temporarily focused into regions of lithosphere that more generally exhibit plate-like behaviour. There is a general consensus that intracratonic orogeny is driven by stresses generated at plate boundaries. If this assertion is true, there should be a strong correspondence between the evolution of plate margin systems and events within mechanically coupled continental interiors.

The intracratonic Petermann and Alice Springs orogens in central Australia form components of a shifting pattern of intraplate deformation whose duration spans the early stages of Gondwanan assembly (c. 600 Ma) to the establishment of a (c. 450-300 Ma) convergent margin along east Gondwana. These orogens have two important similarities. Firstly is the development of comparatively narrow deep foreland basins, which may be coupled with large-scale footwall depression beneath crustal-scale thrust sheets. These observations point to the involvement of weak lithosphere in the intraplate orogenesis. Secondly both record apparently long (> 70 Ma) durations of deformation. The 450-300 Ma Alice Springs Orogeny terminated rifting and associated basaltic magmatism, providing an obvious thermal link for localizing the deformation. However an intriguing aspect of the Alice Springs Orogeny is the existence of a long-lived high-T thermal regime marked by the emplacement of crustally derived melts throughout the entire c. 100 Ma orogenic history. Simple calculations suggest that it would be difficult for the lower crust to remain above the solidus for c.100 Ma without significant inputs of heat from the mantle.

The Alice Springs Orogeny coincided with the development of a long-lived convergent margin along eastern Gondwana. The development of the margin was characterised by upper plate extension punctuated by transient collision/accretion linked to the incorporation of buoyant colliders. A challenge in understanding the geodynamic evolution of the continental margin-interior system is to decipher event timing within the overall long-lived record of intracratonic deformation in comparison with events on the margin. Within the Alice Springs Orogen, phases of contractional deformation generally coincide with collisional events on the adjacent margin with the locus of most intense deformation coinciding with the footprint of pre-orogenic rifting and mantle-derived magmatism. This suggests that the mantle-driven thermal regime initially associated with rifting, played a central and on-going role in controlling the intracratonic response during the development of the adjacent east Gondwana plate margin.

## Processes and timescales of magma genesis and differentiation at Lopevi Volcano, Vanuatu, SW Pacific

H.K. HANDLEY<sup>1</sup>, S.P. TURNER<sup>1</sup>, S.J. CRONIN<sup>2</sup> AND I.E. M. SMITH<sup>3</sup>

<sup>1</sup>GEMOC, Dept. of Earth and Planetary Sciences, Macquarie University, Sydney, NSW 2109, Australia  
(hhandley@els.mq.edu.au; sturner@els.mq.edu.au).

<sup>2</sup>Institute of Natural Resources, Massey University, Private Bag 11 222, Palmerston North, New Zealand  
(s.j.cronin@massey.ac.nz).

<sup>3</sup>Department of Geology, University of Auckland, Private Bag 92019, Auckland, New Zealand  
(ie.smith@auckland.ac.nz).

Recently erupted basaltic and andesitic lavas of Lopevi Volcano, one of the most active in Vanuatu, were analysed for whole rock major and trace element abundances, Sr and Nd isotopic ratios and U, Th and Ra isotopic compositions; forming the first detailed U-series study of an individual volcanic centre within the Vanuatu (New Hebrides) arc. The data are used to constrain the processes and timescales of magma genesis and evolution beneath the volcano, leading towards a better understanding of the relationship between magma supply and eruption, which is invaluable for volcanic hazard assessment.

MgO contents of lavas erupted throughout 2000-2003 cluster at around 4-5 wt%, whereas those from earlier eruptions (during the 1930's and 1960's) exhibit a wider range, extending to more primitive MgO contents (up to 8.5 wt%). Fractional crystallisation is an important mechanism of differentiation at Lopevi, exerting strong control on major and trace element variations. Increases in SiO<sub>2</sub>, Na<sub>2</sub>O, Al<sub>2</sub>O<sub>3</sub>, TiO<sub>2</sub> (and to a lesser extent K<sub>2</sub>O and P<sub>2</sub>O<sub>5</sub>) and decreases of CaO and Fe<sub>2</sub>O<sub>3</sub> with decreasing MgO are consistent with the removal of a mineral assemblage dominated by olivine and pyroxene. Unlike volcanic rock suites of many other arc volcanoes, Dy/Yb ratios at Lopevi do not systematically decrease with increasing SiO<sub>2</sub>, demonstrating that amphibole cannot be an important fractionating mineral during magmatic differentiation at mid-lower crustal depths beneath the volcano.

Enrichment of LREE relative to HFSE and HREE, high Ba/La ratios relative to MORB, uniform HFSE/HFSE ratios (e.g. Ta/Nb) along with <sup>238</sup>U excesses (1.250-1.400) in Lopevi lavas identify the contribution of a fluid component to a relatively homogeneous, slightly depleted mantle source. Furthermore, the sub horizontal array displayed by the data on a U-Th equiline diagram indicates this addition occurred significantly recently. <sup>226</sup>Ra excesses in the lavas suggest that crustal residence times of magmas at Lopevi are <8000 years. <sup>87</sup>Sr/<sup>86</sup>Sr ratios lie between 0.703992 and 0.704078 and are characteristic of volcanoes similarly located in the central Vanuatu arc, above where the D'Entrecasteaux Ridge is being subducted and accreted (cf. northern and southern sections of the Vanuatu arc).

## Functionally diverse chemosynthetic bacteria in hydrothermal sediment, Santorini, Greece: Geochemical implications

K.M. HANDLEY<sup>1</sup>, C. BOOTHMAN<sup>1</sup>, R.A. MILLS<sup>2</sup> AND J.R. LLOYD<sup>1</sup>

<sup>1</sup>School of Earth, Atmospheric and Environmental Sciences, The University of Manchester, Manchester M13 9PL, UK (kim.handley@postgrad.manchester.ac.uk; christopher.boothman@manchester.ac.uk; jon.lloyd@manchester.ac.uk)

<sup>2</sup>School of Ocean and Earth Science, National Oceanography Centre, University of Southampton, Southampton SO14 3ZH, UK (ram1@noc.soton.ac.uk)

A chemosynthetic microbial community displaying diverse respiratory processes was identified within iron- and arsenic-rich shallow marine sediment (20-40°C, pH 6.0-6.3) from an area of active hydrothermalism in Santorini, Greece. Marine hydrothermal sediments are host to abundant microbial life that exploits the steep geochemical gradients generated by the confluence of reduced metal-rich fluids and oxidised seawater. However, there is relatively little information on the functional range of prokaryotes in these settings, and their impact on geochemical cycling. Microbial functional diversity in the Santorini sediment was determined by enrichment culturing (from the suboxic to anoxic transition zone, Eh 0 to -138 mV), coupled with phylogenetic molecular techniques. Enrichment cultures were successfully obtained for: (1) Fe(III), NO<sub>3</sub><sup>-</sup>, SO<sub>4</sub><sup>2-</sup>, and As(V) reducers (with acetate and lactate); (2) anaerobic and microaerophilic Fe(II) oxidisers; and (3) Na<sub>2</sub>S and As(III) oxidisers. Most-probable number (MPN) counts for these functional groups ranged from 7.50 x 10<sup>7</sup> to 2.30 x 10<sup>2</sup> cells ml<sup>-1</sup>, with relative abundances decreasing as follows: NO<sub>3</sub><sup>-</sup>, As(V) and Fe(III) reducers; Na<sub>2</sub>S and FeS oxidisers; SO<sub>4</sub><sup>2-</sup> reducers; and As(III) and anaerobic Fe(II) oxidisers. 16S rRNA and specific functional gene analyses, utilising the clone library method, revealed a phylogenetically diverse range of enriched bacteria, including a number of novel organisms, and also sequences with close affinity for bacteria known to occur in deep-sea hydrothermal vent sediments (e.g. *Shewanella* sp., *Thiomicrospira* sp., *Desulfovibrio* spp., and *Marinobacter* spp.). Phylogenetic bacterial and archaeal sediment communities were dominated by δ-Proteobacteria, Chloroflexi, Bacteroidetes, Chlorobi, and Crenarchaeota. Dominant bacteria displayed closest affinities to known iron and sulphur respirers. In particular, community analyses of the oxidised orange surface sediment (Eh 0) were found to be dominated by an enriched anaerobic, nitrate-dependant Fe(II) oxidiser. Overall, results demonstrate the potential for bacteria to respire inorganic substrates important within the Santorini sediment, namely forms of iron, arsenic, sulphur and nitrogen. Moreover, solid-phase and pore water geochemical data allow correlation between the microbial community structure and the sequence of down-core biogeochemical (redox) zonation.

## Behaviour of PGEs in sills from the Jurassic Ferrar Large Igneous Province, Antarctica

R. HANEMANN AND L. VIERECK-GOETTE

Institut fuer Geowissenschaften, Universitaet Jena, Germany (ricarda.hanemann@uni-jena.de)

The Jurassic Ferrar Large Igneous Province, exposed in a > 3000 km long belt along the margin of the East Antarctic craton, comprises numerous sills, dikes and lava flows as well as the layered mafic Dufek intrusion. Uniform crust-like trace element and isotope data indicate a single magma source within the subcontinental lithospheric mantle characterised by crustal enrichment due to Palaeozoic subduction along the Panthallasia margin of Gondwana. However, the thermal source for the voluminous melt generation is still under debate as the crust-like isotope signatures obscure the detection of a possible mantle plume involvement.

In addition to mineral and bulk-rock chemical data for basaltic andesites and andesites from sills in northern Victoria-land, a subset of 23 samples has so far been analysed for platinum-group elements (PGE) to further describe the genesis of the Ferrar magmatic rocks. The abundances of Ir, Ru, Rh, Pt and Pd were determined by ICP-MS using isotope dilution (except Rh) after sample preparation by NiS-fire assay at the University of Karlsruhe, Germany.

The studied rocks exhibit the common phase assemblage of tholeiitic differentiation sequences composed of varying amounts of pyroxenes, plagioclase, oxides and mesostasis. Most of the wide compositional variations (2-13 wt% MgO) are attributed to low-pressure differentiation after magma intrusion at upper-crustal levels. Compositional differences between rocks that are not affected by in-situ differentiation are ascribed to distinct conditions during pre-emplacement differentiation assuming an identical primary magma.

The PGE totals range from ~ 4 to 40 ppb. The single element abundances exhibit good correlations with the MgO contents of the distinctly evolved samples and are thus interpreted to result mainly from in-situ differentiation as well. While the IPGE (Ir, Ru) are highly compatible during differentiation of the Ferrar magmas, the PPGE (Rh, Pt, Pd) show bimodal variations. They decrease in cumulates, but either increase or decrease in differentiates. The distinct PGE fractionation behaviour results in strongly fractionated primitive mantle-normalised patterns for all analysed samples with considerable enrichment of the PPGE over the IPGE.

Compared to tholeiitic rocks from other magmatic provinces, only the Ferrar rocks exhibit coupled enrichment of Pd, Pt and Cu even in most evolved samples. The decrease of Pt and Pd in some of the more evolved samples does not necessarily signify sulphide fractionation, but may indicate the formation of other PGE-compounds. The inferred sulphur-undersaturated conditions during pre- and post-emplacement differentiation processes are in agreement with the elevated melting degrees as well as the refractory nature of the proposed subcontinental lithospheric mantle source.

## Synthetic melt inclusion and quartz-trap methods for determining Pt solubility in a mafic mineral – Halide melt system at 750°C, 400 bar

JACOB J. HANLEY AND CHRISTOPH A. HEINRICH

IGMR, ETH Zürich, Zürich, Switzerland, CH-8092  
(hanley@erdw.ethz.ch; heinrich@erdw.ethz.ch)

The solubility of platinum in a hydrous salt melt (S-free; ~75 wt% CaCl<sub>2</sub>+MgCl<sub>2</sub>, 25 wt% H<sub>2</sub>O) was investigated at conditions consistent with the post-cumulus metamorphism of layered intrusions that host platinum-group element deposits. The salt melts were reacted with metallic Pt or Pt-PtAs<sub>2</sub> (sperrylite) in Pt capsules using conventional Rene 41 cold seal vessels which buffer *f*O<sub>2</sub> at FMQ-1. The activities of relevant metal-complexing species (e.g., HCl<sup>0</sup>) were buffered by the assemblage tremolite-diopside-enstatite-quartz. Salt melts were trapped (simultaneously) in the matrix of a quartz trap (granulated natural quartz partially isolated in a smaller gold capsule) and in synthetic melt inclusions trapped in pre-fractured quartz. After quenching, the melt inclusions and quartz trap material were analyzed by laser ablation ICP-MS.

Platinum solubility is in the low ppm range. Analysis of different portions of the quartz traps using a 90 µm pit size yielded relatively consistent platinum concentrations of 14.4 ± 6.7 ppm (2σ, n=6; Pt metal source), and 4.6 ppm ± 1.9 ppm (2σ, n=6; Pt-PtAs<sub>2</sub>). Based on the consistency of the metal concentrations from different parts of the trap, it is considered that these concentrations are most representative of metal solubility at run conditions and that the laser sampling size sufficiently overcomes local heterogeneity in the distribution of Pt quench products. By contrast, Pt concentrations in hydrosaline melt inclusions from different areas of a 3 mm x 10 mm quartz cylinder range from below detection limits (~0.1 ppm) to 14.4 ppm (n=28; Pt) and to 6.6 ppm (n=31; Pt-PtAs<sub>2</sub>). The range in observed metal concentrations in this trapping medium increases with the number of inclusions analyzed, and varies between different areas in the quartz cylinder. This confirms observations that saline inclusions trapped in pre-fractured quartz heal quickly (as early as several hours) at elevated temperatures, and may trap disequilibrium metal concentrations in mineral- or melt-buffered systems (Hanley *et al.*, 2005); thus, they are suitable only for qualitative evaluation of trace metal solubility.

The data demonstrates that Pt is highly soluble at conditions consistent with post-cumulus metamorphic activity in layered intrusions, and that salt melts may significantly modify primary metal concentrations in layered intrusions and redistribute these metals. Additionally, Pt solubility in the hydrosaline melt was reduced by a factor of ~ 3 in the presence of a platinum arsenide phase.

### References

Hanley, J. J., Pettke, T., Mungall, J.E., and Spooner, E.T.C. (2005), *Geochim. Cosmochim. Acta* **69** 2593-2611.

## ~560 Ma and ~300 Ma Re-Os ages constrain Neoproterozoic glaciation and record Variscan hydrocarbon migration on extension of Oslo rift

J.L. HANNAH<sup>1,2</sup>, G. YANG<sup>1</sup>, B. BINGEN<sup>2</sup>, H.J. STEIN<sup>1,2</sup>, AND A. ZIMMERMAN<sup>1</sup>

<sup>1</sup>AIRIE Program, Geosciences Dept., Colorado State Univ., Fort Collins, CO 80523-1482 (jhannah@cnr.colostate.edu)

<sup>2</sup>Geological Survey of Norway, 7491 Trondheim, Norway

The Moelv tillite, exposed in the Lower Allochthon of the Scandinavian Caledonides represents the Neoproterozoic Varanger glaciation, which is generally correlated with the ~580 Ma Gaskiers glaciation in Laurentia. To refine a 620 ± 14 Ma maximum age for the Moelv tillite based on detrital zircons [1], Re-Os data were collected from a C-rich shale horizon in the Biri Formation underlying the tillite.

East of the town of Biri, the weakly deformed Biri shale contains a significant silt component, minor but ubiquitous fine-grained pyrite, and an average TOC of 0.7%. Exposures in a steep bedrock stream channel (Djupdalsbekken) show little bleaching or oxidation. Here, where the Biri shale is separated from the Moelv tillite by the Ring conglomerate, two localities were sampled. Seven analyses of four samples taken about 50 m below the Biri-Ring contact yield a statistically tight Re-Os age of ~560 Ma, with an initial <sup>187</sup>Os/<sup>188</sup>Os (Os<sub>i</sub>) near 1. Four additional samples, taken ~48 m below the contact, scatter slightly, but all samples regressed together still yield an age within uncertainty of 560 Ma. Re-Os data from samples taken ~3 m below the Biri-Ring contact scatter about a reference line of 600 Ma with Os<sub>i</sub> = 1.0. Scatter may result from minor Re and lesser Os loss during recent oxidative weathering. Thus, there is some true geologic variation in the data, but the results clearly support an age close to that of the ~580 Ma Gaskiers glaciation.

A second Biri locality near Øvre Rendal lies on the northern extension of the ~300 Ma Oslo rift. Here, the shale shows strong cleavage, has an average TOC of 2.7%, contains lenses of pyritic sandstone, is unusually thick, and directly underlies the Moelv tillite. Road-cut exposures are locally rusty, but fresh, black samples were obtainable. Ten analyses from six samples taken in a 1-m stratigraphic interval scatter about a reference line of 300 Ma with Os<sub>i</sub> = 1.1. Greenschist-facies, dynamic metamorphism does not disturb the Re-Os system in shales [2,3]. We therefore propose that heat from the ~300 Ma rifting event induced hydrocarbon maturation and migration, and that the organic material analyzed was isotopically homogenized (or introduced) during this event.

### References

- [1] Bingen, B., Griffin, W.L., Torsvik, T.H., and Saeed, A. (2005) *Terra Nova* **17**, 250-258.
- [2] Kendall, B.S., Creaser, R.A., Ross, G.M., and Selby, D. (2004) *Earth Planet Sci Lett* **222**, 729-740.
- [3] Hannah, J.L., *et al* (2006) *Geochim Cosmochim Acta* **70**, no. 18S, A228.



## Colloidal green rust behaviour: Adhesion, transformation and mobility

E. B. HANSSON AND S. L. S. STIPP

NanoGeoScience, Department of Chemistry, University of Copenhagen, Universitetsparken 5, 2100 Copenhagen Ø, Denmark (ehansson@geol.ku.dk; stipp@geol.ku.dk)

One of the more poorly understood processes in nature is the transport mechanisms of solutes and particles. In order to predict the behavior of unwanted compounds in nature, we need to establish these processes. Colloidal transport is believed to be one of the major pathways for distributing contaminants. These contaminants might come from general pollution or from leaking radioactive waste repositories. One very interesting compound that forms colloids and which is believed to exist in such environments is green rust.

Green rust is a layered double hydroxide (LDH) of high reactivity. It consists of ordered layers of Fe(II) and Fe(III), alternating with hydroxide layers and intercalating anions, cations (see poster by Christensen *et al.*) and water. It can form from partial oxidation of ferrous iron in the groundwater or directly from corrosion of metallic iron, which we use in reactive barriers and for reinforcement of underground radioactive waste repositories. Green rust reacts readily with redox sensitive contaminants due to the Fe in the layered structure and allows for a high degree of adsorption due to a large external and internal surface area.

Immobilisation of contaminants in or on a solid is desirable, but if the solid is transported as a colloid, the contaminant is mobilised anyway. Therefore, we investigated the attachment ability of green rust using atomic force microscopy (AFM). To survey general colloid behaviour, we examined adhesion on 11 substrates chosen to represent common natural solids. Green rust colloids adhered well to all these substrates regardless of their surface charge.

The mobility of the particles formed from aerial oxidation of green rust was also examined. Upon oxidation, the green rust crystals showed dissolution along the edges. On hydrophilic substrates, elongated goethite crystals typically formed on and near original green rust particles. The stickiness of green rust suggests that it also serves as a substrate for other colloids which might have contaminants adsorbed.

From our experiments we interpret that the presence of green rust will generally limit contaminant transport in the groundwater system.

## Mantle magma chambers beneath Gran Canaria

T.H. HANSTEEN

IFM-GEOMAR, Kiel, Germany (thansteen@ifm-geomar.de)

A suite of basanite-hosted mantle xenoliths from the Quaternary Bandama volcanic center, Gran Canaria, comprises spinel harzburgites, spinel dunites and wehrlites, where Mg# of olivine range from 81 to 91, and clinopyroxenes encompass both igneous (Ti-augite to aegirine-augite) and upper mantle (Cr-diopside) types. They contain abundant silicate melt and CO<sub>2</sub>-dominated fluid inclusions. Clinopyroxene rim-melt thermobarometry of the host basanites indicates significant crystallization at pressures between 0.9 and 1.2 GPa. Barometry of primary magmatic CO<sub>2</sub>-inclusions in basanite olivines similarly yields minimum formation pressures between 0.7 and 1.0 GPa indicating cotectic olivine-clinopyroxene-Ti-magnetite crystallization at such pressures.

In the xenoliths, texturally late fluid inclusions coexist with melt inclusions thus indicating higher formation temperatures than the early fluid inclusions, which do not coexist with melt inclusions. The observed density differences of fluid inclusions is interpreted as *in situ* isobaric heating of the xenoliths in the upper mantle at 0.75 ± 0.1 GPa (26 ± 3 km depth), from about 750°C to near host-magma temperatures. This depth coincides with a change in the upper mantle P-wave velocity structure from anomalously low velocities of 7.5 - 7.8 kms<sup>-1</sup> between the Moho and 26 km depth, to normal values of 8.3 kms<sup>-1</sup> below [1]. This low-velocity zone is interpreted as a clinopyroxene-enriched underplating zone in upper mantle, i.e. a region containing a complex mixture of harzburgite, wehrlite, and partly crystallized melt pockets. The xenoliths represent fragments of wall-rocks from a magma chamber within this region. A genetic link between magma chamber formation in the uppermost mantle, metasomatic overprinting and magmatic underplating is proposed for Gran Canaria, where a localized underplating zone has developed possibly from the late Pliocene to the Holocene through repeated metasomatic interaction between mantle rocks and ascending magmas.

### References

- [1] Ye *et al.* (1999) *J Geodyn* **28**: 3-26

## **Metasomatically induced alteration and re-equilibration of orthophosphate and silicate minerals: Textures, fluids, and mass transfer**

DANIEL E. HARLOV

GeoForschungsZentrum Potsdam, Telegrafenberg, D-14473  
Potsdam, Germany (dharlov@gfz-potsdam.de)

In nature, total re-equilibration of minerals and mineral assemblages under prevailing P-T-X conditions is greatly enhanced when suitably reactive fluids are involved. Oft times, however, re-equilibration is only partial and limited to those areas of the grain in immediate contact with the fluid. This can be due to a variety of factors including limited amounts of fluid, a limited reactivity between the fluid and the mineral and/or sufficiently low P-T conditions thus guaranteeing very low reaction rates. In general re-equilibration, whether localised or total, occurs as a result of dissolution-precipitation processes, which can also allow for the nucleation and growth of mineral inclusions of one phase within minerals of another phase.

Here a series of different orthophosphate and silicate mineral textures with or without mineral inclusions will be described and interpreted. Each of these textures is the direct result of fluid-induced dissolution-precipitation processes and represents the re-equilibration of the orthophosphate mineral on a localised scale. Such re-equilibration textures can have profound implications with regard to dating metasomatic events as well as allowing for P-T-X conditions to be estimated.

From a broader perspective, these fluids have not only interacted with the orthophosphate and silicate minerals but also potentially with the rock as a whole. As a consequence, the documentation and interpretation of metasomatically induced alteration in orthophosphate and silicate minerals has broader implications with respect to obtaining deeper insights into the nature and role of fluids in the crust and upper mantle.

## **LIBS: A new paradigm for real-time and in-field geochemical analysis**

R.S. HARMON<sup>1</sup>, F.C. DELUCIA<sup>2</sup>, N.J. MCMILLAN<sup>3</sup>,  
A.W. MIZIOLEK<sup>2</sup> AND A. WHITEHOUSE<sup>4</sup>

<sup>1</sup>Army Research Office, Research Triangle Park, NC

<sup>2</sup>Army Research Laboratory, Aberdeen Proving Ground, MD

<sup>3</sup>New Mexico State Univ., Las Cruces, NM

<sup>4</sup>Applied Photonics Ltd, Skipton, UK

Laser Induced Breakdown Spectroscopy (LIBS) is a simple atomic emission spectroscopy technique capable of essentially non-destructive determination of the elemental composition of any substance in real time. In LIBS, a focused and pulsed laser beam is directed at a sample surface, where laser energy absorption and resulting material ablation produces a high-temperature microplasma at the sample surface. Small amounts (nanograms) of material are dissociated and ionized, with both continuum and atomic/ionic emission generated by the plasma during cooling. A broadband spectrometer equipped with a CCD array detector can be used to spectrally and temporally resolve the light from the plasma to record emission lines of the full suite of elements present in the sample.

Important attributes of a LIBS sensor system for geochemical analysis include (i) real-time response, (ii) in-situ analysis with no sample preparation required, (iii) a high sensitivity to low atomic weight elements which are often difficult to determine by other techniques, and (iv) standoff detection. LIBS technology is now sufficiently mature, inherently rugged, and affordable to offer a capability for both laboratory and field-deployable analysis. Successful laboratory benchtop and 30-m standoff feasibility studies have been conducted that highlight the potential of LIBS for variety of geochemical, mineralogical, and environmental applications that require either real-time or in-field chemical analysis.

## Magmatic processes recorded by garnets from the AD 79 eruption of Vesuvius

D. HARRIES, A. HEUMANN, K. SIMON AND A. KRONZ

Geowissenschaftliche Zentrum Göttingen, Abt. Geochemie,  
Georg-August-Universität Göttingen, Germany  
(dennis.harries@stud.uni-goettingen.de)

### Introduction

Evolved K-phonolitic tephra of Mt. Somma-Vesuvius volcano (Campania, Italy) contains Ti-rich garnets of the andradite-grossular solid solution series ('melanite') which are interpreted to be of magmatic origin in the Mercato (~8.1 ka) and Avellino (~3.7 ka) eruptive products (Scheibner *et al.*, 2007).

Here we present data on REE distribution patterns obtained by laser ablation ICP-MS profiles in garnets of similar composition from tephra of the AD 79 eruption of Vesuvius in order to potentially distinguish metasomatic and magmatic garnets. The studied garnets have melanitic compositions and show core/rim structures with higher Fe<sup>3+</sup>/Al ratios in the rims and resorption features at the interfaces.

### Samples and Analytical Methods

Garnet phenocrysts (~0.3-0.8 mm) were separated from crushed pumice samples taken from the basis of the chemically most evolved white tephra and from basis and top of the less evolved grey tephra at Pompeii ('Necropolis', Cioni *et al.*, 1995).

Continuous profiles through sectioned garnet crystals were obtained by ICP-MS coupled to a 193 nm ArF excimer laser. Profile width/spot size was 30 µm and resulting profile depth was ~60 µm. Detection limits ranged between 1 to 7 ppm for REE. Major element quantification was accomplished by wavelength dispersive EPMA.

### Results and Discussion

LREE concentrations peak at Nd and show almost no variations through cores and rims, in contrast HREE are strongly depleted in the cores by a factor of up to 30 (2 to 10 for individual crystals) relative to the rims. Very high partition coefficients for HREE in melanitic garnets (Scheibner *et al.*, 2007) suggest crystallisation of the cores from a highly fractionated magma unlike any of the eruption products of AD 79. These findings imply a significant contribution of a residual, highly evolved magma from previous eruptive cycles to the reservoir of the AD 79 eruption as previously outlined by other works (e.g. Cioni *et al.*, 1995).

### References

Cioni R., Civetta L., Marianelli P., Metrich N., Santacroce R. and Sbrana A. (1995), *J. Petrol.* **36**, 739-776.  
Scheibner B., Wörner G., Civetta L., Stosch H.-G., Simon K. and Kronz A. (2007), *Contrib. Mineral. Petrol.* **in press**, DOI: 10.1007/s00410-006-0179-z.

## Using Pb isotopic analyses of fluid and melt inclusions to trace sources of Cu-Au porphyry deposits

C.R. HARRIS<sup>1</sup>, T. PETTKE<sup>2</sup>, C.A. HEINRICH<sup>1</sup> AND T. KLEINE<sup>1</sup>

<sup>1</sup>IGMR, ETH Zurich, Clausiusstrasse 25, 8092 Zurich, Switzerland (harris@erdw.ethz.ch; heinrich@erdw.ethz.ch; kleine@erdw.ethz.ch)

<sup>2</sup>Institute of Geological Sciences, 3012 Bern, Switzerland (pettke@geo.unibe.ch)

We have analyzed Pb isotopic ratios of natural fluid and melt inclusions by LA-MC-ICPMS and demonstrate the ability to use Pb ratios normalized to both <sup>204</sup>Pb and <sup>206</sup>Pb in tracing ore mineralization. The case study follows extensive feasibility tests (Pettke *et al.*, in prep) using synthetic Pb fluid inclusions, in which we attained within run precisions (± 2SE) of as good as 200 ppm (normalized to <sup>206</sup>Pb) and 400 ppm (normalized to <sup>204</sup>Pb) and shot to shot reproducibilities (± 2SD) of 800 ppm and 7000 ppm, respectively.

Fluid inclusions in this study are from quartz veins in two different Cu-Au porphyry systems in the Apuseni Mountains, Romania. The Apuseni Mountains represent the richest concentration of metal deposits in Europe, and have been mined since pre-Roman times. Mineralization is hosted by sub-volcanic Miocene magmas intruded in a transtensional geodynamic environment. The magmatic rocks are mostly andesitic in composition, several of which contain high Sr and Pb concentrations, LILE enrichment and MORB-like Sr and Nd isotopic compositions characteristic of adakite-like magmas. Stocks hosting the porphyry deposits have adakite-like chemical signatures. Whole rock major, trace, and Pb-Sr-Nd isotopic analyses on the magmatic rocks represent the maximum range in age and composition, including endmembers of hybrid magmas recognized in the field from mingling textures. Pb isotopic ratios of whole rock solutions were measured with MC-ICPMS using Tl normalization. Fluid inclusions were measured by LA-MC-ICPMS while admixing desolvated 997-Tl standard solution. In high temperature stockwork veins, fluid inclusion ratios are indistinguishable from high temperature sulfides but less radiogenic than galena from the same deposit. Pb ratios of fluids and sulfides overlap ratios from the magmatic host rocks. Feldspar cores and several melt inclusions hosted in the feldspar cores, however, exhibit Pb isotopes more radiogenic than the magmatic rocks and fluids, consistent with observed inverse feldspar zoning. Results will be explored in consideration of the idea that ore deposition is linked to a pulse of more primitive magma into the system (e.g., Kamenov *et al.*, 2005).

### References

Kamenov, G., Perfít, M., Jonasson, I., and Mueller, P., 2005, *Chemical Geology*, v. 219, p. 131-148.  
Pettke, T., Audetat, A., Oberli, F., Wiechert, U., Harris, C. R., and Heinrich, C.A., in preparation.

## Evidence for water on Hadean Earth

T.M. HARRISON

Dept. of Earth and Space Sciences & IGPP, UCLA, Los Angeles, CA 90095 U.S.A. (tmh@oro.ess.ucla.edu)

The criteria thought necessary for life are: an energy source, organic molecules, and liquid water. Since the necessary energy sources and molecular building blocks for life were surely available during the formative stages of planetary evolution, the question of when life could first have emerged on Earth reduces to: When did liquid water first appear at the Earth's surface? While exposure of >3.83 Ga marine sediments indicates the presence of oceans by that time, strategies to assess an earlier hydrosphere are limited by the fact that there is no known Hadean (4.5-4.0 Ga) rock record. However, detrital zircons as old as nearly 4.4 Ga from the Jack Hills, Western Australia, present four kinds of evidence that suggest the presence of liquid water at or near the Earth's surface during the Hadean. Oxygen isotopes analyses of zircon provides a means to assess the isotopic composition of the protolith. High  $\delta^{18}\text{O}$  values of some Hadean zircons, indicative of a clay-rich protolith, are interpreted as indicating crust-hydrosphere interactions prior to 4 Ga. Inclusion assemblages in Hadean zircons characteristic of hydrated, peraluminous parent magmas are suggestive of the melt protolith having originated at the Earth's surface and further suggest early development of sedimentary cycling in the presence of a hydrosphere. While specific circumstances could be convolved to create a high  $\delta^{18}\text{O}$  signal along with peraluminous inclusions outside a surficial environment, they represent exceptional occurrences. Crystallization temperatures of >4 Ga granitoid zircons cluster strongly at  $680\pm 25^\circ\text{C}$  from which we infer a regulated mechanism producing wet, minimum-melting conditions throughout the Hadean. This distribution is indisputably different from that produced by cooling of mafic and intermediate magmas and we conclude that the vast majority of Hadean zircons could not plausibly be derived from such sources. Instead, the simplest explanation for the dominant low temperature Hadean peak is that it reflects prograde melting under shallow conditions at or near water saturation. In effect, as soon as the source reached anatexis conditions, the majority of melt fertility was lost in the presence of excess water. Comparisons of U-Pb and U-Xe ages in Hadean zircons show varying degrees of Xe loss, but in some cases are concordant within uncertainty. Variable plutonium/uranium ratios in these zircons suggest that Pu and U could be mobile with respect to each other during the Hadean. As Pu and U can be strongly fractionated in aqueous systems, this may indicate, at least locally, the presence oxidized aqueous fluids in the Hadean crust. Although circumstantial, the four lines of evidence discussed above provide a cogent case for the presence of liquid water at or near the Earth's surface during much of the Hadean.

## Rutile $^{207}\text{Pb}$ - $^{206}\text{Pb}$ ages in the Jack Hills quartzite, Western Australia

T.M. HARRISON<sup>1</sup>, D. TRAIL<sup>2</sup>, A.K. SCHMITT<sup>1</sup> AND E.B. WATSON<sup>2</sup>

<sup>1</sup>Dept. of Earth & Space Sci. & IGPP, UCLA, Los Angeles, CA 90095 USA

<sup>2</sup>Dept. of Earth & Environmental Sci., Rensselaer Polytechnic Institute, Troy, NY 12180, USA

The Narryer Gneiss Complex of Western Australia is comprised of 3.73–3.30 Ga orthogneisses and ~3 Ga supracrustal rocks that experienced regional metamorphism and local granite emplacement at ~2.5 Ga. In the western Jack Hills, upper greenschist grade quartzites contain detrital zircons approaching 4.4 Ga and thus efforts have been made to date other detrital phases (e.g., monazite, chromite) but as yet the age distribution of rutile has not been assessed. The significance of discovering >4 Ga rutile grains is heightened by possible application of the recently calibrated Zr-in-rutile thermometer which permits a test the Hadean minimum-melting hypothesis of Watson & Harrison (2005). However, the lower bound of estimates of  $T_c$  for Pb in rutile, which range from 400-600°C, overlaps with the estimated peak metamorphic temperature in which case the potential for rutile to retain its primary crystallization age would be greatly reduced.

388  $^{207}\text{Pb}/^{206}\text{Pb}$  SIMS multi-collector analyses of 369 rutile grains from Jack Hills quartzite sample JH0113 yield a distinct age peak at ca. 2.5 Ga and an average age of  $2.3\pm 0.2$  Ga. Age uncertainty for a 1 min analysis is typically  $\pm 2\%$ . A traverse across one large grain revealed significant  $^{207}\text{Pb}/^{206}\text{Pb}$  age variability. 33 of the dated grains were also analyzed for Zr by EMPA, counting with four spectrometers simultaneously. [Zr] was converted into crystallization temperature using the Watson *et al.* (2006) thermometer yielding a broadly normal distribution at  $665\pm 18^\circ\text{C}$ . The highest recorded temperature ( $718^\circ\text{C}$ ) was obtained near the rim of a ~200  $\mu\text{m}$  rutile grain with the core of the grain closer to the average value.

Given that crystallization temperatures are substantially higher than that attained during greenschist metamorphism, one interpretation is that the Zr-in-rutile thermometer has not been reset but that essentially complete Pb isotope exchange occurred at ca. 2.5 Ga. Alternatively, the very high Ti contents in cracks in detrital zircons from the Jack Hills suggests high Ti mobility during regional metamorphism due to dissolution/precipitation of Ti-bearing detrital grains. Evidence supporting this view comes from 2.5 Ga EMPA chemical Pb ages of monazites included in rutile which further suggest fluid-mediated dissolution/precipitation reactions at that time. This would explain the substantial disturbance to the <sup>142,143</sup>Nd systems in Hadean zircons (Caro *et al.*, 2006) if monazite inclusions are the principal host of LREE's. This interpretation, however, does not explain the level and uniformity of the Zr-in-rutile temperatures and could suggest non-equilibrium Zr abundances in rutile.

## Intra-test variation in the trace element composition of planktonic foraminifera: Implications for biomineralization processes

ED C. HATHORNE<sup>1\*</sup>, RACHAEL H. JAMES<sup>2</sup> AND RICHARD LAMPITT<sup>3</sup>

<sup>1</sup>DFG-Research Center Ocean Margins (RCOM), University of Bremen, Bremen, Germany (ehathorne@marum.de)  
\*previously at<sup>2</sup>

<sup>2</sup>Department of Earth Sciences, The Open University, Milton Keynes, U.K. (R.H.James@open.ac.uk)

<sup>3</sup>National Oceanography Centre, Southampton, U.K. (R.Lampitt@noc.soton.ac.uk)

The trace element chemistry of the calcite shells (tests) of planktonic foraminifera is a prime source of palaeoenvironmental information. Trace element partition coefficients are usually determined empirically, yet it is clear that calcification is biologically controlled. Better interpretation of the chemistry of foraminiferal calcite thus requires an understanding of the fundamental processes of mineralization and their influence on the resulting mineral chemistry.

To this end we have analysed the intra-test variation of a number of trace elements in the planktonic foraminifera species *Gr. inflata*, *Gr. scitula* and *O. universa*. Samples were recovered from a deep sediment trap (3km water depth) in the N. Atlantic (48.6N, 16.3W). The chemical and physical characteristics of the water column at this site are monitored, so the conditions under which calcification took place can be assessed. Measurements were made by laser ablation (LA) inductively-coupled plasma mass spectrometry (ICP-MS). A 193nm ArF Excimer laser was used to ablate through the test walls and time resolved signals from the quadrupole ICP-MS provide depth profiles of trace elements. Internal standardisation was performed using Ca and signals were calibrated using a calcite powder pellet and NIST 612 glass.

All three species display a 100- 200% increase in Mg/Ca through the test wall which is far greater than expected as a result of vertical migration of the foraminifera and associated changes in water temperature. Other light trace elements (Li/Ca and B/Ca) show similar behaviour, but Sr/Ca ratios show no variation greater than the analytical uncertainty (~10% RSD). The change in Mg/Ca, Li/Ca and B/Ca through the test wall is most likely due to biomineralization processes. The implications of these data for foraminifera calcification models will be discussed.

## Hydrogeochemical Properties of Ladik Hot Water Spring (Samsun, Turkey)

E. HATIPOĞLU, F. GÜLTEKİN AND A. FIRAT ERSOY

Karadeniz Technical University, Department of Geological Engineering, 61080, Trabzon Turkey  
(esrahatipoglu@ktu.edu.tr)

In this investigation Ladik (Samsun) hot water spring has been studied from the point of geology, hydrogeochemistry and discharge. The study area is located around middle-north of Turkey. The geology of the study area and its vicinity consist of Permian aged recrystallized limestone, Jurassic-Cretaceous limestone, Eocene- Neogene aged sandstone and claystone and Quaternary aged alluvium. The North Anatolian Fault (NAF) is situated near the hot water spring. Ladik hot water is come out to the surface where cross cut the NS and NW-SE directed fault, which is parallel to the NAF. Spring has 18 l/s discharge rate and 36.7 °C temperature. Hot water is analysed by Hacettepe University, Hydrogeochemistry Laboratory. According to the analyse results total dissolved ion matter for Ladik spring 339 mg/l, Hamamayağı River 192 mg/l and Kocapınar cold water spring 378 mg/l are obtained. The hot spring are classified according to the following criterias:

- according to the structural properties "fault spring"
- according to the temperature "medium hot water"
- according to the geothermal energy "low enthalpy geothermal system"

-according to the hot water analyse result cation and anion trend of the springs are;

for Ladik hot water spring, Kocapınar cold water spring and Hamamayağı River

$$rCa^{+2} > rMg^{+2} > rNa^{+} > rK^{+} \text{ and } rHCO_3^{-} > rSO_4^{-2} > rCl^{-}$$

Saturation indexes of the hot and cold water springs have been calculated in PHREEQC Programme. Springs are not saturated with respect to the calcite, dolomite and aragonite. According to the Schoeller and Piper Diagrame, springs and river waters have similar chemical properties but Ladik hot spring has high  $Mg^{+2}$ ,  $Na^{+}$  and  $K^{+}$  ion values. The reason of these high concentrations have been assumed that the hot water add the ions of the recrystallized limestone and limestone.

### References

- MTA, (2005) *Envanter of the Geothermal Springs of the Turkey*, Ankara (in Turkish).
- Pipper, A.M., (1944), *Trans. Amer. Geophys. Union*, **25**, pp.914-923.
- Schoeller, H., (1962), *Les Aus Souterraines*, Mason et Cie Eiturs.

## Laser ablation inductively coupled plasma mass spectrometry - The role of the ion source for quantitative analysis

BODO HATTENDORF<sup>1</sup>, ZHONGKE WANG<sup>2</sup> AND DETLEF GÜNTHER<sup>1</sup>

<sup>1</sup>ETH Zurich, Laboratory of Inorganic Chemistry, 8093 Zürich, Switzerland (bodo@inorg.chem.ethz.ch, guenther@inorg.chem.ethz.ch)

<sup>2</sup>ETH Zurich, Laboratory of Inorganic Chemistry; now at: RIKEN, Laser Technology Laboratory, Wako, Japan (z-wang@riken.jp)

### Abstract

Laser ablation inductively coupled plasma mass spectrometry (LA-ICPMS) is frequently used for spatially resolved chemical characterization of a wide variety of minerals, soils and many other samples. Despite its successful use, accurate quantification of elemental concentrations can still be problematic, due to effects commonly summarized under the term “elemental fractionation”. This is most pronounced when matrix matched calibration standards are not available, which may result in variations of the relative sensitivities of the elements. This has been mainly attributed to non-representative laser sampling due to variations in the ablation process, causing preferential vaporization of elements. Recent reports, however, indicate that vaporization, ionization of the aerosol inside the ICP as well as the transfer of ions through the vacuum interface of the ICPMS are affecting the relative responses of individual elements significantly [1, 2, 3]. To describe these effects in detail the dependence of relative elemental sensitivities on the operating parameters of the ICPMS was studied for different samples using different laser ablation units (266 nm and 193 nm lasers). It can be shown that the relative sensitivities can vary significantly with the particle size distribution of the laser generated aerosol and the total mass load presented to the ICP. These variations are least pronounced when helium is used as carrier gas with 193 nm laser ablation which produces the aerosol with the lowest fraction of particles > 100 nm. Specific optimization of the ICP operating conditions, on the other hand can reduce the variation in the relative sensitivities and significantly improve the quantification even when the aerosol contains a large fraction of bigger particles and for argon as carrier gas. The change in elemental sensitivity was found to be different for two different ICPMS instruments compared. For one instrument sensitivities varied by not more than a factor of two, while for the other instrument the change was up to a factor of 15, depending on the element.

### References

- [1] Wang, Z.K., Hattendorf, B., Günther, D., (2006), *J. Am. Soc. Mass Spectrom* **17**, 641-651
- [2] Rodushkin, I., Axelsson, M.D., Malinovsky, D., Baxter, D.C., (2002) *J. Anal. At. Spectrom*, **17**, 1223-1230
- [3] Krosiakova, I., Günther, D., (2006), *J. Anal. At. Spectrom*, **22**, 51-62

## What comes around goes around: Mantle convection and the meaning of mantle isochrons

E. H. HAURI<sup>1</sup>, J.P. BRANDENBURG<sup>2</sup> AND P.E. VAN KEKEN<sup>2</sup>

<sup>1</sup>Dept. of Terrestrial Magnetism, Carnegie Institution of Washington, Washington, DC 20015, USA

<sup>2</sup>Dept. of Geological Sciences, University of Michigan, Ann Arbor, MI 02543, USA

The perceived significance of isotopic data arrays for oceanic basalts has long occupied a middle ground between the endmember interpretations of mixing and age. Brooks *et al.* [1] were the first to attach age significance to the correlations between parent-daughter ratios (e.g. <sup>87</sup>Rb/<sup>86</sup>Sr) and daughter isotope ratios (e.g. <sup>87</sup>Sr/<sup>86</sup>Sr) that are a regular feature of the geochemistry of OIB and MORB [e.g. 2,3]. Pseudo-isochrons derived from mixed mantle can still have age significance if the various packets of source material have been physically juxtaposed for long periods of time, yet the current paradigm has generally been to focus on daughter ratios alone, and to interpret their variations in terms of multi-component mixing.

Numerous high-quality geochemical data sets now exist, and continue to be generated, for specific regions of OIB and MORB volcanism. In order to take the next step in a more accurate interpretation of this data, a forward model is needed that delimits the bounds of chemical variability and isotopic correlations expected to arise from the major processes operative during terrestrial mantle convection. In this talk, we will present the results of cylindrical 2D convection models with force-balanced plates [4] and examine specifically the role of subduction and convective mixing of oceanic crust.

In these models, melting occurs at divergent plate boundaries and geochemical evolution is recorded by millions of passive (harzburgite) and active (basalt) tracers that record the times, extents of melting, and extents of degassing at every melting event, allowing the geochemical evolution of any isotope system to be easily calculated (and recalculated) in a post-processing algorithm that operates on the tracer data independently from the dynamic calculations. We will explore the range of isotopic variability in these models as functions of partition coefficients, chemical density of basalt tracers, and convective vigor. In particular, these models reveal relationships between mantle isochron “ages” and true tracer ages that is not obtainable from statistical box-model calculations incorporating idealized mixing scenarios [e.g. 3-5].

### References:

- [1] Brooks, C., Hart S.R., Hofmann A.W. & James D.E. (1976) *EPSL* **32**, 51-61.
- [2] Albarede F. (2001) *EPSL* **189**, 59-73.
- [3] Donnelly, K.E., Goldstein, S.L., Langmuir C.H. & Spiegelman, M. (2004) *EPSL* **226**, 347-366.
- [4] Brandenburg, J.P. *et al* (2007) *in prep.*
- [5] Rudge J.F. (2006) *EPSL* **249**, 494-513.

## Giant impacts, late veneers and the gradual hydration of the earth's mantle by subduction

E. H. HAURI<sup>1</sup>, A.M. SHAW<sup>2</sup> AND A.E. SAAL<sup>3</sup>

<sup>1</sup>Dept. of Terrestrial Magnetism, Carnegie Institution of Washington, Washington, DC 20015, USA

<sup>2</sup>Dept. of Geology & Geophysics, Woods Hole Oceanographic Institution, Woods Hole, MA 02543, USA

<sup>3</sup>Dept. of Geological Sciences, Brown University, Providence RI 02912, USA

The likelihood of one or more giant impact events occurring during the accretion of the Earth is very high [1,2], and most of these late-stage impact events impart enough energy to completely melt the silicate portion of the proto-Earth [3,4]. Despite the uncertain nature and composition of the terrestrial atmosphere immediately after such impacts, it seems inescapable that the Earth's mantle suffered a catastrophic loss of volatiles (including H<sub>2</sub>O, CO<sub>2</sub> and noble gases) within the first 100 Ma of the planet's history.

For these volatile species, the subsequent evolution of the Earth's mantle has thus involved a gradual re-hydration from without, via the subduction of lithosphere altered by water from an exosphere whose existence has been dated to 4.4 Ga [5,6]. The estimated composition of this exosphere shows many similarities to a mass-fractionated proto-atmosphere mixed with volatiles released during impact degassing of a chondritic late veneer.

We will present the results of forward-modelling the evolution of volatiles in the Earth's interior via subduction hydration of an initially dry mantle, with an emphasis on H<sub>2</sub>O. The model estimates the extent of (de)hydration of subducted hydrated lithosphere, and any associated isotopic (D/H) fractionations, based on studies of altered oceanic crust and Mariana arc magmas [7,8]. A defining characteristic of these models is the prediction of an initially high mantle viscosity, with gradual growth of a low-viscosity upper mantle due to the introduction of water at subduction zones. The fraction of the mantle that exchanges water with the exosphere thus grows with time, but the details of this growth depend on the extent of mixing between a hot, dry primordial mantle and a cooler and wet subduction-modified mantle. Nevertheless, virtually all conditions are expected to result in temporal shifts of the D/H ratios of the mantle and atmosphere that never reach steady-state, even over the age of the Earth.

### References

- [1] Wetherill G.W. (1996) *Science* **228**, 887-879. [2] Chambers J.E. & Wetherill, G.W. (1998) *Icarus* **136**, 304-327. [3] Tonks W.B. & Melosh H.J. (1993) *JGR Planets* **98**, 5319-5333. [4] Nimmo F. and Agnor, C.B. (2006) *EPSL* **243**, 26-43. [5] Wilde, S. A., Valley, J. W., Peck, W. H. & Graham, C. M. (2001) *Nature* **409**, 175-178. [6] Mojzsis, S. J., Harrison, T. M. & Pidgeon, R. T. (2001) *Nature* **409**, 178-181. [7] Agriner, P., Hekinian, R., Bideau, D. and Javoy, M. (1995) *EPSL* **136**, 183-196. [8] Shaw, A.M., Hauri E.H., Fischer, T., Hilton D.R. and Kelley, K.A. (2007) in prep.

## Determination of trace metal-nanoparticle associations in contaminated riverine systems using analytical TEM

K.L. HAUS<sup>1</sup>, J.R. JINSCHEK<sup>1,2,3</sup>, J.N. MOORE<sup>4</sup> AND M. HOHELLA, JR<sup>1,2</sup>

<sup>1</sup>Department of Geosciences, 4044 Derring Hall, Virginia Tech, Blacksburg, VA 24061 USA

<sup>2</sup>Institute for Critical Technology and Applied Science (ICTAS), Virginia Tech, Blacksburg, VA 24061 USA

<sup>3</sup>Department of Materials Science and Engineering, Virginia Tech, Blacksburg, VA 24061 USA

<sup>4</sup>Department of Geology, University of Montana, Missoula, MT 59812 USA

Analytical electron microscopy (AEM) is being used to study the associations between trace metals and nanoparticulate material in riverine systems. Seven samples have been taken from the Clark Fork River system in western Montana, USA, over a distance of 200 river kilometers, and during normal summertime flow. This river is being used as a model site because it is contaminated with toxic trace metals (principally Pb, As, Zn, and Cu) from over 150 years of copper and silver mining activities, and it has been studied in great detail. All samples were digested and analyzed using Inductively Coupled Plasma Mass Spectroscopy (ICPMS) to determine total metal concentrations and it was found that every sample contained significant amounts of at least two of the toxic metals of greatest interest. To date, extensive AEM analysis using an FEI Titan high resolution scanning/transmission electron microscope (S/TEM) (equipped with EDS and EELS detectors) on one water sample has been performed. Grains of aragonite, titanium oxide and hematite, bearing Zn, Pb and As, respectively, have been identified. These particles range in size from 8 to 200 nm in diameter, show various stages of crystallinity, and are often heterogeneous even on a nanometer scale. The nanometer size range is important not only because grains this small represent a disproportionately large amount of surface area available in the biogeochemical system, but also because the properties of these materials are expected to be dramatically altered from larger grains of the same material. These property changes, along with a potential for increased activity, may have a large impact on the bioavailability and toxicity of trace metals in natural systems. Further sampling and AEM analysis of existing samples will lead to a better understanding of trace metals in riverine systems and how nanoparticles are likely influencing their fate and availability.

## Basalt weathering rates on Earth and the duration of water on Mars

E.M. HAUSRATH<sup>1</sup>, A.K. NAVARRE-SITCHLER<sup>1</sup>,  
P.B. SAK<sup>2</sup>, C. STEEFEL<sup>3</sup> AND S.L. BRANTLEY<sup>1</sup>

<sup>1</sup>Department of Geosciences, Penn State University,  
University Park, PA 16802 (emh191@psu.edu)

<sup>2</sup>Department of Geology, Dickinson College, Carlisle, PA  
17013

<sup>3</sup>Earth Sciences Division, Lawrence Berkeley National  
Laboratory, Berkeley, CA 94720

Understanding the duration of time that Martian rocks were exposed to liquid water is of great interest because it influences the interpretation of the climate history and the potential for life on that planet. The presence or absence of primary minerals may provide constraints for the presence, duration and characteristics of liquid surface water on Mars.

Weathering rates are very sensitive to the pH of the reacting fluid. If pH values of terrestrial and Martian weathering solutions were similar, then mineral persistence ages on Mars are likely to be  $\geq$  those on Earth. We present a compilation of field terrestrial persistence ages for 8 common rock-forming phases (plagioclase, volcanic glass, quartz, feldspar, micas, pyroxene, amphibole, and olivine) collected from dated chronosequences representing a wide climatic spectrum ranging from -10°C to 30°C mean annual temperature and 400 mm to 4500 mm mean annual precipitation. The extent to which these minerals persist may help constrain the rates at which primary phases weather under field conditions on Earth, and likely represent minimum mineral persistence times on Mars if pH values were similar.

However, Mars weathering solutions may have been more acidic than on Earth. Relative mineral dissolution rates at different pH values can be predicted from laboratory dissolution experiments. Here we compare relative mineral weathering rates observed in the field with laboratory predicted trends. Relative mineral weathering rates observed for basalt in Svalbard (Norway), Pennsylvania, and Costa Rica are explainable by pH. These results suggest that the pH-dependence of laboratory rates can be used to interpret relative mineral persistence on Mars to yield information about the pH of the reacting fluid.

We also interpret both terrestrial and Martian weathering profiles using reactive transport modeling, which can yield insights into the duration of weathering. The interpretation of weathering profiles on Mars is a promising approach to study that planet's aqueous history, and highlights the need for additional depth profiles.

## The generation and evolution of the continental crust

CHRIS HAWKESWORTH<sup>1</sup> AND TONY KEMP<sup>2</sup>

<sup>1</sup>Department of Earth Sciences, University of Bristol, Bristol,  
BS8 1RJ UK (c.j.hawkesworth@bristol.ac.uk)

<sup>2</sup>School of Earth Sciences, James Cook University, Townsville  
QLD, 4811 Australia (tony.kemp@jcu.edu.au)

Detrital and inherited zircons encapsulate a more representative record of igneous events than the rock record, and their hafnium isotope ratios reflect the time since the source of the parental magmas separated from the mantle. O and Hf isotope ratios on well-dated zircons are used (i) to distinguish crust formation ages that reflect involvement in the sedimentary cycle, and those that do not, and (ii) to reconcile the crust formation ages of material whose isotope ratios reflect evolution in the igneous and sedimentary reservoirs.

Global peaks in juvenile igneous activity have been identified at 2.7, 1.9 and 1.2 Ga from the geological record. An initial study on samples from the Lachlan Fold belt revealed sharp peaks in Hf model ages in zircons with  $\delta^{18}\text{O}$  of  $< 6.5$  per mil at 1.9 Ga and 3.3 Ga. It is rare to find zircons with similar crystallization and Hf model ages. At issue are the links between such peaks in the geological and zircon records, and the time periods between initial crust formation and the generation of high silica magmas that might crystallize zircon in different tectonic settings.

The sedimentary record shows no evidence for major pulses of crust generation, and one interpretation is that it can take up to one billion years for new crust to dominate the sedimentary record. The residence times of material in the lower crust appears to be much lower than in the upper crust. Finally, the development of granulite facies rocks, and their effects on the deformation history of the continental crust, will be briefly explored.

## Paleoproterozoic post-orogenic evolution of the North China Craton: Geochemical and isotopic constraints from the Xiyanghe Group along the southern margin of the North China Craton

YANHONG HE, GUOCHUN ZHAO AND MIN SUN

Department of Earth Sciences, the University of Hong Kong, Hong Kong (h0492037@hkusua.hku.hk)

There is now a coherent outline of the timing and tectonic processes involved in the Palaeoproterozoic amalgamation and much intensive knowledge concerning the pre-collisional history of the North China Craton. However, much of the post-collisional history of the craton remains unknown. The Xiyanghe volcanics, together with the Xiong'er volcanics, constitute a large Paleo-Mesoproterozoic volcanic belt along the southern margin of the North China Craton. In this study, we provide geochemical and Sr-Nd isotopic data for the Xiyanghe volcanics, which provide important constraints on their petrogenesis and tectonic environment.

The Xiyanghe volcanics could be subdivided into three units: BA1 (basaltic andesites-1), BA2 (basaltic andesites-2) and andesites, all of which show consistent  $\epsilon_{Nd}(t)$ , La/Nb and Th/Nb values irrespectively of  $SiO_2$ , precluding significant crustal contamination during ascent. Based on the covariation between La and La/Sm<sub>N</sub>, the basaltic andesites show the trend of partial melting processes with the BA1 unit representing the major products of a magma chamber, whereas the andesites may fractionally crystallize from the BA1. The BA1 rocks and andesites show HSFE enrichments (especially Nb>6 ppm) and high Fe-Ti contents, comparable with Nb-enriched basalts, suggesting that the Xiyanghe volcanics were derived from a melt-metasomatized mantle source. The BA2 unit is characterized with variable Ti/Eu, Zr/Sm and Nb/La ratios, suggesting that amphiboles have been involved in a partial melting process, which implies that the Xiyanghe volcanics were derived from hydrous magma. A large range in initial Sr (0.7039 to 0.7111) and a relatively narrow range in  $^{143}Nd/^{144}Nd$  ( $\epsilon_{Nd}=-6.8\sim-10$ ) suggest inheritance of the enriched Nd-isotopic composition from the mantle wedge metasomatized by slab derived fluid. On the primitive mantle normalized trace-element diagrams, the Xiyanghe volcanic rocks show enrichments in the LILE and LREE and negative anomalies on the Nb-Ta-Ti, similar to arc-related volcanics produced by the hydrous melting of the metasomatized mantle wedge. The arc-related characteristics of the Xiyanghe volcanic rocks suggest that the southern margin of the North China Craton may have recorded the outbuilding history of the Columbia Supercontinent during Paleo-Mesoproterozoic time.

This research was financially supported by Hong Kong RGC grants (HKU7055/05P, 7048/04P and 7063/06P), China NSFC grant (40429001) and a HKU Seed Funding for Basic Research (200411159122), all to G.C. Zhao.

## Np(V) coprecipitation with calcite

FRANK HEBERLING, MELISSA A. DENECKE AND DIRK BOSBACH

<sup>1</sup>Institute for Nuclear Waste Disposal, Forschungszentrum Karlsruhe, PO Box 3640, 76021 Karlsruhe, Germany

The actinide elements U, Np and Pu form oxo-cations ('actinyl-cations') in oxidizing aqueous environments. The environmental behaviour of the actinyl ions U(VI), Np(V) and Pu(V,VI) is to a large extent controlled by sorption reactions (adsorption, coprecipitation / structural incorporation) with minerals. We study the structural incorporation of Np(V) into the host mineral calcite by coprecipitation in mixed flow reactors under steady-state conditions at room temperature. In this way reaction rates and partitioning coefficients can be determined under varying conditions. We found that homogeneous partition coefficients for Np in calcite (0.5 - 11) are significantly higher than those reported for U(VI) (0.01 - 0.2 [1]). The local structural environment of incorporated Np(V) is characterized from the Np L3 EXAFS. Measurements are performed at the INE-Beamline at ANKA (Forschungszentrum Karlsruhe). Our data suggest that the Np(V)-ions occupy calcium lattice sites, but with two missing carbonate groups in the first coordination sphere. The two axial oxygen atoms of the linear neptunyl-ions are likely oriented towards these vacant sites. Consequently, only four carbonates are observed to coordinate the Np(V)-ion. Np-O and Np-C interatomic distances (2,41Å, 3,34Å, respectively) indicate slight structural relaxation of the carbonate groups from their ideal sites. A similar structural model was reported for U(VI) incorporated into natural calcite [2].

### References

- [1] E.Curti (1997) Coprecipitation of radionuclides: basic concepts literature review and first applications. In *PSI-Bericht 97*, PSI.
- [2] Kelly *et al.* (2003) Uranyl Incorporation in Natural Calcite, *Environmental Science and Technology* **37**, pp 1284-1287.

## Geochemistry and mechanic emplacement of Late proterozoic dyke swarms, Eastern Desert, Egypt

HUSSEIN A. HEGAZY

Geology Department, Faculty of Science, Assiut University, Assiut, Egypt (hegazy 512000@yahoo.com)

Geologic and geochemical data of intraplate Late Pan-African (493±7Ma) dykes assemblage in the Eastern Desert of Egypt are presented. The dyke swarms consist of a bimodal mafic-felsic suite of transitional alkaline to subalkaline chemistry and exhibit a broad compositional range. Geochemical studies show that they can be subdivided into three distinct chemical groups with two distinct compositional gaps and correlate fairly well with other occurrences of late Pan –African dykes in Egypt. This bimodal suite bears a genetic relation to corresponding rock types in the study area.

These dykes trend predominantly in NW and NNW directions and less frequently in NW and N orientations; parallel to the major fracture pattern and lineament trends. Despite of the small geographic area and limited time interval in which the dykes were extruded, their complex geochemistry requires multiple sources together with varying amounts of open system fractionation assimilation. It is believed that the crystallization of the studied dykes follow the one-step emplacement either in open or closed system under both brittle and ductile crustal conditions. The time (ts) required to solidify these types of dykes is generally longer in the acidic than the basic variety.

## Nb-depleted calc-alkaline dacites from Iceland: Implications for Archean crust formation

E. HEGNER<sup>1</sup>, M. WILLBOLD<sup>2</sup>, A. STRACKE<sup>3</sup> AND A. ROCHOLL<sup>1</sup>

<sup>1</sup>Universität München, Department für Geowissenschaften, Luisenstrasse 36, 80333 München, Germany

<sup>2</sup>University of Bristol, Department of Earth Sciences, Bristol, BS8 1RJ, United Kingdom

<sup>3</sup>ETH Zürich, Institut für Isotopengeologie, Clausiusstr. 25, 8092 Zürich, Switzerland

Samples from the dacitic Krokksfjordur volcanic center, NW Iceland, have calc-alkaline compositions contrasting the alkaline to tholeiitic composition commonly observed for felsic rocks from ocean islands or plateaus (JÓNASSON, 2006). New major, trace element, and isotope data show that these samples display a distinct depletion of Nb ( $La/Nb_{PM} = 2.7 \pm 0.4$ ;  $1\sigma$ ) and enrichment of Pb ( $Ce/Pb_{PM} = 0.7 \pm 0.1$ ) in primitive mantle normalized trace element plots, and high Na/K ratios ( $3.6 \pm 0.3$ ).

The Sr-Nd-Hf-Pb isotopic compositions preclude the involvement of old continental lithosphere in the petrogenesis of the dacitic melts. The limited variation in major element data and the small though systematic variation of La/Nb and Ce/Pb ratios with  $TiO_2$  and Ce concentrations, respectively, suggest that the dacites were derived by partial melting of a mafic protolith comprising plagioclase + clinopyroxene + amphibole + Fe-Ti oxides. Inverse modelling shows that the calculated trace element composition of the source is similar to that of mafic crustal xenoliths hosted by one of the dacitic bodies. This observation suggests that partial melting of Icelandic mafic lower crust, most likely during magmatic underplating, has produced the calc-alkaline dacites at Krokksfjordur.

The major and trace element composition of the dacites closely resembles that of Archean tonalite - trondjemite - granodiorite (TTG) associations. Depletion of Nb and enrichment of Pb in TTG associations have hitherto been interpreted as evidence for their exclusive formation in Archean subduction zones (e.g. DRUMMOND and DEFANT, 1990; MARTIN, 1999). The new findings from the Krokksfjordur volcano demonstrate that partial melting of mafic protoliths in an oceanic intra-plate setting can also lead to chemical signatures similar to that of magmatic rocks generated in subduction zone environments. This provides evidence that the Archean continental crust could have been formed in a variety of geodynamic settings including intra-plate as well as plate margin settings.

### References

- Drummond M. S. and Defant M. J. (1990), *Journal of Geophysical Research* **95** 21503-21521.  
 Jónasson K. (2006), *Journal of Geodynamics* **43** 101-117.  
 Martin H. (1999), *Lithos* **46** 411-429.

## Mineralized microbial mats with extreme lanthanum enrichments in the tunnel of Äspö, Sweden

C. HEIM, K. SIMON, N.-V. QUÉRIC AND V. THIEL

Geoscience Centre, University of Göttingen, Germany  
(cheim@gwdg.de)

Microbial mats precipitating iron oxides and thereby accumulating trace and rare earth elements (REE) are widely recognized [1, 2, 3]. A key role in that biomineralization process is assigned to negatively charged organic surfaces (cell surfaces and extracellular polymeric substances, EPS) binding cations and forming complexes [2,3,4]. Depending on the nature of these surfaces, a fractionation of specific cations may occur, thus giving the resulting minerals an inorganic “biosignature”. Bacteriogenic iron oxides covering granitic surfaces in the 450m deep Äspö Hard Rock Laboratory (Sweden) were analysed for inorganic biosignatures using LA-ICPMS. The study revealed an extreme enrichment (about 1000fold) in lanthanum (La) compared the other REE (Fig. 1). According to the similar chemical behaviour of the light REE (La - Nd), this phenomenon cannot be explained by an inorganic precipitation of REE. Likewise, the REE concentration of the water supplying the microbial mat did not show a positive La anomaly. This points to a biologically driven, selective fractionation of La by the bacterial community involved. The resulting biosignature may help to build a better understanding of modern and fossil microbially induced minerals and rocks, even in the absence of fossil remains and organic molecular indicators.

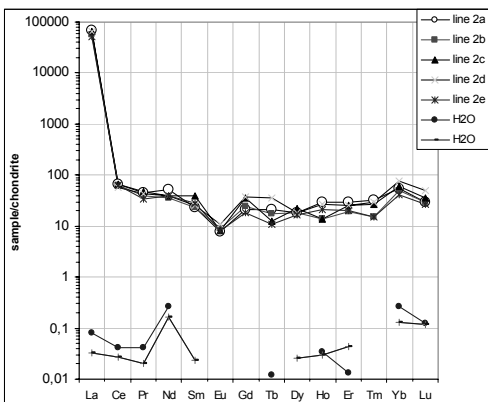


**Figure 1:** REE plot of mineral precipitates (line 2a-2e on the mineralized microbial mat), and the supplying water (H<sub>2</sub>O).

### References

- [1] Anderson *et al.* 2006 *Geobiology* **4**, 29–42
- [2] Ferris 2005, *Geomicrobiology Journal* **22**, 79–85
- [3] Konhauser 1998 *Earth-Science Reviews* **43**, 91–121
- [4] Takahashi *et al.* 2005 *Chemical Geology* **219**, 53–67

## Fe isotopes in siliceous igneous rocks: Evidence for fluid-rock interaction in plutons

A. HEIMANN, B. BEARD AND C. JOHNSON

Univ. Wisconsin – Madison (aheimann@geology.wisc.edu;  
beardb@geology.wisc.edu; clarkj@geology.wisc.edu)

The average  $\delta^{56}\text{Fe}$  value of bulk plutonic rocks (PR) with >70wt% SiO<sub>2</sub> is  $0.18 \pm 0.08\text{‰}$  (1-SD; n=19; data from Poitrasson and Freydier 2005 CG; Poitrasson 2006 EPSL; this study). In contrast, the average  $\delta^{56}\text{Fe}$  value of bulk volcanic rocks (VR) with >70wt% SiO<sub>2</sub> is  $0.02 \pm 0.07\text{‰}$  (1-SD; n=6; data from Beard *et al.*, 2003 CG; Beard and Johnson, 2004 GCA; this study). We have conducted a detailed study of minerals and bulk PR and VR samples using high-precision Fe isotope analysis ( $\pm 0.06\text{‰}$ , 2SD) to evaluate the origin of these differences.

Magnetite in PR has consistently higher  $\delta^{56}\text{Fe}$  values ( $\delta^{56}\text{Fe} = +0.13$  to  $+0.51\text{‰}$ ) than its host rock, whereas VR magnetite has lower  $\delta^{56}\text{Fe}$  values ( $-0.05$  to  $+0.27\text{‰}$ ). Silicates in both PR and VR have  $\delta^{56}\text{Fe}$  values that fall within the range for mafic VR ( $\delta^{56}\text{Fe} = -0.14$  to  $+0.10\text{‰}$ ). Fractionation factors between magnetite and silicates are larger for magnetite-biotite pairs in PR ( $\Delta^{56}\text{Fe}_{\text{mag-bt}} = +0.15$  to  $+0.58\text{‰}$ ) than for magnetite-silicate pairs in VR ( $\Delta^{56}\text{Fe}_{\text{mag-sil}} = -0.02$  to  $+0.19\text{‰}$ , one at  $+0.34\text{‰}$ ). Both are positively correlated with the  $\delta^{56}\text{Fe}$  values of magnetite and show a weak negative correlation with those of silicates, but in PR they are also correlated with  $\delta^{56}\text{Fe}$  of the host rock. The positive correlation between  $\Delta^{56}\text{Fe}_{\text{mag-bt}}$  and bulk  $\delta^{56}\text{Fe}$  in PR indicates that magnetite and bulk PR underwent open-system Fe exchange; the near-zero  $\delta^{56}\text{Fe}$  values in VR indicate that high  $\delta^{56}\text{Fe}$  values in silicic igneous rocks do not reflect crystal fractionation.

Open-system Fe isotope exchange in PR is influenced by cooling rates, Fe content, crystallization temperatures,  $f\text{O}_2$  conditions, Fe diffusion rates in minerals, and interaction with late-stage exsolved fluids and/or saline hydrothermal fluids. There is no correlation between  $\delta^{56}\text{Fe}$  and  $\delta^{18}\text{O}$  values for PR, indicating that Fe was not mobilized by dilute meteoric fluids; the largest range in  $\delta^{56}\text{Fe}$  values of minerals and bulk samples occurs in PR that have been mineralized. Fe isotope shifts likely occurred during exsolution of Fe-rich brines during solidification and deuteric alteration. The relatively high  $\delta^{56}\text{Fe}$  values of magnetite from PR probably reflect sub-solidus isotopic equilibration upon cooling and the high Fe diffusion rates in this mineral relative to silicates. Exsolved Fe-chloride solutions will have low  $\delta^{56}\text{Fe}$  values as compared to silicates or magnetite based on theory (Polyakov and Mineev, 2000 GCA; Schauble *et al.*, 2001 GCA), suggesting that the remaining pluton will increase in its  $\delta^{56}\text{Fe}$  value; this effect will be most significant in low-Fe, high-SiO<sub>2</sub> rocks, matching the observation that  $\delta^{56}\text{Fe}$  values for bulk samples and magnetite in PR are higher at higher SiO<sub>2</sub> contents.

## Synthetic forsterite grain boundaries: Tilt [100] and 9.9° to 21.5°

S. HEINEMANN<sup>1,2</sup>, R. WIRTH<sup>1</sup> AND G. DRESEN<sup>1</sup>

<sup>1</sup>GeoForschungsZentrum Potsdam, Germany

<sup>2</sup>Present address: AMD, Center for Complex Analysis,  
Dresden, Germany (stefan.heinemann@amd.com)

Forsterite is a main constituent of rocks in the Earth's mantle. The refractory nature of forsterite makes it suitable for ceramics used in thermal insulations. The properties of rocks and ceramics are largely determined by their grain boundaries. Structure and transport properties of grain boundaries in rocks are still poorly understood. In general grain boundary structure, grain boundary energy and grain boundary properties depend on orientation. Low angle grain boundaries show dislocations, have low grain boundary energy and their transport properties (e.g. grain boundary chemical and thermal diffusion, grain boundary migration and sliding) are slow. High angle grain boundaries do not reveal dislocations, have high grain boundary energy and their transport properties are fast. In oxides, the transition from low to high angle grain boundaries is not studied in detail, but the transition to a high angle grain boundary is commonly defined at an angular lattice misorientation of ~ 10°-15°.

We synthesized a series of symmetric tilt grain boundaries in forsterite bicrystals with tilt axis **a** and increasing tilt angle from 9°-21° by direct bonding (Heinemann *et al.* 2001, 2005). For each bicrystal two oriented and polished synthetic forsterite single crystal plates were joined at room temperature and annealed at 400°C in vacuum for one week. All bicrystals were cut in two parts and one part was annealed further at 1650°C for 48h. Specimens were prepared for investigations in the TEM with focused ion beam (FIB).

HRTEM investigations of the grain boundaries parallel to tilt axis **a** show symmetric tilt grain boundaries with arrays of regular spaced edge dislocations between undisturbed crystal regions for all annealing temperatures and all tilt angles. The grain boundary structure developed below 400°C and did not change till 1650°C. All grain boundaries with tilt angles from 9°-21° are low angle grain boundaries. The Burgers vector of the edge dislocations is **c**. The regular dislocation spacings decrease with increasing tilt angles and dislocation cores do not overlap up to a tilt angle of 21°.

The dislocation model of low angle grain boundaries can be applied and the observed dislocation spacings  $d$  are related to tilt angle  $\theta$  and Burgers vector length  $b$  by Frank's formula:  
$$d = b / (2 \sin(2/\theta)) \approx b / \theta \quad \text{for small } \theta$$
with tilt angles increasing from 9° to 21° the dislocation spacing decreased.

Using Frank's equation and a rough estimation of the dislocation core radius of  $r_0 \sim 0.4 \text{ nm} \sim 2/3b$  we propose that in forsterite the transition between low and high angle grain boundary occurs at a misorientation of ~ 42°.

### References

- Heinemann S. *et al.* (2001) *Phys Chem Minerals* **28** 685-692  
Heinemann S. *et al.* (2005) *Phys Chem Minerals* **32** 229-240

## Formation of oceanic zircons

E. HELLEBRAND<sup>1</sup>, A. MÖLLER<sup>2</sup>, M. WHITEHOUSE<sup>3</sup> AND  
M. CANNAT<sup>4</sup>

<sup>1</sup>Geology and Geophysics Dept., University of Hawaii,  
Honolulu, USA (ericwgh@hawaii.edu)

<sup>2</sup>Institut für Geowissenschaften, Universität Potsdam,  
Germany (amoeller@geo.uni-potsdam.de)

<sup>3</sup>Laboratory for Isotope Geology, Swedish Museum of Natural  
History, Stockholm, Sweden  
(Martin.Whitehouse@nrm.se)

<sup>4</sup>Laboratoire de Petrologie, Paris, France  
(cannat@ipggp.jussieu.fr)

Zircon is an omnipresent accessory phase in gabbroic rocks collected along mid-ocean ridges. We obtained *in situ* U-Pb ages and REE compositions of well-documented (BSE, color-CL imaging) zircons from three locations along the Mid-Atlantic Ridge. In order to avoid contamination, we only used zircons found within petrographic thin sections.

The medium to coarse grained zircons of this study were found in highly evolved, oxide gabbro veins crosscutting mantle peridotites and are as abundant as 15 modal percent. They are generally subhedral to perfectly euhedral in shape, can exceed 1 mm and appear homogeneous in BSE images. Color-CL reveals a dominant sector zoning in dark and bright blueish-grey. Within the individual sectors, a fine oscillatory zoning can be generally resolved as well.

All near-ridge zircons have U concentrations less than 50 ppm and yield ages of approx. 1 Ma and younger. This contrasts strongly with Paleozoic-Proterozoic ages reported on similar samples from the same locations, which may have resulted from contamination during sample preparation. The steep REE patterns of all samples are very similar: low LREE and very high (up to 10,000x CI-chondrite) HREE with pronounced positive Ce and negative Eu anomalies. Their absolute REE abundances are bimodal. The CL-bright sectors have a factor 2 to 3 times lower REE concentrations than the associated darker sectors. Average CL-bright zones from all samples are chemically virtually indistinguishable. Significant core-rim zoning is absent. These features are consistent with a cumulate-type origin from nearly identical highly evolved melts. This requires relatively large melt volumes that would not change in HREE concentration during zircon formation.

Titanium concentrations are sector-independent and yield temperatures around 830°C. This suggests that there is no temperature gradient between the evolved melt and the peridotite wall rock. Along cracks, rare patchy yellow and very bright blue luminescence domains occur, generally characterized by low trace element abundances except for high U (up to 290 ppm) and significantly lower Ti-in-zircon temperatures. This suggests that low-T hydrothermal dissolution-recrystallization reactions are possible, which potentially affect whole-grain U-Pb (-He) systematics.

## Evaluating the role of superoxide ( $O_2^-$ ) and hydrogen peroxide ( $H_2O_2$ ) in the dissolution of Saharan dust in the Tropical Atlantic

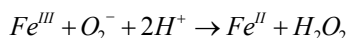
M. HELLER AND P. CROOT

IFM-Geomar, Kiel, Germany

(mheller@ifm-geomar.de; pcroot@ifm-geomar.de)

### Method and Theory

The major source of iron to the Tropical Atlantic is through aeolian deposition of Saharan dust. Presently within SOPRAN (German SOLAS) we are investigating, at the TENATSO site in Cape Verde, water column processes that control the dissolution of Saharan dust deposited at the seawater surface. The thermodynamic solubility of Fe(III) in surface seawater is thought to be controlled by the presence of iron complexing organic ligands. However in tropical waters, where high fluxes of superoxide ( $O_2^-$ ) may exist, due to photochemical reactions of dissolved organic material, there exists the possibility of a kinetic controlled reduction of Fe in colloids and particles to the more soluble Fe(II) [Kustka *et al.*, 2005; Rose and Waite, 2006].



Photochemistry may not be the only source of  $O_2^-$  in seawater as recent work suggests a significant biological source also [Kim *et al.*, 2004]. Overall these processes may lead to longer residence times for dissolved Fe in surface waters [Croot *et al.*, 2004].

### Discussion

Current work focuses on laboratory work evaluating analytical methodologies and focuses on three key aspects:

- (i) The influence of temperature on the dismutation rate of  $O_2^-$  in seawater.
- (ii) How  $O_2^-$  can alter the Fe organic speciation in seawater.
- (iii) Assessment of the enhancement of Fe dissolution from Saharan dust via increased  $O_2^-$

### Conclusion

Using this approach we hope to be able to critically examine the role in which photochemistry and biology play in solubilizing Fe from Saharan dust in Tropical seawater. Overall this information will help in better assessing the key processes controlling iron bioavailability in natural seawater.

### References

- Croot, P. L., P. Streu, and A. R. Baker (2004), *GRL*, **31**, L23S08, doi.1029/2004GL020153.
- Kim, D., M. Watanabe, Y. Nakayasu, and K. Kohata (2004), *Aquatic Microbial Ecology*, **35**, 57-64.
- Kustka, A. B., Y. Shaked, A. J. Milligan, D. W. King, and F. M. M. Morel (2005), *L&O*, **50**, 1172-1180.
- Rose, A. L., and D. Waite (2006), *GCA*, **70**, 3869-3882.

## The reactivity of ferric (oxy)hydroxides toward dissolved sulphide between pH 3 to 9

K. HELLIGE AND S. PEIFFER

Dept. of Hydrology, University of Bayreuth, Germany

(katrin.hellige@uni-bayreuth.de;

s.peiffer@uni-bayreuth.de)

The reaction between  $H_2S$  and ferric (oxy)hydroxides exerts a major role for the sulphur and iron cycle as for the electron and carbon flow in many aquatic systems (e. g. Canfield, 1992). The reaction mechanism is reasonably well understood (Dos Santos Afonso *et al.*, 1992; Peiffer *et al.*, 1992). The reaction rate depends on pH which can be explained by a surface speciation model according to which the electron transfer is preceded by an adsorption step of a sulphide species to the neutral ferric oxide surface  $>FeOH$ .

In a recent study, steady-state experiments have been performed at low pH ( $< 5$ ) using a fluidized-bed reactor that is supplied with a constant flow of electrochemically generated hydrogen sulphide (Peiffer & Gade, 2007). The surface area normalized experimental reaction rates depended on bulk properties of the used minerals and decreased in a sequence  $Gt > 2lfh > 6lfh$ . These observations are in contrast to results from batch experiments obtained at pH 7.5 where mineral reactivity seemed to be related to the free energy of their formation (Poulton *et al.*, 2004). Under these conditions  $Fe^{2+}$  strongly adsorbs to the mineral surface and thereby interacts with dissolved sulfide.

In this study we attempt to resolve these contradictions. Using the same experimental approach as described in Peiffer & Gade (2007), we have extended the experimental pH range to study the steady-state reactivity of various iron (hydr)oxides to values between 3 and 9. In this poster we will present the first results from these experiments.

### References

- Canfield D. E. and Raiswell R. and Bottrell S. (1992), The reactivity of sedimentary iron minerals toward sulphide. *Amer. J. Sci.* **292**, 659-683.
- Dos Santos Afonso M. and Stumm W. (1992), Reductive Dissolution of Iron(III) (Hydr)oxides by Hydrogen Sulfide. *Langmuir* **8**, 1671-1675.
- Peiffer S. and Dos Santos Afonso M. and Wehrll B. and Gächter R. (1992), Kinetics and mechanism of the reaction of  $H_2S$  with lepidocrocite. *Environ. Sci. Technol.* **26**(12), 2408-2413.
- Peiffer S. and Gade W. (2007), Reactivity of ferric oxides toward  $H_2S$  at low pH. *Environ. Sci. Technol.* In press.
- Poulton, S. W. and Krom M. D. and Raiswell R. (2004), A revised scheme for the reactivity of iron (oxyhydr)oxide minerals towards dissolved sulphide. *Geochim. Cosmochim. Acta.* **68**, 3703-3716.

## Investigating the dependence of feldspar dissolution rates on Gibbs free energy in the presence of high $p\text{CO}_2$

R. HELLMANN<sup>1</sup>, D. DAVAL<sup>2</sup> AND D. TISSERAND<sup>3</sup>

<sup>1</sup>LGIT, CNRS UMR C5559-Univ. Grenoble, France  
(hellmann@obs.ujf-grenoble.fr)

<sup>2</sup>IPGP, Paris and Laboratoire de Géologie, ENS, UMR 8538  
Paris, France (daval@ipgp.jussieu.fr)

<sup>3</sup>LGIT, CNRS UMR C5559-Univ. Grenoble, France  
(tisserand@obs.ujf-grenoble.fr)

Here we report on results from an ongoing experimental investigation of the dissolution kinetics of albite feldspar at 100 °C in aqueous solutions significantly enriched in dissolved carbon dioxide ( $p\text{CO}_2 = 9$  MPa). The purpose of this study is to measure  $\text{CO}_2$ -water-rock interactions as a function of solution saturation ( $\Delta G$ ), thereby providing data needed to model physico-chemical interactions associated with mobile  $\text{CO}_2$ -plumes in subsurface environments. Over the fluid saturation range of  $-70$  to  $-40$  kJ mol<sup>-1</sup> the dissolution rates can be characterized by a dissolution rate plateau, where the rates are roughly equal and independent of dissolved Na, Al, and Si. At higher solution saturation states, the rates begin to decrease sharply. In addition, the stoichiometry of dissolution changes from stoichiometric to non-stoichiometric, and is most probably due to the precipitation of an Al phase. Current experiments are being run to measure the kinetics at  $\Delta G > -30$  kJ mol<sup>-1</sup>. The present data set, even though incomplete, is in general accord with many other studies that show a sigmoidal dissolution rate-free energy relation (e.g. Hellmann and Tisserand, 2006; and refs therein). Most importantly, the data also deviate dramatically from the behavior predicted by transition state theory (TST).

### Reference

Hellmann, R. and Tisserand, D., (2006) Dissolution kinetics as a function of the Gibbs free energy of reaction: An experimental study based on albite feldspar. *Geochim. Cosmochim. Acta* **70**, 364-383.

## Lower mantle phase-boundary variability

DON V. HELMBERGER AND DAOYUAN SUN

Seismological Laboratory 252-21, California Institute of Technology

A lower mantle S-wave triplication with a Scd branch occurring between S and ScS appears to be explained by a recently discovered Perovskite (PV) to Post-Perovskite (PPV) phase-change. It is predicted to have a positive Clapeyron slope ( $\gamma$ ) between 5 to 13 MPa/K with a small S-velocity jump (1.5 to 4%) and an even smaller 1 to 2% jump in P-velocity. Seismic observations indicate that Scd arrives earlier and stronger beneath fast regions indicating a positive  $\gamma$  (circum-Pacific) than slow regions (super plumes). However, it proves difficult to separate effects produced by down-welling (slab debris) from up-welling (plumes) in refining the actual physical properties. Here we model dense record sections collected from USArray and existing PASSCAL data to isolate effects produced by lower mantle structure as evidenced by P and S-waves, to better define the seismic phase-change properties beneath Central America. We find that the PV-PPV velocity jump is twice as strong beneath slow regions than fast regions requiring distinct reference heights indicative of changing chemistry. Moreover, the edges of the supposed buckled slabs delimited by both P and S-waves display very rapid changes in phase-boundary heights producing Scd multipathing. These features can explain the unstable nature of this phase with easy detection to no detection commonly observed. The fine structure at the base of the mantle beneath these edges contains particularly strong reflections indicative of local ultralow velocity zones, which is predicted in some dynamic models.

### References

- Sun D.Y., Tan E., Helmberger D., and Gurnis M., (2007), Seismological support for the metastable superplume model, sharp features, and phase changes within the lower mantle, *PNAS* **10**.1073/pnas.0608160104.
- Sun D.Y., Helmberger D., Song X.D. and Grand S., (2007), Predicting Global Perovskite and Post-Perovskite Phase Boundary, AGU Monograph, *The Last phase Transition*, in press.

## Different origin for mafic and intermediate/felsic lavas from Moorea island (Society, French Polynesia)

C. HÉMOND<sup>1</sup>, C. CHAUVEL<sup>2</sup>, R.C. MAURY<sup>3</sup> AND E. LEWIN<sup>2</sup>

<sup>1</sup>Domaines océaniques, IUEM, Brest University 29200 Plouzané, France (chhemond@univ-brest.fr)

<sup>2</sup>LGCA, Grenoble University, 38041 Grenoble cedex, France.

Moorea, a Quaternary volcanic island in the linear Society chain (French Polynesia) is made up of shield (alkali basalt to trachybasalt) capped by intermediate lavas (basaltic trachyandesites, trachyandesites, tephri-phonolites) and alkali trachytes. These intermediate to evolved lavas were emplaced between 1.55 and 1.35 Ma, just after the end of the shield stage which started at 1.72 Ma. The Moorea alkali basaltic suite cannot, however, be easily explained by closed-system fractionation processes because (i) the suite is bimodal in terms of rock abundances (60% mafic lavas and 40% intermediate/felsic ones), and (ii) fractional crystallisation tests fail to account for the transition between these two types.

In order to understand the relationship between basalts and felsic lavas, we determined trace element concentrations, as well as high precision Pb isotope ratios, and Hf, Sr and Nd isotopic compositions of a selection of 18 samples representing the various lava types. Basalts have relatively uniform <sup>206</sup>Pb/<sup>204</sup>Pb (~ 19.2) but variable Nd, Hf and Sr ratios (i.e., <sup>87</sup>Sr/<sup>86</sup>Sr between 0.7044 and 0.7052). In contrast, the felsic lavas have uniform Nd and Hf isotopic ratios but variable Sr and Pb ratios. The high precision Pb isotopic data define a straight line for the felsic lavas while the basalts form a cluster. Interestingly, the felsic lava straight line does not intersect the basalt cluster.

The composition of the basalts can be explained by conventional models involving partial melting of a garnet peridotite within a plume with EMII characteristics. The composition of the felsic material requires a completely different origin. We suggest that the felsic lavas originate from melting of a basaltic component and not from fractional crystallization of the plume derived basalts. This basaltic component is isotopically heterogeneous but its location is uncertain: it could be located at the base of the oceanic crust below the island or it could be an integral part of the plume.

## Schwertmannite transformation to hematite by heating: Implications for pedogenesis, water quality and CO<sub>2</sub>/SO<sub>2</sub> export in acid sulfate soil landscapes

S.P. HENDERSON\*, L.A. SULLIVAN, R.T. BUSH AND E.D. BURTON

Southern Cross University, PO Box 157, Lismore, NSW 2480, Australia (\*scott.henderson@scu.edu.au)

Naturally occurring schwertmannite (Fe<sub>8</sub>O<sub>8</sub>(OH)<sub>5.5</sub>(SO<sub>4</sub>)<sub>1.25</sub>), a product of acid sulfate soil oxidation and severe acidification, has been identified as a labile source of iron, sulfate and acidity. Schwertmannite forms surface accumulations on coastal flood plains of eastern Australia that are subject to wild fire events. We report experimental evidence that fire in acid sulfate soil landscapes will convert schwertmannite to hematite (α-Fe<sub>2</sub>O<sub>3</sub>), consequently reducing the potential acidity store whilst liberating greenhouse gases. At ≥ 800°C, naturally occurring schwertmannite was transformed completely to hematite. Thermal gravimetric analysis of this transformation process showed that CO<sub>2</sub> and SO<sub>2</sub> evolved simultaneously at relatively low temperatures (200-250°C and 300-340°C respectively). Aqueous dissolution experiments with samples of the initial schwertmannite and the resultant hematite showed that there was a significant decrease in the acidity potential associated with the heating-induced conversion to hematite. The data clearly shows natural fires may convert schwertmannitic surface accumulations to hematite. Hematite surficial layers have been observed previously in these landscapes and this study provides an explanation for their pedogenesis. Theoretical acid loads, based on this research, indicate fire can greatly reduce potential acidity. Relatively low temperature fires in these landscapes can combust schwertmannitic accumulations resulting in the discharge of CO<sub>2</sub> and SO<sub>2</sub>. These results have implications for the assessment of acidity and the sustainable management of acid sulfate soil landscapes.

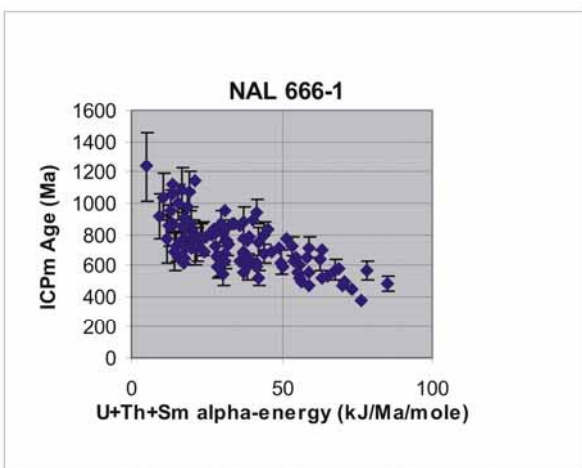
## Evidence for natural, non-thermal annealing of fission tracks in apatite

B.W.H. HENDRIKS<sup>1</sup>, R.A. DONELICK<sup>2</sup>, P.B. O'SULLIVAN<sup>2</sup>  
AND T.F. REDFIELD<sup>1</sup>

<sup>1</sup>Geological Survey of Norway, Trondheim, Norway  
(bart.hendriks@ngu.no, tim.redfield@ngu.no)

<sup>2</sup>Apatite to Zircon, Inc., Viola, Idaho, USA  
(donelick@apatite.com, osullivan@apatite.com)

Apatite fission-track (AFT) analyses using a LA-ICP-MS based approach on samples from Finland and Canada provide evidence for a non-thermal AFT annealing process that is dependent on the present-day concentration of alpha-emitter actinides (U,Th,Sm) within grains. In one example, 118 grains were dated from a sample from central Finland (see below).



Because all of the dated grains are from a single hand sample, the inverse correlation between the concentrations of alpha-emitter actinides and AFT age cannot be explained simply by intra-grain variations in temperature history. Electron microprobe analysis of the dated grains indicates that chemical elements that are known to control the annealing rates in apatite (Cl, Mn, Fe, REE, etc.) do not show a similar correlation.

Electron beam induced annealing of fission tracks in apatite (Paul and Fitzgerald 1992) and studies of phosphates as nuclear waste forms (e.g. Ewing and Wang 2002) indicate that processes other than thermal annealing can cause fading of fission tracks under laboratory conditions. The above example from Finland represents a natural example of non-thermal, radiation-induced annealing.

Modelling of AFT data from cratonic settings with annealing models that do not incorporate non-thermal annealing processes will lead to overestimation of paleotemperatures.

### References

- Paul and Fitzgerald 1992, *American Mineralogist* 77.  
Ewing and Wang 2002, Phosphates, *Reviews in Mineralogy and Geochemistry* 48

## Trace element distributions and coral skeleton micromorphology following a bleaching event

E.J. HENDY<sup>1</sup>, A. LANZIOTTI<sup>2</sup>, T. RASBURY<sup>3</sup> AND  
J. LOUGH<sup>4</sup>

<sup>1</sup>Department of Earth Sciences, University of Bristol, UK  
(e.hendy@bristol.ac.uk)

<sup>2</sup>The University of Chicago – CARS, Brookhaven National Laboratory, Upton, NY, USA (lanziotti@bnl.gov)

<sup>3</sup>Department of Geosciences, SUNY Stony Brook, NY, USA  
(erasbury@notes.cc.sunysb.edu)

<sup>4</sup>Australian Institute of Marine Science, Townsville, Australia  
(j.lough@aims.gov.au)

The massive tropical corals commonly used as palaeoclimate archives, such as *Porites* sp., contain zooxanthellae (symbiotic photosynthesizing algae). Coral bleaching occurs when these pigmented zooxanthellae are expelled from the coral tissue. In this study we investigate how the biomineralization process and trace element distribution within the coral skeleton are impacted by zooxanthellae population dynamics following a bleaching event. The non-destructive, high resolution in-situ mapping capabilities of synchrotron  $\mu$ -XRF is an ideal tool to investigate differences in trace element partitioning that correspond to the fine-scale architecture of coral skeleton.

A healthy ~30 year old *Porites australensis* colony was collected 2 ½ years after the February 1998 mass coral bleaching event from the inshore central Great Barrier Reef, Australia (18.48°S, 146.26°E). During the 1998 coral reef bleaching event ~80% of coral to a depth of 10m bleached at this reef, and bleaching mortality subsequently reduced coral cover by ~20%. At the time of collection (August 2000) there were no signs that the specimen had bleached, however, x-ray images show a marked and sustained skeletal growth response with lower extension and calcification rates and higher skeletal density.

Synchrotron  $\mu$ -XRF mapping was carried out at Beamline X26A (NSLS, BNL) with the beam set at 16.5 keV to target elements up to Sr and a 10 $\mu$ m spot size. Sr, Ca, Br, Zn, Ni, Cu, Fe Pb and Ba were mapped in 20 $\mu$ m steps (equivalent to daily growth rate) down the width of a single corallite for a 4-year period of skeleton growth including the 1998 bleaching event. Skeletal structures are compositionally zoned, with a strong response 6 months after the start of the bleaching event. An adjacent CT-X-ray microtomography scan recorded the contemporary morphological changes in skeleton micro-architecture. Bulk analyses of Sr/Ca, Mg/Ca,  $\delta^{13}\text{C}$ ,  $\delta^{18}\text{O}$  were measured on a parallel milled transect. To isolate the role of tissue smoothing on the seasonal signal  $\mu$ -XRF elemental maps were also collected across the most recent skeleton deposited within the tissue zone of specimens collected in both summer and winter seasons.

## Tourmaline in evaporites and meta-evaporites: Perspectives from Namibian metasediments

DARRELL J. HENRY<sup>1</sup>, HAITING SUN<sup>1</sup>,  
BARBARA L. DUTROW<sup>1</sup> AND JOHN F. SLACK<sup>2</sup>

<sup>1</sup>Dept. of Geology and Geophysics, Louisiana State Univ.,  
Baton Rouge, LA 70803, USA (dhenry@geol.lsu.edu)

<sup>2</sup>U.S. Geological Survey, National Center, MS 954, Reston,  
VA 20192

Tourmalines associated with evaporitic or meta-evaporitic rocks commonly exhibit a compositional trend where there is low Al in the structural formula that is compensated by the introduction of Fe i.e., Al = Fe<sup>3+</sup> exchange. This compositional trend has been found in the few occurrences of known evaporitic tourmalines: the caprock of a salt dome in the Gulf of Mexico, a brecciated and metamorphosed cap rock from Alto Chapare (Bolivia), an amphibolite-facies metabasite deposit from eastern Liaoning (China), and some tourmaline in tourmalinites from the meta-evaporitic sequence of the Duruchaus Formation (Damara Belt, Namibia – this study). These tourmalines follow a trend that defines a complete solid solution between

dravite (NaMg<sub>3</sub>Al<sub>6</sub>(Si<sub>6</sub>O<sub>18</sub>)(BO<sub>3</sub>)<sub>3</sub>(OH)<sub>3</sub>(OH)) or “oxy-dravite” (Na(MgAl<sub>2</sub>)(MgAl<sub>5</sub>(Si<sub>6</sub>O<sub>18</sub>)(BO<sub>3</sub>)<sub>3</sub>(OH)<sub>3</sub>O) and povondraite (NaFe<sup>3+</sup><sub>3</sub>(Fe<sup>3+</sup><sub>4</sub>Mg<sub>2</sub>)(Si<sub>6</sub>O<sub>18</sub>)(BO<sub>3</sub>)<sub>3</sub>(OH)<sub>3</sub>O). These trends are interpreted to represent tourmalines developed in an Al-poor, Fe<sup>3+</sup>-rich environment, consistent with evaporitic settings.

Although some of the tourmalines from the Duruchaus Formation follow this Al for Fe<sup>3+</sup> trend, a number of clearly meta-evaporitic tourmalines do not. The tourmalinites in two of the three localities studied are interlayered with biotite- and muscovite- semipelite and with calcite-dolomite marble. Despite their derivation from evaporitic sediments (tourmalinites preserve pseudomorphs after a variety of primary evaporitic minerals), the tourmalines in these tourmalinites exhibit an Al- and Mg-rich composition that appears to reflect a local compositional influence from the semipelitic interlayers. In fact, these Al-Mg-rich compositions are similar to those found by Prof. Werner Schreyer and his colleagues in tourmalines from the ultrahigh-pressure rocks of the Dora Maira massif (Italy) that they interpreted as meta-evaporites.

## Geochemistry of cold vent fluids at the Central American Convergent Margin

C. HENSEN<sup>1</sup>, K. WALLMANN<sup>1</sup>, M. SCHMIDT<sup>2</sup>,  
V. LIEBETRAU<sup>1</sup>, U. FEHN<sup>3</sup>, D. GARBE-SCHÖNBERG<sup>2</sup> AND  
W. BRÜCKMANN<sup>1</sup>

<sup>1</sup>IFM-Geomar, Kiel, Germany

(chensen@ifm-geomar.de; kwallmann@ifm-geomar.de;  
vliebetr@ifm-geomar.de;  
wbrueckmann@ifm-geomar.de)

<sup>2</sup>Geosciences, CAU, Kiel, Germany

(mas@gpi.uni-kiel.de; dgs@gpi.uni-kiel.de)

<sup>3</sup>Univ. of Rochester, NY, USA (fehn@earth.rochester.edu)

The active continental margin offshore Central America is characterised by a high number of cold vent sites associated with typical sea floor features such as mud volcanoes and diapirs (mounds) or submarine slides. Over the past couple of years a solid geochemical data base of fluid samples has been collected from various locations along the Costa Rica - Nicaragua forearc. Similar to pore fluids from other, mostly accretionary convergent margins, these fluids are typically less saline than normal seawater. There is clear evidence (using oxygen and hydrogen isotope ratios) that chloride-depleted fluids originate from clay-mineral dehydration processes at elevated temperature and pressure conditions. This interpretation is supported by a number of additional observations such as the occurrence of thermal methane and highly elevated boron concentrations. Due to the lack of suitable conditions for the presumed processes within the sedimentary sequence of the overriding plate, it has been hypothesized that the fluids may originate from mineral dehydration in subducted sediments at about 10 km depth (Hensen *et al.* 2004). This is supported by mass balance estimates between input of mineral-bound water by subducting sediments and output through known vent sites. At many sites, however, the geochemical signature does not reveal clear evidence for a “deep” origin, such as the abundant occurrence of shallow biogenic gas. Conspicuous differences in the geochemical composition of fluids from various locations allow a general subdivision into regional, potentially structurally-controlled, types. We will present a comprehensive description of the available data set – covering the main element composition and various isotope systems ( $\delta^{18}\text{O}$ ,  $\delta\text{D}$ ,  $\delta^{13}\text{C}$ ,  $^{87}\text{Sr}/^{86}\text{Sr}$ ,  $\delta^{44}\text{Ca}$ ,  $^{129}\text{I}/\text{I}$ ) – and discuss fluid sources and potential ages as well as processes of formation and alteration. In addition, we will present an outline of current efforts to drill key sites of the most prominent dewatering structures within IODP (633 full2, Costa Rica Mounds).

### Reference

Hensen C., Wallmann K., Schmidt M., Ranero C. R., and Suess E., (2004), *Geology* **32**, 201-204.

## The application of granular activated carbon on remediation in trichloroethylene contaminated groundwater

JOONG-HYEOK HEO<sup>1</sup>, DAL-HEUI LEE<sup>2</sup> AND HO-WAN CHANG<sup>1</sup>

<sup>1</sup>School of Earth and Environmental Sciences, Seoul National University, Korea

<sup>2</sup>Research Institute of Groundwater and Soil Environment, Yonsei University, Korea

The objective of this study is to evaluate the effect of ionic strength and hardness of trichloroethylene (TCE) contaminated groundwater on remediation using granular activated carbon (GAC). The sorption rate of TCE by GAC was observed by batch experiments. The sorption kinetic of GAC was analyzed by kinetic models. As the ionic strength and hardness of the synthetic groundwater increased, the TCE sorption rates of GAC in the synthetic groundwater decreased. The TCE sorption rates of GAC in synthetic groundwater were 100%, 93.0%, 90.2%, and 86.2%, respectively. These results showed that the TCE sorption rates were affected by the relationship between the ionic strength and the hardness of the synthetic groundwater. The Elovich model ( $r^2=0.99$ ) is more precise than Pseudo first order model ( $r^2=0.96$ ). This indicates that the Elovich model is well represented in the contaminated groundwaters which have various factors like ionic strength and hardness. The surface area of the GAC was 958.98 m<sup>2</sup>/g and the calculated sorption areas of TCE & ions were 318.38 m<sup>2</sup>/g, which were 32.2% of the GAC surface area. Therefore, the ionic strength and hardness of groundwaters must be considered in the remediation of TCE-contaminated groundwater using GAC.

## Accessory phase control on the trace element signature of subduction zone fluids

J. HERMANN AND D. RUBATTO

Research School of Earth Sciences, ANU, Canberra 0200  
(joerg.hermann@anu.edu.au; daniela.rubatto@anu.edu.au)

In order to understand the general trace element signature of arc lavas, phase and melting relations in metapelites at sub-arc depth are of first order importance. Here we present results from experimental studies on a trace element doped, hydrous (2-7 wt.% H<sub>2</sub>O), synthetic pelite and granite in the range 20-45 kbar and 600-1050°C, i.e. conditions relevant for the slab at sub-arc depth. In the metapelite, a hydrous melt that quenches to a glass is present at conditions above 700°C, 25 kbar; 750°C, 35 kbar and 800°C, 45 kbar. At lower temperatures, a solute-rich aqueous fluid is present that is not quenchable. This fluid has been captured in diamond traps in the experiments and the quench material as well as the glass have been analysed with LA-ICP-MS.

One surprising feature in the run products is the presence of accessory phases at subsolidus as well as at suprasolidus conditions, even at large melt proportions of 50%. Rutile, apatite and zircon have been found over the entire investigated P-T range. Allanite is present at 2.5 GPa up to 800°C, and at 3.5 and 4.5 up to 750°C. At higher temperatures, monazite is stable up to 1000°C. This has profound bearings on the trace element characteristics of the fluid phase. In a residue consisting of garnet, clinopyroxene, phengite and coesite all trace elements in the fluid phase are governed by partitioning behaviour. In contrast, in the presence of accessory phases, several trace elements are buffered (Ti by rutile, P by apatite, Zr by zircon, LREE by monazite/allanite). Additionally, other HFSE and REE are preferentially retained in the residue with respect to a system without these accessory minerals. This is documented in the measured composition of the fluid phases. For example LREE display only incompatible behaviour at the highest temperature investigated (950-1000°C) whereas at 800°C, LREE are compatible in the residue due to the presence of monazite or allanite. In the aqueous fluid LREE are about an order of magnitude lower than in the hydrous melt at 750°C. Zircon is able to fractionate geochemical twins such as Zr and Hf. Hf decrease in the melt is less pronounced than Zr decrease with decreasing temperature and thus hydrous melts at 750-800°C leaving the slab have a Zr/Hf significantly lower than the primitive mantle value. Aqueous fluids are very dilute in all trace elements and even LILE are higher in the residue than in the fluid. For example Ba is more than 10 times lower in the aqueous fluid than in the residue. This provides evidence that hydrous melts and not aqueous fluids are needed to significantly recycle incompatible elements from the slab to the mantle wedge. This observation provides evidence that top slab temperatures  $\geq 750^\circ\text{C}$  are required below arcs that show significant LILE and LREE enrichment or a Hf contribution from sediments.

## Validation of normalisation concepts for *in situ* $\mu$ -EDXRF data

Y. HERMANN<sup>1,2</sup>, A. WITTENBERG<sup>2</sup>, D. RAMMLMAIR<sup>2</sup>  
AND A. SCHWALB<sup>1</sup>

<sup>1</sup>Institut für Umweltgeologie, TU Braunschweig, Germany  
(y.hermanns@gmx.net)

<sup>2</sup>BGR, Hannover, Germany (a.wittenberg@bgr.de,  
rammlmair@bgr.de)

Column experiments were performed to study hard pan formation processes in mining dumps. The special focus of this study was to develop a better understanding concerning the time-dependent transport behaviour of element towards the capillary fringe. Therefore, three 50 cm long vertical columns were filled with homogenized tailings material from Freiberg/Germany (35cm) and purified silica sand (top part of column). At the bottom of the columns water is injected and because of capillary transport a continuously fluid transport occurs. The resulting changes in the local chemical conditions (e.g. Eh, pH) create the environment for dissolution, transport and precipitation. Hence, an enrichment of mobile behaving elements like Cu, Zn and Fe are expected to occur in the upper levels and accordingly a decrease within the bottom parts of the column.

The measurements were performed by using the  $\mu$ -EDXRF method, which has been described in detail by Rammlmair *et al* (2006). The experiment was set up for a period of six month. Within this time frame 20 runs were achieved to record the changes in the elemental concentrations. The results were calculated by using the Q-Spec 6.5 software (COX Analytical Systems).

There is no way to compare scans of different dates directly, since we haven't found a proper way to calibrate the method yet. In the frame of a student research project the collected  $\mu$ -EDXRF data are studied for comparison using various normalizing methods. Hence, effects due to e.g. matrix or water content changes can be shown.

### Reference

Rammlmair D., Wilke M., Rickers K., Schwarzer R. A., Möller A., and Wittenberg A. (2006) 7.6. *Geology, Mining, Metallurgy*. In *Handbook of Practical X-Ray Fluorescence Analysis* (ed. B. Beckhoff, B. Kanngießner, N. Langhoff, and R. Wedell), pp. 640-687. Springer.

## A high-resolution study of diatom oxygen isotopes in a Late Pleistocene to Early Holocene laminated record from Lake Chungará (Andean Altiplano, Northern Chile)

A. HERNÁNDEZ<sup>1</sup>, R. BAO<sup>2</sup>, S. GIRALT<sup>1</sup>, M.J. LENG<sup>3</sup>,  
P.A. BARKER<sup>4</sup>, J.J. PUEYO<sup>5</sup>, A. SÁEZ<sup>5</sup>, A. MORENO<sup>6</sup>,  
B. VALERO-GARCÉS<sup>7</sup> AND H.J. SLOANE<sup>3</sup>

<sup>1</sup>Institute of Earth Sciences 'Jaume Almera'-CSIC, C/Lluís Solé i Sabarís s/n, 08028 Barcelona, Spain

<sup>2</sup>Faculty of Sciences, University of A Coruña, Campus da Zapateira s/n, 15701 A Coruña, Spain

<sup>3</sup>NERC Isotope Geosciences Laboratory, British Geological Survey, Nottingham NG12 5GG, UK

<sup>4</sup>Department of Geography, Lancaster University, Lancaster LA1 1YB, UK

<sup>5</sup>Faculty of Geology, University of Barcelona, C/ Martí Franquès s/n, 08028 Barcelona, Spain

<sup>6</sup>Limnological Research Center, University of Minnesota, 310 Pillsbury Drive SE, Minneapolis, MN 55455, USA

<sup>7</sup>Pyrenean Institute of Ecology - CSIC, Apdo. 202, 50080 Zaragoza, Spain

Lake Chungará (18°15' S, 69°09' W, 4520 m a.s.l. 22.5 Km<sup>2</sup> and 40 m of water depth) is a hydrologically closed lake located on the Andean Altiplano. The lake is polymictic, meso to eutrophic and currently primary productivity is mainly governed by diatoms and chlorophytes.

Three laminated intervals were selected for detailed petrographical studies as well as a high resolution diatom oxygen isotope analysis. These laminated sediments are made up of bands of white and dark mm-thick laminae and thin layers of diatomaceous ooze with variable carbonates and amorphous organic matter.

Assuming no significant changes in the isotopic compositions of the water sources and according to the diatom microstratigraphy of the laminae, two alternating environmental scenarios can be described. Lower-level water conditions are interpreted during the intervals of white laminae deposition (high values of  $\delta^{18}\text{O}$ ), since those conditions are more favourable for the massive short-term deposition of monospecific large centric diatom blooms and  $\delta^{18}\text{O}$  enrichment. These white laminae are probably the result of exceptional periods of mixing of the shallow water column during lowstands, which recycle nutrients from the hypolimnion. Lower  $\delta^{18}\text{O}$  values, and therefore deeper water conditions, are more favourable for the development of dark laminae (normal annual cycle of the lake with alternating phases of stratification and mixing).

These conditions would lead to the development of a complex diatom community, among other algal groups.

## The energy balance at the core-mantle boundary

J. W. HERNLUND<sup>1</sup>, S. LABROSSE<sup>2</sup> AND N. COLTICE<sup>3</sup>

<sup>1</sup>Department of Earth and Ocean Sciences, University of British Columbia, Canada (hernlund@gmail.com)

<sup>2</sup>Laboratoire des Sciences de la Terre, Ecole Normale Supérieure de Lyon, CNRS, Université Lyon 1, France (stephane.labrosse@ens-lyon.fr)

<sup>3</sup>Laboratoire des Sciences de la Terre, Ecole Normale Supérieure de Lyon, CNRS, Université Lyon 1, France (coltice@univ-lyon1.fr)

Cooling of Earth's core occurs because relatively cool rocks sink to the core-mantle boundary (CMB) and absorb heat by conduction in a continuous cycle of sluggish mantle convection. A thermal boundary layer (TBL) is formed where heat is conducted from the core into the mantle and is characterized by an increased geothermal gradient in the D'' region. The recent discovery of post-perovskite (pPv) and increasing seismic evidence for a double-crossing of the pPv phase boundary by the TBL geotherm provides auspicious new constraints on the heat flow in D'', yielding lower bounds in the range 5-15 TW. However, if a several km thick layer of partially molten material just above the CMB was much thicker in the past when Earth's deep interior was hotter, then it is possible that the layer fractionally crystallized over time to achieve its present state and could therefore retain a significant budget of incompatible radioactive species. The power released by radioactivity (on the order of several TW) in this ultralow-velocity zone (ULVZ) layer would contribute to overall D'' heat flow and have potentially important consequences for the structure and dynamics of the mantle and core. Numerical models of mantle convection including a thin dense radioactive layer show that significant lateral variations in the thickness of the ULVZ arise which enhance variations in heat flux at the top of the core, with the thickest and hence most internally heated patches swept up beneath upwelling plumes. On the other hand, inclusion of larger modestly dense chemical piles (or "crypto-continents") moderates the excess heat that would otherwise be transferred into upwelling plumes.

## An integrated NMR and FTCIR mass spectroscopic study to characterize a new and major refractory component of (marine) natural organic matter (NOM) at the molecular level, CRAM: Carboxyl-rich alicyclic molecules

N. HERTKORN<sup>1</sup>, R. BENNER<sup>2</sup>, M. WITT<sup>3</sup>,  
M. FROMMBERGER<sup>1</sup>, PH. SCHMITT-KOPPLIN<sup>1</sup>,  
K. KAISER<sup>2</sup>, A. KETTRUP<sup>1</sup> AND I. J. HEDGES<sup>4</sup>

<sup>1</sup>GSF Research Center for Environment and Health, Institute of Ecological Chemistry, Ingolstaedter Landstrasse 1, D-85764 Neuherberg, Germany (hertkorn@gsf.de);

<sup>2</sup>Department of Biological Sciences and Marine Science Program, University of South Carolina, Columbia, SC 29208, USA (benner@biol.sc.edu);

<sup>3</sup>Bruker Daltonics, Fahrenheitstrasse 4, D-28359 Bremen, Germany (matthias.witt@bdal.de);

<sup>4</sup>School of Oceanography, Box 355351, University of Washington, Seattle, WA 98195-5351, USA (deceased).

Advances in organic structural spectroscopy have enabled a direct molecular level analysis of very complex natural mixtures such as the very abundant natural organic matter (NOM), a key contributor to the global carbon cycle and other element cycles (N, P, S,...). NOM often defines the chemical environment and the bioavailability of toxic and nutrient metal ions in the biosphere. Little is known about the chemical composition of NOM and the reason for its refractory nature.

Recently we have identified a new and major constituent of NOM, namely carboxyl-rich alicyclic molecules (CRAM), using nuclear magnetic resonance spectroscopy and ultrahigh resolution mass spectrometry [Fourier transform ion cyclotron mass spectrometry (FTICR-MS)]. CRAM are compositionally and structurally more heterogeneous than other NOM constituents (like peptides and carbohydrates), and are comprised of a complex mixture of carboxylated and fused alicyclic aliphatics with a carboxyl-C:aliphatic-C ratio of 1:2 to 1:7. The structural diversity found within CRAM and their substantial content of alicyclic rings and branching contribute to their resistance to biodegradation and refractory nature.

CRAM are expected to constitute a strong ligand for metal binding, and multiple coordination across cations could promote aggregation and marine gel formation thereby affecting CRAM reactivity and the bioavailability of nutrients and trace metals. It appears CRAM are ultimately derived from biomolecules with structural similarities to sterols and hopanoids. The occurrence of CRAM in freshwater and terrestrial environments seems likely, considering the global distribution of biomolecules and the similarities of biogeochemical processes among environments.

## Modelling the geochemical variation of granitic mushes

J. HERTOGEN AND J. MAREELS

Geo-Instituut, K.U.Leuven, Celestijnenlaan 200E, B-3001  
Leuven, Belgium (jan.hertogen@geo.kuleuven.be)

Straightforward Rayleigh-type fractional crystallisation models have merits to outline the main factors that caused geochemical evolutionary trends of granites, but the implied complete separation of mineral phases from residual liquid is at best a poor approximation of reality. A more elaborate crystallisation model of granitic 'mushes' tracks the trace element variation in two subsystems - a 'congealed mush' and a 'residual mush' - that develop as crystallisation proceeds. It takes into account any separation of less-viscous, water-rich melts and fluid phases from the residual mush during the final stages of solidification. Special attention is paid to the role of accessory minerals on the evolution of the Rare Earth Element (REE) patterns. Petrography learns that accessories are often present as clusters of minerals that crystallised from pockets of trapped interstitial melts. These accessory minerals crystallised too late to significantly affect fractionation trends. Moreover, these clusters frustrate efforts to estimate effective crystallisation rates from modal abundances. Parameters of the model are the fraction of crystals trapped in the congealed mush, and the crystal-to-trapped liquid ratio in the congealed mush. Calculations are based on a 'finite step' numerical simulation of crystallisation and melt expulsion processes.

The model calculations will be illustrated with results for two closely related leuco-granitic series from the Variscan Northern Vosges (France): the Natzwiller granite and the highly evolved Kagenfels granite. The variation trends of the Natzwiller granite demonstrate the crucial role of the accessory minerals apatite, sphene, allanite and zircon. The pronounced decrease of the concentrations of the middle REE (relative to Light and Heavy REE) of the Kagenfels granite cannot be explained by models based on reasonable values of modal abundances of accessory minerals and of partition coefficients. It is argued that the Kagenfels granite matches the composition of expelled liquids from the residual mush at 50 to 60 % solidification of the Natzwiller body. The expulsion of interstitial liquids is presumably promoted by tectonic activity.

## The first Lu-Hf garnet ages of North Penninic alpine eclogites

D. HERWARTZ<sup>1</sup>, C. MÜNKER<sup>1,2</sup>, E. E. SCHERER<sup>2</sup>,  
T. NAGEL<sup>1</sup>, J. PLEUGER<sup>1</sup> AND N. FROITZHEIM<sup>1</sup>

<sup>1</sup>Universität Bonn, Germany (danielherwartz@gmx.de)

<sup>2</sup>Universität Münster, Germany

Despite a large geochronological database there are still various models for the tectonic evolution of the Alps. Current rapid progress in dating metamorphic minerals such as garnet has given this technique a key role in the ongoing discussion. Recently, [1] recognized the so called Balma Unit in the upper Sesia valley, previously interpreted as part of the Zermatt-Saas Zone (South Penninic Ocean), as a fragment of the North Penninic Ocean. Most previous studies dating peak metamorphism of Alpine ophiolites have focussed on the Zermatt-Saas zone. Here, we present the first Lu-Hf garnet data for eclogites from the North Penninic Ocean.

Electron microprobe analyses show typical prograde zoning profiles in garnet. A selective digestion procedure for garnet was applied, where zircon and rutile inclusions are not dissolved. The garnet-whole rock Lu-Hf ages obtained for three samples are  $42.19 \pm 0.47$  Ma (MSWD: 1.8),  $43.19 \pm 0.36$  Ma (MSWD: 1.2) and  $45.4 \pm 1.1$  Ma (MSWD: 2.3), which is significantly younger than all Lu-Hf ages established so far for South Penninic Units. Notably, existing SHRIMP U-Pb zircon ages [2] of  $93.4 \pm 1.7$  Ma (syngmatic core) and  $40.4 \pm 0.7$  Ma (synmetamorphic rim) for the sample in which the Lu-Hf age of 42.19 Ma was obtained, indicate that growth of metamorphic zircon postdates garnet growth.

Despite the fact that all three samples originate from the same tectonic unit, their Lu-Hf ages differ outside of error. The cause of this is not yet known, but if the garnets grew over a long time interval (several million years) it is possible that varying core-to-rim distributions of Lu in garnet could result in the observed age range. Such Lu zoning can occur by Rayleigh fractionation during garnet growth [3] or by diffusion-limited garnet growth [4]. Our new Lu-Hf data indicate that garnet growth, and possibly peak pressure conditions in the North Penninic ophiolites postdates those in the South Penninic ophiolites.

### References

- [1] Pleuger J., Froitzheim N. and Jansen E., (2005), *Tectonics* **24**, TC4013, DOI 10.1029/2004TC001737.
- [2] Liati A. and Froitzheim N., (2006), *Eur. J. Min.* **18**, 299-308.
- [3] Lapen, T.J., Johnson C.M., Baumgartner L.P., Mahlen N.J., Beard B.L. and Amato J.M., (2003), *Earth Planet. Sci. Lett.*, **215**, 57-72.
- [4] Skora S., Baumgartner L.P., Mahlen N.J., Johnson C.M., Pilet S. and Hellebrand E., (2006), *Contrib. Mineral. Petrol.* **152**, 703-720.

## Convective Dissolution of CO<sub>2</sub> in Saline Aquifers

M.A. HESSE, A. RIAZ AND H.A. TCHELEPI

Department of Energy Resources Engineering, Stanford University (mhesse@stanford.edu; ariaz@stanford.edu; tchelepi@stanford.edu)

Dissolution of CO<sub>2</sub> into the brine is one of the major trapping mechanisms that increases storage security. The increase in density of the brine that occurs when CO<sub>2</sub> dissolves drives convective motion that enhances the dissolution rate of CO<sub>2</sub>. We present the results of a hydrodynamic stability analysis that describes the onset of convective motion. We have obtained expressions for the critical time necessary for the onset and the initial wavelength of the fastest growing disturbance. In high permeability aquifers onset of convection will be rapid (<1 yr), but wavelength are very small (~1 m). Resolution of these small length scales is a challenge standard reservoir simulators.

We present numerical results of the long term evolution of the convection in the brine and the dissolution rate of the CO<sub>2</sub>. The numerical simulations show three mass transport regimes, an early diffusive regime, followed by an infinite-acting convective regime, and finally a finite-acting convective regime. The infinite acting convection regime is characterised by a constant dissolution rate. The depth of the aquifer determines the duration of this highly efficient convective mass transfer regime. As the plumes of CO<sub>2</sub>-rich brine reach the bottom of the aquifer mass transfer decays rapidly, despite continued convective motion (finite acting convection).

We conclude that dissolution trapping will be an important mechanism in high permeability aquifers, because the onset time is short, the dissolution rate is high. In large aquifers the high infinite-acting dissolution rate can be maintained longer and therefore dissolution trapping will be more important in large aquifers.

### Reference

Riaz A, Hesse M. A., Tchelepi H. A., Orr Jr. F. M. (2006) Onset of Convection in a Gravitationally Unstable, Diffusive Boundary Layer in Porous Media. *J. Fluid Mechanics*, **548**, 87 - 111

## Microbial life in a hydrothermal spring rich in arsenic compounds

A. HETZER<sup>1</sup>, H. MORGAN<sup>1</sup>, I. McDONALD<sup>1</sup> AND C. DAUGHNEY<sup>2</sup>

<sup>1</sup>University of Waikato, Hamilton, New Zealand (hetzer.adrian@web.de)

<sup>2</sup>Institute of Geological and Nuclear Sciences, Lower Hutt, New Zealand (C.Daughney@gns.cri.nz)

The geothermal spring Champagne Pool in Waiotapu, New Zealand has an estimated volume of 50,000 m<sup>3</sup> and discharges fluid at 75° C, which is oversaturated with arsenic and antimony compounds such as orpiment (As<sub>2</sub>S<sub>3</sub>) and stibnite (Sb<sub>2</sub>S<sub>3</sub>) that precipitate and form orange deposits. Although Champagne Pool is geochemically well characterized only few studies addressed its role as a potential habitat for microbial life. In the current investigation, a combined approach of first culture-independent studies followed by culturing experiments was applied to describe microbial density and diversity within Champagne Pool. ATP measurements and epifluorescence microscopy showed relatively low biomass in Champagne Pool compare to other terrestrial hot springs within New Zealand and relatively low cell numbers of  $5.6 \pm 0.5 \times 10^6$  cells per ml. Denaturing Gradient Gel Electrophoresis and 16S rRNA gene clone libraries analyses indicated low microbial diversity and the abundance of hydrogen-oxidizing and sulfur-dependent populations, which were dominated by members belonging to the order *Aquificales*. On account of the results culture media were designed and two novel bacteria and a novel archaeon were successfully isolated. Experiments suggested that the observed relatively low biomass and biodiversity might be due to the presence of volatile components (H<sub>2</sub>S, methyl and hydride derivatives of arsenic and antimony) within the spring which are inhibiting microbial growth.

## Carbon isotopic compositions of acetate as proxies for biogeochemical processes in gas hydrate bearing sediments

VERENA HEUER<sup>1</sup>, JOHN POHLMAN<sup>2</sup>, MARCUS ELVERT<sup>1</sup>,  
AND KAI-UWE HINRICHS<sup>1</sup>

<sup>1</sup>Dept. of Geosciences, University of Bremen, 28359 Bremen,  
Germany (vheuer@uni-bremen.de,  
melvert@uni-bremen.de, khinrichs@uni-bremen.de)

<sup>2</sup>U.S. Geological Survey, Woods Hole, USA  
(jpohlman@usgs.gov)

A large fraction of methane in marine gas hydrates results from biogenic sources, but the processes that generate methane in the deeply buried sediments remain to be elucidated. IODP Expedition 311 drilled a transect across the Cascadia Margin, NE Pacific, to study the distribution and evolution of gas hydrates in an active continental margin. In our post-cruise research, we seek to identify processes and reactants involved in methane formation by compound-specific isotopic analysis (CSIA) of dissolved carbon-bearing compounds such as acetate. So far, deep pore-water profiles of acetate concentration are rare and  $\delta^{13}\text{C}$  values of acetate are largely lacking due to analytical obstacles.

Our recent survey of a wide range of natural sediments and sediment incubations has revealed a large variability in the carbon isotopic compositions of acetate and incubation experiments suggest a systematic link between the carbon isotopic composition of acetate and the dominant carbon transforming processes of the sediments, i.e., fermentation, methanogenesis and homoacetogenesis (Heuer *et al.*, 2006).

At the Cascadia Margin, both concentrations and  $\delta^{13}\text{C}$  of acetate vary considerably. Acetate concentrations increase from  $<5\ \mu\text{M}$  at the sediment-water interface to  $670\ \mu\text{M}$  at 250 meters below seafloor.  $\delta^{13}\text{C}$  values of acetate range from  $-50$  to  $-8\text{‰}$  vs VPDB. Given uniform  $\delta^{13}\text{C}$  values of dissolved organic carbon (DOC) close to  $-23\text{‰}$ , the low values of acetate require either partial production of acetate from a  $^{13}\text{C}$ -depleted pool of precursors such as biomass from methanotrophs or partial production of acetate by  $\text{CO}_2$  reduction (homoacetogenesis). On the other hand, the high values of  $\delta^{13}\text{C}$  of acetate in some hydrate-bearing sediment intervals likely point to acetoclastic methanogenesis as an important sink of acetate. CSIA of dissolved organic compounds provides novel information on the molecular-scale processes in deeply buried sediments that lead to formation of methane and ultimately methane hydrate.

### Reference

Heuer V., Elvert M., Tille S., Krummen M., Prieto Mollar X., Hmelo L. R., and Hinrichs K.-U., (2006), *Limnol. Oceanogr. Methods* **4**, 346-357.

## Biological fractionation of Ca isotopes ( $\delta^{44/40}\text{Ca}$ ): A study in Göttingen minipigs

A. HEUSER<sup>1</sup>, A. EISENHAEUER<sup>1</sup>, K.E. SCHOLZ-AHRENS<sup>2</sup>  
AND J. SCHREZENMEIR<sup>2</sup>

<sup>1</sup>IFM-GEOMAR, Kiel, Germany (aheuser@ifm-geomar.de)

<sup>2</sup>Institute of Physiology and Biochemistry of Nutrition,  
Federal Research Centre for Nutrition and Food, Kiel,  
Germany

Calcium is an essential element in human physiology and plays an important role in many processes. Due to its important role Ca concentrations are kept within small limits in the extracellular space. This Ca homeostasis is maintained by three organs, the gastrointestinal tract (input of Ca), the skeleton (store of Ca) and the kidney (output of Ca). Physiological ageing processes and many chronic diseases are associated with disturbances of the calcium metabolism.

In a study at the Federal Research Centre for Nutrition and Food several animal trials with the Göttingen miniature pig for generation of osteopathies have been carried out. The Göttingen miniature pig was chosen for these trials as their physiology is comparable to human physiology (e.g. Scholz-Ahrens *et al.*, 2007). We analyzed food, feces, blood, bone and urine samples of six animals from these trials in order to study the calcium metabolism with respect to stable Ca isotopes and their fractionation.

Feces had  $\delta^{44/40}\text{Ca}$  values similar to the  $\delta^{44/40}\text{Ca}$  of the semi-synthetic diet (0.42‰) or exhibit a fractionation which tends to result in lower  $\delta^{44/40}\text{Ca}$  values in feces. Blood  $\delta^{44/40}\text{Ca}$  values vary from 0.06‰ to 0.68‰ and are on average 0.68‰ heavier than the bone  $\delta^{44/40}\text{Ca}$  values (-0.60‰ to -0.03‰) This difference between the  $\delta^{44/40}\text{Ca}$  values of blood and bone is only half of the difference between soft and mineralized tissue reported by Skulan and DePaolo (1999).

$\delta^{44/40}\text{Ca}$  values of urine samples range from 2.05‰ up to 2.68‰ and are approximately 2‰ higher than the corresponding blood  $\delta^{44/40}\text{Ca}$  values of the same animal. Presumably, the observed fractionation between blood and urine mainly occurs in the kidney This enrichment of heavy Ca in urine may be due to preferential transport of  $^{40}\text{Ca}$  by Ca transporters in the renal tubules, by which more than 98% of the calcium of the primary urine is reabsorbed (Hoenderop *et al.* 2005) in a repetitive process.

### References

- Hoenderop J.G.J., Nilius B., and Bindels R.J.M. (2005) *Physiol. Rev.* **85**, 373–422.
- Scholz-Ahrens K.E., Delling G., Stampa B., Helfenstein A., Hahne H.J., Acil Y., Timm W., Barkmann R., Hassenpflug J., Schrezenmeir J., Glüer C.-C. (2007) *Am. J. Physiol. Endocrinol. Metab.* (April 24, 2007)
- Skulan J.L. and DePaolo D.J. (1999). *Proc. Nat. Acad. Sci.* **96**, 13709–13713.

## Continental crust as a source component for NW Central American Arc lavas?

K. HEYDOLPH<sup>1</sup>, K. HOERNLE<sup>1,2</sup>, F. HAUFF<sup>2</sup> AND P.V.D. BOGAARD<sup>1,2</sup>

<sup>1</sup>SFB 574 University of Kiel and Leibniz Institute for Marine Science (IFM-GEOMAR), Wischhof Straße 1-3, 24148 Kiel, GER (kheydolp@ifm-geomar.de)

<sup>2</sup>Leibniz Institute for Marine Sciences (IFM-GEOMAR), Wischhof Straße 1-3, 24148 Kiel, GER

Our group evaluates along and across arc geochemical variations from various volcanoes and volcanic centres in the NW Central American Volcanic Arc from NW Nicaragua to Guatemala. Additional data from several Guatemalan continental crust samples as well as Cocos Plate sediments help to clarify the potential endmember compositions for the observed trends.

Subduction input from the subducting Cocos Plate consists of carbonate to hemipelagic sediments, seawater altered and unaltered igneous crust and serpentinites. Slab dip decreases while the thickness of the continental crust increases beneath the volcanic front (VF) from a maximum in central Nicaragua to NW Guatemala. Continental crustal thickness also increases behind the VF.

Our comprehensive geochemical data set consists of major elements, a wide variety of trace elements and Sr-Nd-Pb-Hf-O isotope data. As shown previously by the Carr group, ratios of fluid mobile to less fluid mobile elements (e.g. Ba/La, Ba/Th and U/Th) decrease and Pb isotope ratios increase systematically from Nicaragua to Guatemala. The <sup>143</sup>Nd/<sup>144</sup>Nd and <sup>176</sup>Hf/<sup>177</sup>Hf isotope ratios decrease systematically from Nicaragua to Guatemala. These geochemical variations suggest a decreasing role for a hydrous fluid component and an increasing role for a sediment or continental crustal melt component in volcanic rocks towards Guatemala (NW) along the VF and behind the volcanic front (BVF). Samples from the back arc in Honduras have the most mid-ocean-ridge basalt (MORB) like compositions and are believed to represent the composition of the mantle wedge. Samples from the Nicaraguan VF have similar Nd but higher Sr isotope compositions most likely reflecting enrichment with slab derived fluids containing a subducted sediment or seawater Sr component.

A positive correlation in <sup>206</sup>Pb/<sup>204</sup>Pb vs. <sup>207</sup>Pb/<sup>204</sup>Pb isotope ratios for VF and BVF volcanic rock samples from El Salvador and Guatemala trends towards the granitic basement in Guatemala. Combined εNd vs εHf isotope data for VF and BVF samples from Nicaragua to Guatemala tend from high εNd and εHf MORB like compositions towards continental crust like compositions with increasingly lower εNd and εHf values. Supplementary εNd vs εHf isotope data from Guatemalan continental crust and Cocos Plate sediment samples provide further support for a continental crustal component in the generation of the NW CAVA magmas.

## Melt/wallrock interaction shown by silicate melt inclusions in peridotite xenoliths from Pannonian Basin

KÁROLY HIDAS<sup>1</sup>, CSABA SZABÓ<sup>1</sup>, TIBOR GUZMICS<sup>1</sup>, ENIKŐ BALI<sup>2,1</sup>, ZOLTÁN ZAJACZ<sup>3,1</sup> AND ISTVÁN KOVÁCS<sup>4,1</sup>

<sup>1</sup>Lithosphere Fluid Research Lab, Eötvös University Budapest, H-1117 Pázmány P. stny. 1/C, Budapest, Hungary (cszabo@elte.hu)

<sup>2</sup>Bayerisches Geoinstitut, University of Bayreuth, D-95447 Universitatstrasse 30, Bayreuth, Germany (eniko.bali@uni-bayreuth.de)

<sup>3</sup>Department of Earth Sciences, Institute of Isotope Geochemistry and Mineral Resources, ETH Zürich, 8092 Zürich, Switzerland (zajacz@erdw.ethz.ch)

<sup>4</sup>Research School of Earth Sciences, The Australian National University, ACT0200 Building 61 Mills Road, Canberra, Australia (istvan.kovacs@anu.edu.au)

### Samples

Primary silicate melt inclusions (SMI) in clinopyroxene (cpx) rims and secondary ones in orthopyroxenes (opx) along healed fractures from two equigranular amphibole-bearing spinel lherzolite xenoliths representing the subcontinental lithospheric mantle (Szigliget, Pannonian Basin, Hungary) have been studied. Microthermometry of dense CO<sub>2</sub>-bearing fluid inclusions, associated with SMI, was also carried out.

### Discussion

Electron microprobe analysis reveals in both xenoliths that cpx and opx are zoned, especially in terms of basaltic major elements. Cores of both cpxs show trace element distribution close to the primitive mantle. Rims display an overall enrichment with high positive anomalies in Th, U and moderate LREE content, as an indication for metasomatism. The pargasitic amphiboles, formed after rims of the cpx, exhibit elevated Rb, Ba, Nb, Ta and moderate LREE content. The SMI are composed mostly of silicate glass and dense CO<sub>2</sub> bubble. The primary SMI show evidence for significant crystallization on the wall of the host cpx. The major element composition of glass in SMI, regardless of xenoliths and host minerals, covers a wide range, mostly with trachyandesitic composition. The SMI, either primary or secondary ones, are extremely enriched in incompatible elements (particularly in U, Th, La, Zr) with a slight negative Hf anomaly.

### Conclusion

The development of zoned pyroxenes, and the trapping of primary SMI in the cpx rims happened after the partial melting and subsequent crystallization of cpxs, most probably due to an interaction between a hot volatile-rich mafic melt and mantle wallrock. This interaction resulted in evolved silicate melts, which filled microfractures in opxs, leading to the formation of secondary SMI and, via metasomatism, the development of zoned pyroxenes. Most probably the formation of amphiboles is not related to this evolution.

## Accessing the surface area of natural nanoparticles

TJISSE HIEMSTRA<sup>1</sup>, JUAN ANTELO, RASOUL RAHNEAIE,  
AND WILLEM H. VAN RIESMDIJK

<sup>1</sup>(tjisse.hiemstra@wur.nl)

Information on the reactive surface area of natural samples is essential for the application of surface complexation models (SCM). The PO<sub>4</sub>-CO<sub>3</sub> interaction on iron oxide is used to quantify the reactive surface area of soil particles. In the approach, phosphate is used to act as probe ion in natural samples brought at well-chosen solution conditions enforced by a 0.5 M NaHCO<sub>3</sub> extract solution. This matrix suppresses the influence of Ca<sup>2+</sup> ions, desorbs organic matter (further stimulated by adding active carbon), and fixes the pH and ionic strength, leading to dominance of the PO<sub>4</sub>-CO<sub>3</sub> interaction. Samples were equilibrated for solid/solution ratios between 1/6 and 1/300.

The CO<sub>3</sub>-PO<sub>4</sub> interaction is calibrated by studying it for goethite, using the CD model [1] with an Extended Stern (ES) double layer option. The CD values are independently obtained from MO/DFT optimized geometries of iron-carbonate and -phosphate complexes and are additionally corrected for dipole orientation effects [2]. The surface speciation derived from the data analysis of the CO<sub>3</sub>-PO<sub>4</sub> interaction on goethite agrees with ATR-FTIR spectroscopy.

Application to data of natural samples shows SA values from ~1000-10.000m<sup>2</sup>/kg soil. The SA correlates to the organic matter (OM) content of the samples, which is due to the correlation of OM with the Fe oxide fraction, suggesting that the natural oxide particles are embedded in an OM matrix. Scaling of SA on the experimental soil oxide contents shows high values for the specific surface area (~200-900 m<sup>2</sup>/g extracted oxide), pointing to the presence of nanometer-sized particles (~1-5 nm).

### References

- [1] Hiemstra, T.; Van Riemsdijk, W. H. A surface Structural Approach to Ion Adsorption: The Charge Distribution (CD) Model *J. Colloid Interf. Sci.* 1996, **179**, 488-508.
- [2] Hiemstra, T.; Van Riemsdijk, W. H. On the relationship between charge distribution, surface hydration and the structure of the interface of metal hydroxides *J. Colloid Interf. Sci.* 2006, **301**, 1-18.

## In situ Hf and O isotopic data from Archean zircons of SW Greenland

J. HIESS<sup>1</sup>, V. BENNETT<sup>1</sup>, A. NUTMAN<sup>2</sup> AND  
I.S. WILLIAMS<sup>1</sup>

<sup>1</sup>Research School of Earth Sciences, The Australian National University, Canberra, Australia (joe.hiess@anu.edu.au; vickie.bennett@anu.edu.au; ian.williams@anu.edu.au)

<sup>2</sup>Chinese Academy of Geological Sciences, Beijing, China (nutman@bjshrimp.cn)

We have obtained new, coupled U-Pb, O and Hf isotopic data from Archean TTG suites in Southwest Greenland in order to explore mechanisms for Archean tonalite genesis and crust formation. The dataset comprises analyses of >250 zircon spots from 11 rocks ranging in age from 3.85 Ga to 2.55 Ga, including the most ancient tonalites of the Itsaq Gneiss Complex through to late Archean granitoids of the Qôrqt Granite Complex. All grains were characterized by CL, reflected and transmitted light imaging prior to analysis. U-Pb ages were determined using either SHRIMP RG or SHRIMP II; <sup>18</sup>O/<sup>16</sup>O ratios were measured on the same zircon spots using SHRIMP II in multi-collector configuration; <sup>176</sup>Hf/<sup>177</sup>Hf data was subsequently acquired by LA-MC-ICPMS (ANU Neptune).

Zircons from the oldest, ca. 3.85 Ga, tonalites record δ<sup>18</sup>O compositions within 1‰ of mantle values (δ<sup>18</sup>O mantle = 5.3 ± 0.3 [e.g. 1]) and initial ε<sub>Hf</sub> values largely within ±1 epsilon unit of chondritic composition (calculated using λ<sup>176</sup>Lu = 1.867×10<sup>-11</sup>yr<sup>-1</sup>). These narrow, mantle-like, O-Hf fields contrast markedly with results from studies of Phanerozoic suites [2, 3], which show diverse Hf-O isotopic arrays, displaced from mantle compositions.

Hf isotopic compositions of zircons from the youngest sample analysed, the 2.55 Ga Qôrqt Granite Complex (initial ε<sub>Hf</sub> ≈ -25), are in agreement with earlier Pb isotopic studies [4] suggesting the origin of the Complex by the remelting of >3.7 Ga crust. The O isotope data from this suite however lie 1-2‰ below mantle compositions, again in contrast with results for Phanerozoic suites.

A striking feature of the overall dataset is the absence of high (>7‰) δ<sup>18</sup>O values highlighting the lack of recycled supracrustal material in the genesis of the TTG. Of particular note is the prevalence of low δ<sup>18</sup>O values, with 4 out of 11 samples, with ages from 3.7 to 2.55 Ga, having compositions 1-3‰ below mantle values. Low δ<sup>18</sup>O values are a relatively rare feature in granitic suites (e.g. [1]) and typically result from hydrothermal alteration by surface waters, in some cases enhanced by glaciation. The presence of low δ<sup>18</sup>O in these mid-crustal level Archean granitoids is unexpected and may reflect different surface conditions and hence fluid compositions in the Archean.

### References

- [1] Valley J.W., *et al.*, (2005), *CMP* **150** 561-580.
- [2] Kemp A.I.S., *et al.*, (2006), *Nature* **439** 580-583.
- [3] Kemp A.I.S., *et al.*, (2007), *Science* **315** 980-983.
- [4] Moorbath S. and Taylor P.N. (1981), In: Kroner (Ed.), *Precambrian Plate Tectonics*. Elsevier 491-525.

## Confocal micro-Raman spectroscopy: A tool for the allocation of organic and inorganic components in calcified biominerals

S. HILD<sup>1</sup>, U. SCHMIDT<sup>2</sup> AND A. ZIEGLER<sup>1</sup>

<sup>1</sup>Central Facility for Electron Microscopy; University of Ulm,  
Albert-Einstein-Allee 11, D89081 Ulm

<sup>2</sup>WITec Wissenschaftliche Instrumente und Technologie  
GmbH, Hoervelsinger Weg 6, D89081 Ulm

Mineralized biological composites have attracted increasing interest because of their outstanding mechanical properties that are well adapted to their function. Microcharacterization of these materials allows a better understanding of the structure-properties relationship of these materials. Since the mineralized exoskeleton (cuticle) of crustaceans is composed of various types of calcified biominerals e.g. calcium phosphate, calcite, and amorphous calcium carbonate (ACC) embedded in a chitin matrix this material is an excellent model for a biocomposite. High resolution scanning electron microscopy has been extensively used to investigate the morphology of the crustacean cuticle. However, to allocate of the spatial resolution of the various organic and inorganic components an additional chemical characterization is required. Scanning confocal  $\mu$ -Raman spectroscopy (SC $\mu$ -RS) provides complementary important information about the spatial distribution of both the organic and the inorganic components because the Raman spectrum can be unequivocally attributed to a certain compound even when its concentration is very low. Additionally, SC $\mu$ -RS enables one to allocate the different calcium carbonate polymorphs.

For these studies the cuticle of the terrestrial isopod *Porcellio scaber* is used as a model system. The spatial distribution of minerals, elements, and organic compounds was studied on the sub-micrometer scale using cross sections of the cuticle. Calcite and amorphous calcium carbonate (ACC) were found to be the main biominerals within the cuticle. For the first time, it was shown that the minerals are arranged in distinct layers. Calcite is restricted to the outer area of the cuticle, whereas ACC is localized in the middle having only little overlap with the calcite layer. The proximal region of the cuticle mainly consists of chitin. Since the cuticle is subjected to periodic molting it is periodically decalcified and shed. A new larger cuticle, synthesized before shedding, is mineralized after every molt. These processes cause spatial and temporal variations of the mineral distribution. The change in mineral during the molting cycle was monitored with respect to the organic matrix. It was shown that the protective outer calcite layer is shed away during each molt, while ACC is recycled to quickly re-establish the protective calcite layer in the new cuticle. Thus, ACC is used as a transient reservoir for calcium and carbonate ions.

## Demonstrating equilibrium Fe-isotope fractionation in Fe-Cl solutions

P.S. HILL, E.A. SCHAUBLE, E.D. YOUNG AND  
A. SHAHAR

Dept Earth and Space Sciences, UCLA (phill@ess.ucla.edu)

A major problem when conducting isotopic fractionation experiments in aqueous solutions is determining if isotopic equilibrium has been reached. We have successfully demonstrated the attainment of equilibrium isotopic fractionation in a two-phase aqueous/ether system containing a mixture of Fe-Cl complexes, using the Fe three-isotope equilibrium method of Shahar *et al.* (2006; Matsuhisa *et al.*, 1978). The immiscible liquid/spiked reversal procedure should also be applicable to other aqueous systems. These reversal experiments are part of our continuing integrated theoretical and experimental studies of the effects of changing bond environments on Fe fractionation. We use aqueous Fe-Cl complexes as an example of possible Fe-ligands because of the structural similarity of chloride to other potential iron-ligands, such as sulfides (e.g., pyrite, FeS<sub>2</sub>) and small organic ligands (e.g., rubredoxin, FeS<sub>4</sub>R<sub>4</sub> similar in structure to tetrahedral FeCl<sub>4</sub><sup>-</sup>), and the tractability of chloride in aqueous experiments.

Our experiments consist of a series of low pH solutions of ferric chloride, with total chlorinity varying from 0.5 to 5.0 M, to which an equal amount of immiscible diethyl ether has been added. As the aqueous-ether mixture equilibrates, FeCl<sub>4</sub><sup>-</sup>, the only Fe-Cl complex soluble in the ether, moves from the aqueous into the ether phase. We use measurements of  $\delta^{56}\text{Fe}(\text{aq}) - \delta^{56}\text{Fe}(\text{ether})$ , in conjunction with a speciation model, to determine the relative fractionations among the complexes. At [Cl<sup>-</sup>]=1M the aq-ether fractionation is ~0.8%.

To establish the attainment of equilibrium between the ether and aqueous phases, we paired an aq/ether mixture of unspiked <sup>56</sup>Fe/<sup>54</sup>Fe with an equivalent mixture prepared with <sup>54</sup>Fe spike. Once both mixtures had equilibrated, half the ether from the spiked experiment was added to the ether of the normal Fe experiment, so that spiked FeCl<sub>4</sub><sup>-</sup> from the ether phase would have to pass into the aqueous phase of the unspiked experiment to reach equilibrium. We removed small aliquots from both the ether and aqueous phases after 20, 30, and 40 minutes, without disturbing the equilibrium of the mixture, and measured the aqueous-ether fractionation.

At 20 minutes, the ether and aqueous solutions were ~80% equilibrated, and they were totally equilibrated by 30 minutes. Equilibrium was demonstrated by the reversal in two ways: 1) both the aqueous and ether phases arrived at the same mass fractionation line; and 2) the final aqueous-ether fractionation of the reversal experiment was ~0.8%, in agreement with the unspiked forward experiments.

### References

- Shahar A., Manning, C.E. and Young, E.D. (2006) *EOS Trans AGU 87*, Fall Meet. Suppl., Abstract V13E-03;  
Matsuhisa, Y., Goldsmith, J.R., and Clayton, R.N. (1978) *Geochim. Cosmochim. Acta* **42**, 173-182.

## Potassium as a heat source in the core? Metal-Silicate partitioning of K and other alkali metals

VALERE J. HILLGREN, BEATE SCHWAGER AND  
REINHARD BOEHLER

Max Planck Institut für Chemie, Postfach 3030, 55020 Mainz,  
Germany [hillgren@mpch-mainz.mpg.de]

The alkali metals (Li, Na, K, Rb, and Cs) are depleted to varying degrees in the Earth's upper mantle. This is generally assumed to be due to volatility of these elements during accretion of the Earth. However, it is also often argued that some amount of K may have partitioned into the core and act as an additional heat source for the core dynamo. If K could partition into the core, it is not unreasonable to assume that the other alkali metals might also do so. Therefore, we have begun an experimental study of the partitioning of K and the other alkali metals between metals and silicates at lower mantle conditions using the laser-heated diamond anvil cell.

Our samples consisted of either pure Fe-metal or an Fe-S mix containing 10 wt. % S surrounded by either a K-silicate glass, a (Li, Na, K, Rb, Cs)-silicate glass, or a mixture of a (Na, K, Rb, Cs)-silicate glass and San Carlos olivine and overlain by an Al<sub>2</sub>O<sub>3</sub> disk (to act as an optical window and to insulate the sample from the diamond). Pressures for the runs ranged from 23 to 110 GPa, and the temperatures for each sample were above the melting point of Fe for that pressure. Samples were recovered, polished and analyzed with the electron microprobe.

Experiments with pure Fe-metal and K-silicate glass in the pressure range 38-77 GPa showed no pressure dependence for the partitioning of K into metal. They also implied a maximum of 5 ppm K in the core.

Results from the experiments with the alkali-silicate glass or alkali-silicate glass mixed with olivine and Fe or Fe-S mix suggest that all the alkalis partition more readily into a sulfide than pure metal, and we found the general trend that  $D_{\text{MET/SIL}}$  for Na > K ≥ Cs > Rb. However, under all conditions all the alkalis remained distinctly lithophile, and even at 110 GPa and 3200 K with 5 wt. % S and 1.5 wt. % O in the metal, the results suggest no more than 10 ppm K in the Earth's core. Thus, K could only be responsible for less than 1% of the core's heat budget.

## Helium isotope studies in seismically-active regions of Turkey and California

D.R. HILTON<sup>1</sup>, G. DE LEEUW<sup>1</sup>, E. FUERI<sup>1</sup>, N. GULEC<sup>2</sup>,  
H. MUTLU<sup>3</sup>, M.D. TRYON<sup>1</sup> AND K.M. BROWN<sup>1</sup>

<sup>1</sup>Scripps Inst. Oceanography, La Jolla, CA, USA  
(drhilton@ucsd.edu; gdeleeuw@ucsd.edu;  
efueri@ucsd.edu; mtryon@ucsd.edu;  
kmbrown@ucsd.edu)

<sup>2</sup>METU, Ankara, Turkey (nilgun@metu.edu.tr)

<sup>3</sup>Osmangazi University, Eskisehir, Turkey  
(hmutlu@ogu.edu.tr)

He isotopes in groundwaters and geothermal fluids are sensitive indicators of crustal-mantle interaction. Here, we present new He isotope (and associated carbon) data from two of the world's great fault systems - the North Anatolian Fault Zone, Turkey (NAFZ) and the San Andreas Fault, California (SAF) - to further utilize He isotopes in regions of crustal unrest.

Following the catastrophic earthquakes in 1999, we initiated a periodic monitoring program (4 times/yr for 3 yrs) targeting geothermal fluids at 9 localities along an 800-km stretch of the NAFZ. <sup>3</sup>He/<sup>4</sup>He ratios vary between 0.29 R<sub>A</sub> (Yalova, Gozlek) and 2.2 R<sub>A</sub> (Mudurnu) (R<sub>A</sub> = air <sup>3</sup>He/<sup>4</sup>He) indicating a magmatic He contribution throughout. There were no large earthquakes over the monitoring period and little variation in <sup>3</sup>He/<sup>4</sup>He values at individual localities. However, there are significant changes in the CO<sub>2</sub>/<sup>3</sup>He ratio and especially δ<sup>13</sup>C. We discuss these changes with respect to the regional stress pattern in Turkey.

Mantle-derived He is also pervasive in the vicinity of the SAF: <sup>3</sup>He/<sup>4</sup>He reaches 0.11 R<sub>A</sub> (Mojave River Basin); 0.26R<sub>A</sub> (East Morongo Basin) and 3.4 R<sub>A</sub> (Monterey Bay). The whole region adjacent to the SAF is therefore leaking mantle-derived He to the surface albeit heavily diluted with crustal He. At Monterey Bay, cold seep fluids collected in long Cu-coils preserve temporal variability in He isotopes. This technique has enormous potential in future monitoring studies of earthquake-prone regions as it produces a continuous record of He isotope and gas chemistry variations.

## Accessory mineral dating by ims-1270 ion microprobe

R. W. HINTON

Edinburgh Ion Microprobe Facility (EIMF), Grant Institute of  
Earth Science, University of Edinburgh, West Mains  
Road, Edinburgh, EH9 3JW, UK;  
(Richard.Hinton@ed.ac.uk)

A number of accessory minerals concentrate small amounts of U and Th and if they (initially) contain very little Pb they will be amenable to ion microprobe analysis. Each mineral presents different analytical problems not the least of which is the identification of well characterised standards. Changes between analyses in the ionisation and detection of  $Pb^+$  relative to  $U^+$  ions (i.e. in the  $Pb^+/U^+$  ratio) do occur but can be shown to correlate with measured  $UO^+/U^+$  ratios and corrections applied. At the EIMF we believe that measurement of a second molecular species e.g.  $UO_2^+$  or  $ThO_2^+$  can improve the correction procedures or, at least, be simply used to give confidence in the correlating ratios. Routinely, Pb, U, UO, ThO and  $UO_2$  are all measured.

In monazite the high Th/U ratios make it possible to utilise both U and Th decay systems. Corrections are applied using a combination of Pb, Th, ThO and  $ThO_2$  peaks. In the work to date monazite has given good reproducibility in the Pb/Th system but some open system behaviour has been observed in the Pb/U system.

Rutile, like zircon, gives good correlations for Pb/U vs UO/U or  $UO_2/UO$  ratios. However, this phase discriminates so strongly against Th that in some cases no Th signal can be detected and any  $^{208}Pb^+$  signal can be assumed to be common Pb. The total background common Pb, either that originally incorporated in the mineral or that added to the surface during sample preparation, can be shown to be less than 1 ppb (and  $^{204}Pb$  less than 0.03 ppb). This increases the confidence that dating rutile with relatively low U content (<5 ppm) should be possible.

Baddeleyite is the only mineral analysed so far where variations in the Pb/U ratio have been shown to be dependent on crystal orientation (Wingate and Compston, 2000). Similar effects have been observed in baddeleyite analyses made on the Edinburgh ion probe. Future EBSD work will be used to study the effects of crystallographic orientation and whether corrections can be systematically applied.

### Reference

Wingate M.T.D. and Compston W., (2000), *Chem. Geol.* **168**, 75-97.

## The origin of compositional variation of mafic magma and genesis of associated silicic magma in the Shirataka volcano, NE Japan: Constraints from Sr isotopic compositions of mafic inclusions and their hosts, with detailed petrologic features of the mafic inclusions

SHIHO HIROTANI<sup>1</sup>, MASAO BAN<sup>2</sup> AND  
MITSUHIRO NAKAGAWA<sup>3</sup>

<sup>1</sup>Graduate School of Science and Engineering, Yamagata  
University, Japan (ss073@kdw.kj.yamagata-u.ac.jp)

<sup>2</sup>Department of Earth and Environmental Science, Faculty of  
Science, Yamagata University, Japan  
(ban@sci.kj.yamagata-u.ac.jp)

<sup>3</sup>Graduate School of Science, Hokkaido University, Japan  
(nakagawa@mail.sci.hokudai.ac.jp)

Eruptive products of Shirataka volcano (0.9-0.7 Ma) in NE Japan are calc-alkaline andesite-dacite (57-66%  $SiO_2$ ), and are divided into six petrologic groups (G1-6). Mafic inclusions, basalt-andesite (48-58%  $SiO_2$ ), are always observed in G1, G2, G5 and G6.

All rocks are mixing rocks formed by mixing/mingling between mafic and silicic end-members judging from many petrologic aspects, such as linear trends defined by hosts and inclusions in variation diagrams and coexistence of mafic and silicic magmas origin phenocrysts in each group. The mixing trends defined by hosts and inclusions are divided into high- and low-Cr-Ni types, and both types coexist in G1, G2 and G5. Cr and Ni contents of the high type show some variation. Estimated mafic end-members are high-Cr-Ni (1120-1150°C, 47-52%  $SiO_2$ , Fo-rich olv±Mg-rich cpx±An-rich plg) and low-Cr-Ni type magmas (ca.1100°C, 48-52%  $SiO_2$ , Mg-rich cpx±An-rich plg), while the silicic end-members of both types have similar petrologic features in the same petrologic group (790-840°C, 63-68%  $SiO_2$ , hbl±qtz±Mg-poor px±An-poor plg). The high-Cr-Ni type mafic end-member magma is richer in compatible elements and poorer in incompatible elements than the low type one. Besides,  $^{87}Sr/^{86}Sr$  data of all rocks show broad ranges (0.70377-0.70537), but the compositional range of each group is restricted. In each petrologic group, the high-Cr-Ni type mafic and associated silicic end-members have lower values in  $^{87}Sr/^{86}Sr$  ratio than the low type ones, indicating that mafic and silicic end-members in the same type have co-genetic relationships. The MELTS and trace element model calculations suggest that the low-Cr-Ni type mafic end-member magma can be produced through <25% fractional crystallization (olv±cpx±plg) from the high-Cr-Ni type mafic end-member magma accompanied with the assimilation of basement plutonic rocks ( $r=0.03-0.07$ ). In terms of associated silicic magmas, the trace element model calculations indicate that the silicic magmas can be produced through <30% partial remelting of corresponding solidified mafic magmas leaving a gabbroic residue.

## Carbonatite-mantle interaction in the formation of highly alkalic oceanic island basalts

MARC M. HIRSCHMANN<sup>1</sup> AND RAJ DASGUPTA<sup>2</sup>

<sup>1</sup>Dept. of Geology and Geophysics, University of Minnesota, Minneapolis, MN 55455 USA  
(Marc.M.Hirschmann-1@umn.edu)

<sup>2</sup>Lamont-Doherty Earth Observatory, Columbia University, Palisades, NY 10964, USA (rajdeep@ldeo.columbia.edu)

In heterogeneous basalt source regions, variations in mantle composition correspond to variations in melt production, leading more enriched compositions to produce partial melts at depths where more refractory lithologies do not. Migrating melts from easily melted heterogeneities can enrich refractory surroundings, which may subsequently partially melt. Thus, there is a direct link between heterogeneity and metasomatism in basalt source regions. In the source regions of oceanic islands, carbonated lithologies partially melt to form small amounts of carbonatite at >300 km. These highly mobile melts react with mantle rocks at shallower depths to form carbonated silicate liquids. Experiments show that these silicate partial melts are stabilized in peridotite and eclogite ~130 °C and ~250 °C cooler, respectively, than the volatile-absent peridotite solidus (Dasgupta *et al.*, 2006; 2007). Thus, migrating carbonatite produces carbonated silicate liquids when it encounters eclogite bodies at depths of >150 km. Such melts may metasomatize surrounding peridotite, which can produce highly alkalic carbonated magmas at depths of 90-150 km that are compositionally similar to basanites, nephelinites, and melilitites common in many OIB localities. Such magmas are expected where potential temperatures are not much greater than those in the MORB-source mantle (weak plumes, the margins of hotter plumes, or petit spots). Implantation of small-degree partial melts produces peridotite that is enriched in highly incompatible elements and that has isotopic signatures of crustal recycling, characteristics typical of sources of highly alkalic OIB.

### References

- Dasgupta, Hirschmann, M.M., and Stalker, K. (2006) *J. Petrol.* **47**, 647-571.  
Dasgupta, R. Hirschmann, M.M., and Smith, N. (2007) *Geology* **35**, 135-138

## How nanoscience has changed our understanding of environmental geochemistry

M.F. HOHELLA, JR.

NanoBioEarth, Department of Geosciences, Virginia Tech, Blacksburg, Virginia, USA (hochella@vt.edu)

Naturally occurring nanoscale materials, many containing trace elements, appear to be ubiquitous in the environment, and it can be hypothesized that due to their behaviour which is unlike both molecules and bulk materials, they play roles that have not yet been appreciated, or even realized. More specifically, nanoscale particles, films, and/or confined fluids are present throughout the Critical Zone, and in the atmosphere and oceans. And it has been well established that the structural and electronic properties of these materials change, often dramatically, as a function of their size in the nanorange. As a result, chemical and physical properties of nanomaterials change as a function of size (in the case of particles) or thickness (in the case of films). Yet we do not understand these nanomaterials very well, even from a fundamental physical chemistry point-of-view. Nevertheless, it is straight forward to hypothesize about their importance because it is becoming more common to observe their deviant behavior (relative to the same material at a larger scale) in laboratory and field studies in both biologically and abiotically dominated systems. In addition, because of the minute sizes involved, the interface to bulk ratios are extremely large in these nanoscale components of bulk systems, and therefore interfaces become even more important than usual. Critical insights into local, regional, and even global phenomena await our understanding of processes that are relevant at the smallest scales of Earth science studies. More and more investigators are beginning to uncover a fascinating story of how the immense surface area, unusual properties, and widespread distribution of natural nanomaterials affect Earth phenomena in ways that are surprising.

## Chromite-rich cumulates in mafic xenoliths, São Vicente, Cape Verde Islands

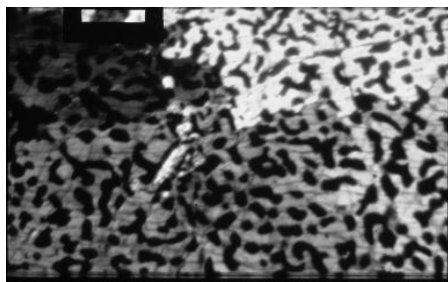
B. HOEJSTEEN<sup>1</sup> AND P.M. HOLM<sup>2</sup>

<sup>1</sup>(b.hoejsteen@webspeed.dk)

<sup>2</sup>Institute of Geography and Geology, University of Copenhagen, Øster Voldgade 10, DK-1350 Copenhagen, Denmark

Mafic xenoliths from two basanitic lavas at São Vicente have mineral compositions and textures indicating that they could be early cumulates, fractionated from magmas similar to the host of the xenoliths. In one of these lavas some xenoliths accumulated up to 25% anhedral chromite in poikilitic olivine (mg# 83-86) and ferri-titan-chromdiopside

The shape of the chromite grains as well as their high concentration has not been reported from other xenoliths from the Cape Verde Islands. We have puzzled our brains over their origin.



The chromites have cr# and  $fe^{2+}$ # ~ 40-60 and are relatively rich in Ti and  $Fe^{3+}$ . Such composition is known from chromite in kimberlites and is thought to be a result of fluid release from the magma during decompression. The anhedral shape could form either

1. By early precipitation and later partly dissolution of chromite in the magma. Complete dissolution of chromite was avoided by the high concentration of chromite buffering the melt, or 2. Matveev and Balhaus reports an experiment on an olivine and chromite saturated basaltic melt which holds sufficient  $H_2O$  (> 4 %  $H_2O$ ) to release fluid when decompressed. Chromite then precipitated as pearls inside the fluid bubbles. They rose towards the top of the magma chamber until the bubbles got overloaded with chromite and sunk. This could be the explanation for the shape and concentration of the São Vicente xenoliths although the chromite concentration maybe never passed the critical mass limit but kept flowing. Based on the primitive nature of olivine and clinopyroxene and because the necessary water may have been present we prefer the second solution.

### References

- Matveev S. and Ballhaus C. (2002). *Earth and Planet. Sci. Lett.* **203**, 235-243.  
 Roeder P.L. and Reynolds I. (1991). *Journal of Petrology* **32**, 5, 909-934.

## Comparison of laser ablation and micromill sampling techniques for MC-ICPMS $^{230}Th$ - $^{234}U$ - $^{238}U$ measurements on speleothems

DIRK L. HOFFMANN<sup>1</sup>, CHRISTOPH SPÖTL<sup>2</sup> AND AUGUSTO MANGINI<sup>3</sup>

<sup>1</sup>Bristol Isotope Group, University of Bristol, Bristol, UK (dirk.hoffmann@bristol.ac.uk)

<sup>2</sup>Institut für Geologie und Paläontologie, Universität Innsbruck, Innsbruck, Austria (christoph.spoetl@uibk.ac.at)

<sup>3</sup>Heidelberger Akademie der Wissenschaften, Heidelberg, Germany (augusto.mangini@iup.uni-heidelberg.de)

*In situ* laser ablation (LA) MC-ICPMS can be used to achieve U-series isotope measurements at very high spatial resolution without prior chemical separation procedures. However, matrix effects especially for mass and elemental fractionation pose significant problems for accurate determinations of  $^{230}Th$ - $^{234}U$ - $^{238}U$  ratios.

Procedures for accurate determinations of U-series isotope ratios using *in situ* laser ablation (LA) and MicroMill techniques for carbonates such as speleothems are presented. For LA analyses we are using a New Wave UP193HE laser and a new multiple ion counting detector system available for the ThermoFinnigan Neptune MC-ICPMS. Multiple ion counting increases the efficiency of low level ion beam collection by allowing simultaneous collection of all ion beams and also circumvents problems associated with unstable, transient beams. We present details of our measurement setup for LA measurements and the correction procedures for instrumental fractionation effects using a matrix matching carbonate standard.

We compare results of LA U-series measurements on a U rich (40 - 90  $\mu g/g$ ) speleothem from Spannagel Cave (Austrian Alps) to results on samples from the same speleothem section prepared using a New Wave MicroMill and processed through separation and purification solution chemistry. For laser ablation results, we currently obtain precisions of  $^{230}Th/^{238}U$  in the range of 3 % ( $2\sigma$ ), the solution analyses yield more precise  $^{230}Th/^{238}U$  isotope ratios in the range of 1 %. Accuracy is assessed by comparison to conventional MC-ICPMS and TIMS measurements.

Key advantages of our LA technique are, for example, a matrix matching calibration standard, high spatial resolution analyses and the possibility of rapid determination of numerous coeval subsamples. We also demonstrate that LA measurements yield accurate but less precise results on speleothem samples with less than 1  $\mu g/g$  U. The results on MicroMill samples are more precise but this sample preparation technique is time consuming and for a single measurement a bigger sample size is needed. For solution U-series MC-ICPMS measurements a minimum total load of about 5 ng for  $^{238}U$  and about 10 fg for  $^{230}Th$  should be used.

## Evidence for Hadean mantle depletion in the sources of ~3.75 Ga subduction-related rocks, Isua, SW Greenland

J.E. HOFFMANN<sup>1,2</sup>, C. MÜNKER<sup>1,2</sup>, A. POLAT<sup>3</sup> AND K. MEZGER<sup>2</sup>

<sup>1</sup>Universität Bonn, Germany (joerg.elis.hoffmann@gmx.de; muenker@uni-bonn.de)

<sup>2</sup>Universität Münster, Germany (klaush@uni-muenster.de)

<sup>3</sup>University of Windsor, Canada (polat@uwindsor.ca)

The Hf isotope compositions of Earth's oldest zircons provide growing evidence that crust-mantle differentiation started as early as 4.4 Ga. Yet, the size of these differentiated Hadean reservoirs and their persistence over Earth's history are still under debate. Lu-Hf studies on zircons younger than 3.8 Ga do not reveal any evidence for the long term presence of ancient depleted mantle reservoirs [e.g. 1].

Rocks from the ~3.71-3.81 Ga Isua supracrustal belt (ISB) comprise the oldest preserved record of mafic crustal material, thus potentially providing evidence for any large scale mantle depletion in the early Archean. Here, we report Hf and Nd isotope data for the least altered samples from a suite of ~3.75 Ga old, submarine boninite-like metabasalts from the central tectonic domain of the eastern ISB [2]. These metabasalts are among Earth's oldest preserved subduction related rocks [2]. They were metamorphosed under amphibolite to greenschist facies conditions.

Initial  $\epsilon_{\text{Hf}}$  values of the boninite-like metabasalts range from -1.3 to +7.9. The samples have  $^{176}\text{Lu}/^{177}\text{Hf}$  values as high as 0.9, indicating a previous depletion of the mantle source(s) in the garnet stability field. These  $\epsilon_{\text{Hf}}$  values are clearly of primary origin, as the initial  $\epsilon_{\text{Hf}}$ ,  $\epsilon_{\text{Nd}}$  and  $\gamma_{\text{Os}}$  [3] correlate with major and trace elements [2], exhibiting a magmatic differentiation trend. All samples follow AFC curves, suggesting assimilation of up to 30 % enriched crustal material, possibly marine sediments or igneous rocks with TTG-like composition. Two different parental mantle sources can be identified: one has an initial  $\epsilon_{\text{Hf}}$  value of ca. +7.9 and the other of ca. +1.3. In order to have an initial  $\epsilon_{\text{Hf}}$  of +7.9, a source must have an old and strong depletion in incompatible elements. Hence the presence of a complementary enriched component is required, which may be the earliest continental crust. These results provide the first evidence from mafic Archean rocks for the persistence of Hadean mantle depletion into the early Archean. As other ISB rocks do not display such strongly depleted initial  $\epsilon_{\text{Hf}}$  values, the volume of these depleted mantle domains was probably small.

### References

- [1] Amelin *et al.* (1999), *Nature* **399**, 252-255.
- [2] Polat, A. *et al.* (2002), *Chem. Geol.* **184**, 231-254.
- [3] Frei, R. *et al.* (2004), *GCA* **68**, 1645-1660.

## Is D'' a low-mu reservoir?

A.W. HOFMANN<sup>1,2</sup>, S.L. GOLDSTEIN<sup>2</sup> AND C. CLASS<sup>3</sup>

<sup>1</sup>Max-Planck-Institut für Chemie, Postfach 3060, 55020

Mainz, Germany (hofmann@mpch-mainz.mpg.de)

<sup>2</sup>Lamont-Doherty Earth Observatory, Palisades, NY, 10964

USA (steveg@ldeo.columbia.edu)

<sup>3</sup>Lamont-Doherty Earth Observatory, Palisades, NY, 10964

USA (class@ldeo.columbia.edu)

Preservation of a "hidden" reservoir in the lowermost mantle, the D'' layer, since the early Earth has recently been proposed to explain unbalanced geochemical signatures of accessible terrestrial reservoirs relative to a chondritic Earth, on the basis of xenon (Tolstikhin and Hofmann, 2005) and  $^{142}\text{Nd}$  isotopes (Boyet and Carlson, 2005). How could such a reservoir have formed and subsequently survive for more than 4 Ga? Here we explore the possibility that following large-scale early mantle melting, the partially molten lowermost mantle solidified by downward migration of a dense melt fraction. This is the inferred consequence of the measured crossover of melting temperatures of silicate perovskite and magnesio-wüstite at about 1200 km depth, and the predicted Fe-rich eutectic and low melting temperatures in the lowermost mantle (Boehler, 2000). This suggests that D'' formed during early solidification of the lower mantle and that it survives because of its Fe-rich composition.

The high melting temperatures of Mg and Ca perovskites in the lowermost mantle suggest that both phases remain in the residual solid. Corgne *et al.* (2005) have measured remarkably high partition coefficients for U and Th in Ca-perovskites. They suggested that this might provide an explanation for the "HIMU" (high mu = high U/Pb) ocean island source reservoir. In contrast, we suggest that the downward solidifying scenario should create a low-mu lowermost mantle region, because Pb is incompatible in the perovskites and is therefore enriched in the liquid, whereas U and Th are enriched in the Ca perovskite of the residual solid. Using the partition coefficients of Corgne *et al.* (2005) with simple fractional crystallization models yields a low-mu D'' layer and a higher-mu overlying mantle. If the time scale of this lower-mantle solidification was on the order of 100 to 500 Ma, this offers a simple solution to the classic "Pb paradox" (estimated bulk silicate lead lying "to the right" of the Pb-Pb geochron) and the well-known two-stage evolution of terrestrial lead. We also explore possible solutions of other geochemical puzzles, such as the high, time-integrated Th/U ratios calculated from early Archean galenas and feldspars, the subchondritic Nb/Ta ratios of accessible terrestrial reservoirs, and the decoupled  $\epsilon(\text{Hf})$  and  $\epsilon(\text{Nd})$  values of early Archean rocks in terms of this model.

### References

- Boehler, R. (2000) *Reviews Geophys.* **38**, 221-235.
- Tolstikhin, I.N. & Hofmann, A.W. (2005) *Phys. Earth Planet. Int.* **148**, 109-130.
- Boyet, M. & Carlson, R.W. (2005) *Science* **309**, 576-581.
- Corgne, A. *et al.* (2005) *Geochim. Cosmochim. Acta.* **69**, 485-496.

## Sub-micron-scale variations in Ti abundance in zircon

A.E. HOFMANN<sup>1</sup>, A.J. CAVOSIE<sup>2</sup>, Y. GUAN<sup>1</sup>,  
J.W. VALLEY<sup>3</sup> AND J.M. EILER<sup>1</sup>

<sup>1</sup>Division of Geological & Planetary Sciences, California Institute of Technology, Pasadena, CA 91125, USA.  
(hofmann@gps.caltech.edu)

<sup>2</sup>University of Puerto Rico, Mayagüez, PR 00681, USA.

<sup>3</sup>University of Wisconsin, Madison, WI 53706, USA.

The Ti-in-zircon geothermometer [1,2] can constrain growth and/or re-equilibration temperatures of zircons and is particularly useful for constraining Archean and Hadean events where detrital zircon is the only surviving mineral. Zircons are often small (ca. <100  $\mu\text{m}$  in the long dimension) and preserve evidence of fine-scale (sub-micron) compositional zonation. Methods for determining Ti abundances in natural zircons typically analyze domains 10s of microns across, which must average fine-scale compositional variations. Although Ti can correlate with coarse cathodoluminescence (CL) zones (e.g., [3]), it is unknown whether Ti exhibits fine-scale variations and thus may be compromised by coarse-scale measurements.

We report Ti abundances in natural and synthetic zircons down to length scales of ca. 250 nm based on measurements made with the Caltech Microanalysis Center Cameca NanoSIMS 50L. All data reported here were calibrated by comparison with primary and secondary standards previously studied in other laboratories. The external precision of our measurements for 2- $\mu\text{m}$  raster images are typically 2%, relative, at 10 ppm Ti, and degrade with decreasing spot size as expected by counting statistics.

We analyzed detrital zircons from Archean metasediment in the Jack Hills (Australia) and from Proterozoic metapelite in the Adirondacks (New York). Ti concentrations commonly vary by factors of 2-3 over distances of ca. 3  $\mu\text{m}$ , conformable to  $\mu\text{m}$ -scale CL zonation and corresponding to nominal temperatures of ~700 to ~750 °C. In some cases, banding extends down to sub-micron scales with gradients at least as sharp as a factor ~3 in concentration over 250 nm. The preservation of such gradients through granulite facies metamorphism attests to slow diffusion of Ti in zircon. Curiously, compositional variations include ca. 1-2  $\mu\text{m}$  bands of very low Ti content (<2 ppm, corresponding to apparent temperatures of <600 °C). Hf concentrations commonly covary with Ti, but the sense of correlation can be either positive or negative; i.e., there is no general correlation among all data. All zircons studied to-date also contain 1-2  $\mu\text{m}$ -wide bands or ca. 1  $\mu\text{m}$  spots having Ti concentrations up to 80 times that of the background, corresponding to nominal temperatures up to 1200 °C. These presumably reflect sampling of micron or sub-micron inclusions of Ti-rich phases.

### References

- [1] Watson, E.B. & Harrison, T.M. (2005) *Science* **308**, 841-844. [2] Watson, E.B., Wark, D.A., & Thomas, J.B. (2006) *CMP* **151**, 413-433. [3] Holden, P. *et al.* (2005) *Eos Trans. AGU* **86** (52) Fall Meet. Suppl., Abstract V41F-1539.

## Ferrihydrite in porous media – An inner-sphere complexation and transport approach to describe multiple reactions and predict colloid mobilization

A. HOFMANN<sup>1</sup> AND L. LIANG<sup>2</sup>

<sup>1</sup>Université des Sciences et Technol. de Lille 1, UMR/CNRS 8110 PBDS, 59655 Villeneuve d'Ascq Cedex, France  
(annette.hofmann@univ-lille1.fr)

<sup>2</sup>Oak Ridge National Laboratory, MS-6250, P.O. Box2008, Oak Ridge, TN 37831-6250 USA (liangl@ornl.gov)

Prediction of colloid release and transport as affected by reactive species remains a significant challenge for field applications. We report experimental and modeling results of ferrihydrite colloid release under the influence of citrate species. Using CD-MUSIC, a 3-plane surface complexation model (1), equilibrium constants were obtained for the three proposed inner-sphere complexes by fitting citrate adsorption isotherm and pH adsorption envelopes. The constants are used in a reactive transport model (implemented in ORCHESTRA (2)) for simulating reaction fronts of dissolved species during injection of citrate in ferrihydrite-coated quartz columns. Simulation results show that sorption alone may not adequately describe the breakthrough curves. Inclusions of ferrihydrite dissolution and re-adsorption of Fe(III) improve the prediction of dissolved species transport. Additionally, matrix diffusion may be needed for a better prediction. The mechanisms of colloidal iron oxide release change over time. At complete breakthrough of citrate, oxide dissolution and interfacial repulsion control particle release from sediment. However, the peak release of colloids, corresponding to the breakthrough front of citrate, was mainly brought by electric double layer forces. These particles underwent detachment-deposition-detachment cycles along the flow path, and emerged in the effluent with the major reaction front. To quantitatively predict colloid release, a semi-empirical linear correlation is proposed, linking the calculated electric potential to experimental colloid release rates. The model works well for the prediction and scaling of field experiments concerned with organic ligand injection in subsurface environments.

### References

- [1] Hiemstra, T.; Van Riemsdijk, W.H. *Colloid Interface Sci.* **1996**, *179*, 488-508.  
[2] Meeussen, J. C. L. *Environ. Sci. Technol* **2003**, *37*, 1175-1182

## Theoretical and experimental arguments for Earth's heat flux being $31 \pm 2$ TW

A.M. HOFMEISTER<sup>1</sup>, V.M. HAMZA<sup>2</sup> AND R.E. CRISS<sup>1</sup>

<sup>1</sup>Dept. of Earth and Planetary Sci., Washington U., St. Louis MO 63130, USA (hofmeist@wustl.edu; criss@wustl.edu)

<sup>2</sup>Observatório Nacional, Rua General José Cristino, 77 Rio de Janeiro, Brazil (Hamza@on.br)

Global power (heat flux averaged over Earth's surface) links to radiogenic content, geodynamic state and thermal evolution. Recent computations involve replacing measured flux over substantial parts of the ocean floors with calculations from 1-D cooling models. Cooling models must support through their alleged prediction of seafloor depths. But, a factor of 3 error exists in equations used to predict depth as a function of seafloor age. Specifically, 1-D models presume that temperature varies in the Z-direction only, so contraction is only in Z and is governed by linear thermal expansivity, not volumetric as mistakenly implemented. Values predicted for depth are 1/3 those measured if reasonable physical parameters are used. To reproduce depth data requires using  $\sim 3000$  K as the basal temperature, which is incompatible with petrology, and provides global power of  $\sim 132$  TW, not 44 TW. Other problems exist with cooling models and the database. Recent assessment of heat flow data, corrected for duplications and errors in location, limits global power to between 28.6 and 34.1 TW, with uncertainties largely stemming from the need to estimate flux in certain geographic regions. Hydrothermal circulation has been rationalized as causing the discrepancy of model with measurements, but practically speaking, measurements are made mostly in strongly sedimented areas where the confining lid prevents effects of hydrothermal circulation, local or extensive. In hydrothermal systems, temperature gradients in the rocks are reduced below ideal conductive values where the water enters the system in recharge regions far from the ridges and robs heat from the rocks, not near the ridges where ascending hot water warms rocks and enhances conductive gradients. The rationalization thus implicitly assumes that measurement sites are preferentially located over recharge zones, which is unlikely. Harmonic expansions, up to degree 36, reveal that previous low-degree hybrid spherical harmonic analysis (wherein high fluxes near the ridges from 1-D cooling models are used in place of data) causes heat flux in the mathematical representation to be overestimated, even in continental regions, due to the importance of lowest order spherical harmonic coefficients. Enstatite chondrite models provide  $\sim 30$  TW, suggesting that additional heat sources, such as K in the core or secular delay, are not necessary to explain Earth's thermal state.

### References

Hamza V.M. (in review) *Internat. J. Earth Sci.*  
Hofmeister A.M. and Criss R.E. (2005) *Tectonophys.* **395**, 159-177; **409**, 193-198; (2006) *Tectonophys.* **428**, 95-100.

## Timescale for metal-silicate separation by metal rainfall in a magma ocean

TOBIAS HÖINK<sup>1</sup>, JÖRG SCHMALZL<sup>2</sup> AND ULRICH HANSEN<sup>2</sup>

<sup>1</sup>Department of Earth Science, MS-126, Rice University, 6100 Main St, Houston TX, 77005, USA

(Tobias.Hoeink@rice.edu)

<sup>2</sup>Institut für Geophysik, WWU Münster, Corrensstr. 24, 48149 Münster, Germany (joergs@uni-muenster.de, hansen@earth.uni-muenster.de)

The largest sequestering event in Earth's evolution, which ultimately lead to the differentiation of Earth's mantle and core, was the separation of metal from silicate in a magma ocean. The only separation mechanism that can explain geochemical observations is metal rainfall. Essential to the metal rainfall mechanism is that metal disperses into small droplets which chemically equilibrate with the surrounding silicate while they sink by means of turbulent density currents. Höink *et al.* (2006) have studied the metal rainfall mechanism under the assumption of constant silicate viscosity and found that the time scale of metal silicate separation under these conditions are on the order of the Stokes' settling time, which for centimeter-sized metal droplets in Earth's magma ocean corresponds to a time scale of weeks.

However, it is well known that magma dynamics are fundamentally influenced by variations in viscosity. A non-constant viscosity, i.e. a temperature dependent viscosity, or even more realistically, a temperature- and pressure dependent viscosity may alter the mechanism of metal rainfall significantly. In the present work we analyse the influence of temperature dependent viscosity and temperature- and pressure dependent viscosity on the rainfall mechanism by employing a numerical convection model combined with a sedimentation method.

We find that the metal-silicate separation time depends on the thermal viscosity contrast and also on the viscosity contrast due to pressure. For values suitable to Earth's magma ocean, the time scale of metal-silicate separation by metal rainfall increases to the order of tens to hundreds of years. Accordingly, metal rainfall is a very rapid mechanism for metal-silicate separation in a magma ocean. This short timescale has profound implications for the timing of Earth's evolution.

### References

Höink, T., J. Schmalzl and U. Hansen, Dynamics of metal-silicate separation in a terrestrial magma ocean, *Geochem. Geophys. Geosyst.*, **7**, Q09008, doi:10.1029/2006GC001268, 2006

## Comparison of the development in melt compositions in the Faroe Islands and East Greenland during continental breakup in the Paleogene

P.M. HOLM AND N. SØAGER

Institute of Geography and Geology, University of Copenhagen, Øster Voldgade 10, DK-1350 Copenhagen, Denmark (paulmh@geol.ku.dk)

The upper part of the Faroe plateau lavas erupted during continental rifting and can be correlated with East Greenland counterparts of the Paleogene North Atlantic Igneous Province (Søager & Holm, this conf.). Low-Ti lavas with typically  $La/Sm_{cho} = 0.3-0.4$  have fractionated  $Dy/Yb_{cho}$  up to 1.25 which require substantial melting with residual garnet and thus a relatively hot source. Compared to late low-Ti lavas, the early tend to have more radiogenic Pb and occur in the northeastern parts. There is also a  $^{87}Sr/^{86}Sr$  decrease from 0 to -3 with time, while positive  $^{87}Sr/^{86}Sr$  show a rough increase with time. The low-Ti basalts with the most radiogenic Pb show a marginal overlap with Icelandic rocks.  $Dy/Yb$  has a negative correlation with  $^{206}Pb/^{204}Pb$  and on formation level there is an increase in  $^{206}Pb/^{204}Pb$  with time.

While the low-Ti basalts seem to be similar on both sides of the rift, the high-Ti basalts in the Faroes indicate decreasing depth of melting throughout the development, whereas the contemporaneous RFF in East Greenland has melts derived at high pressure. However, as in East Greenland, there is a change with time from IE2 to IE1 (Thirlwall & al., 2004) end-member composition. The increasing fraction of high-Ti basalts to the south could be caused by lateral variation in the mantle plume. Relatively low  $Dy/Yb$  indicates lithospheric thinning to have continued at the Faroes in contrast to East Greenland. A MORB-type source dominates the early low-Ti basalts, while NAEM (Ellam & Stuart, 2000) mantle composition is more important in the later development. This depleted two-component source is proposed to be part of the early Iceland plume and contributed much more in Faroes than in East Greenland.

### References

- Ellam R.M., Stuart F.M. (2000), *J. Petrol.* **41**, 919-932.  
Thirlwall M.F., Gee M.A.M., Taylor R.N., Murton B.J. (2004), *Geochim. Cosmochim. Acta* **68**, 361-386.

## Bubble gas-exchange in an artificially aerated lake traced using noble gases

C. P. HOLZNER<sup>1,2</sup>, N. GRASER<sup>1</sup> AND R. KIPFER<sup>1,3</sup>

<sup>1</sup>Eawag, Swiss Federal Institute of Aquatic Science and Technology, Dübendorf, Switzerland  
(christian.holzner@eawag.ch)

<sup>2</sup>Institute of Biogeochemistry and Pollutant Dynamics, ETH Zurich, Switzerland

<sup>3</sup>Institute of Isotope Geochemistry and Mineral Resources, ETH Zurich, Switzerland

The concentrations of dissolved atmospheric noble gases in open waters generally correspond to the equilibrium concentrations determined by temperature and salinity during atmospheric gas exchange. As noble gases are chemically inert, only physical processes may change the noble-gas abundance and hence are responsible for deviations from the initial equilibrium. Gas bubbles that are released at the bottom of a lake will affect the concentrations of dissolved gases in the water column, as the bubbles strip gases from the surrounding water and dissolve simultaneously during their ascent. The effect of these secondary gas exchange processes on the concentrations of dissolved gases varies depending on the solubility and diffusivity of the respective gas and on the initial gas concentrations in the bubbles.

We measured dissolved noble gas concentrations in Lake Hallwil (Switzerland), a small eutrophic lake, to trace the effects of gas release from an aeration system. This installation prevents anoxia in the deep water by the injection of oxygen-rich gas bubbles at the bottom of the lake. Noble gases in both the aeration gas and dissolved in the water of the lake were analyzed.

The measurements show that noble gases in the injected gas are strongly fractionated with respect to air. He, Ne and Ar are enriched, whereas Kr and Xe are virtually absent. Noble gases dissolved in the lake water show corresponding deviations from the atmospheric equilibrium concentrations. Deep-water samples taken at three different locations in the lake are supersaturated in He, Ne and Ar. The magnitude of the enrichment decreases with increasing distance from the bubble source. The observed noble gas supersaturations were also found to vary according to the operation mode of the aeration system, with higher gas flow leading to stronger noble gas enrichment. In contrast, only minor changes of the dissolved oxygen concentrations could be detected due to fast oxygen consumption.

In conclusion, the example of Lake Hallwil demonstrates that gas exchange with injected bubbles affects the noble gas abundance in the water body. Noble gas analyses allow quantifying the effectiveness of the aeration system, i.e. noble gas enrichments can be interpreted as a measure for the oxygen transfer to the lake water. Note that these findings may also help to understand natural systems like gas seeps in lakes and oceans.

## TEM investigations of bacterial effects on biotite dissolution

J. HOPF, F. LANGENHORST AND D. MERTEN

Institute of Geosciences, University of Jena, Burgweg 11,  
D-07749 Jena, Germany (JulianeHopf@web.de)

### Introduction

In natural environments minerals and rocks are not only weathered by chemical and physical processes but also by biological activity. In order to understand the role and interaction between alteration processes, the interface between minerals and bacteria must be investigated at the microscopic to nanometer scale.

### Methods and results

In batch culture experiments three different bacteria strains (*Bacillus subtilis spizizenii*, *Shewanella putrefaciens* and *Streptomyces acidiscabies E13*) were grown for 35 days with ground biotite as main nutrient source. The release of major and minor elements (Al, Fe, K, Mg, Mn, Si, Ti) was measured using inductively coupled plasma-optical emission spectrometry (ICP-OES). In comparison with an abiotic control the sample with *Bacillus subtilis spizizenii* showed an increase in the dissolution of Al and Mg. Compared to the control, the dissolution rates of Al and Mg in experiments with *Shewanella putrefaciens* and *Streptomyces acidiscabies E13* are however slightly decreased. These first results demonstrate that bacteria have a diverse control on the dissolution behaviour of biotite.

To understand this diversity in dissolution behaviour of biotite, we have employed transmission electron microscopy (TEM) and energy dispersive X-ray microanalysis (EDX). These techniques were used to detect changes in structure, morphology, and element chemistry of the untreated and biologically treated biotite. Pure visual TEM observations of the bacteria treated specimens provide clear evidence for intense degradation. The small bacteria treated biotite flakes show frayed rims and etch pits on surfaces, whereas untreated biotite from the control experiment displays the normal shape of unaltered starting biotite with unaffected crystal edges and surfaces. Crystal-chemical changes have been detected in experiments with *Bacillus subtilis spizizenii*, which show a K-Na cation exchange in biotite interlayers. The Na is thereby provided by the liquid media. Additionally, we found small crystals of a secondary phase, which is currently under identification.

### Conclusion

Bacteria are able to influence the dissolution processes of biotite in various ways. Especially the gram-positive soil bacteria *Bacillus subtilis spizizenii* increases the dissolution of certain elements and triggers the precipitation of a secondary phase.

## An evaluation of He, Ne and Ar isotope and element systematics of oceanic mantle sources

JENS HOPP AND MARIO TRIELOFF

Mineralogisches Institut, Universität Heidelberg, Im  
Neuenheimer Feld 236, D-69120 Heidelberg  
(jhopp@min.uni-heidelberg.de)

The more radiogenic character of Mid Ocean Ridge Basalts (MORB), i.e. higher air corrected mantle ratios of  $^4\text{He}/^3\text{He}$ ,  $^{21}\text{Ne}/^{22}\text{Ne}$ ,  $^{40}\text{Ar}/^{36}\text{Ar}$  compared to many Ocean Island Basalts (OIB), is commonly attributed to a higher degree of depletion of primordial noble gases within the MORB source. In addition, He/Ne and He/Ar elemental ratios found in MORB glasses are higher relative to OIBs. This had been considered as evidence for solubility controlled elemental fractionation during gas - melt partitioning. However, the generally lower He concentrations in OIBs compared to a presumed degassed MORB source appears in contradiction with this conclusion.

To resolve this issue in terms of a two-stage fractionation and binary mixing model we evaluated literature data from MORB and Loihi-Kilauea glasses and used their He, Ne and Ar isotope and element systematics and concentrations. We can describe mantle  $^{21}\text{Ne}/^{22}\text{Ne}$  -  $^4\text{He}/^3\text{He}$  isotope systematics by a simple binary mixing process between a MORB and a 'plume' endmember that differ in their  $^3\text{He}/^{22}\text{Ne}$  ratios at time of admixing. The 'plume' endmember is a postulated component, basing on the premise that both endmembers shared a common radiogenic evolution history, i.e. the same initial  $^3\text{He}/^{22}\text{Ne}$  ratio, but a different time integrated accumulation of radiogenic isotopes. Within this model a primary fractionation process must have occurred before admixing of both subcomponents. We performed a back calculation of this mixing process and extended this procedure to the Ar system assuming a linear relationship of mantle  $^{21}\text{Ne}/^{22}\text{Ne}$  and  $^{40}\text{Ar}/^{36}\text{Ar}$  ratios. With the implicit assumption that the composition of basalt glasses represents the melt phase and that the initial He/Ne, He/Ar compositions of the melt will only evolve towards higher values in course of solubility controlled secondary fractionation during magmatic degassing we derive upper limits for the  $^3\text{He}/^{22}\text{Ne}$ ,  $^4\text{He}^*/^{21}\text{Ne}^*$  and  $^4\text{He}^*/^{40}\text{Ar}^*$  ratios of both mixing endmembers. The MORB component appears not or weakly fractionated, in opposite to the 'plume' component displaying a significant He deficit. A simple calculation of unfractonated initial 'plume'  $^3\text{He}/^{22}\text{Ne}$ ,  $^4\text{He}^*/^{21}\text{Ne}^*$  and  $^4\text{He}^*/^{40}\text{Ar}^*$  ratios and He concentrations are in broad agreement with observed MORB data. A more compatible behaviour of He relative to Ne and Ar during crystal - melt partitioning could explain the data: OIB melt could represent low degree melts from an isotopically different source region that admixes with higher degree MORB melts at shallow depths. Alternatively, a more complex magmatic fractionation scenario is addressed.

## The H-, C-, N-, and O-isotopic compositions of cometary matter returned by STARDUST

PETER HOPPE

Max-Planck-Institute for Chemistry, 55020 Mainz, Germany  
(hoppe@mpch-mainz.mpg.de)

### Introduction

The STARDUST spacecraft collected about 1 mg of dust during a flyby in January 2004 of comet 81P/Wild 2 in two collection media, low-density silica aerogel and Al foil (Brownlee *et al.*, 2004). The dust collector was successfully returned to Earth in January 2006 and the cometary dust was analyzed by an international Preliminary Examination Team. These analyses showed that comet Wild 2 is an unequilibrated mixture of materials that have both solar and presolar origins (Brownlee *et al.*, 2006). Here, I will briefly review the results obtained for H-, C-, N-, and O-isotopic compositions by the Isotope subteam (McKeegan *et al.*, 2006; Stadermann *et al.*, 2007).

### Hydrogen

The H-isotopic composition was measured in five particle fragments. Moderate D enrichments were observed with D/H ratios of up to ~3x the terrestrial value. This is qualitatively consistent with the signature found in IDPs and insoluble organic matter (IOM) from chondrites, although the maximum D enrichments are smaller in the Wild 2 samples.

### Carbon and Nitrogen

C- and N-isotopic compositions were measured in several microtome sections, particle fragments, and crater residues in Al foils. No circumstellar C- or N-rich grains were found. Two hotspots enriched in  $^{13}\text{C}$  and depleted in  $^{15}\text{N}$  were recognized, possibly the signature of labile organic material.  $^{15}\text{N}$  enrichments with  $^{15}\text{N}/^{14}\text{N}$  ratios of up to ~2x the terrestrial value are found in bulk samples and as hotspots as similarly observed for IDPs and IOM from chondrites.

### Oxygen

Most studied samples (crater residues, microtome sections) have O-isotopic compositions compatible with those of bulk chondrites. One circumstellar O-rich grain, about 250 nm in size, was found. The  $^{17}\text{O}/^{16}\text{O}$  ratio of ~2.6x solar and  $^{18}\text{O}/^{16}\text{O}$  ratio of ~0.9x solar suggest an origin from a RGB/AGB star. A CAI-like particle exhibits enrichments in  $^{16}\text{O}$  of ~4% as similarly observed for CAIs from chondrites. The presence of a CAI-like particle among cometary matter is suggestive of large-scale radial mixing in the solar nebula.

### References

- Brownlee D. *et al.* (2004), *Science* **304**, 1764-1769.  
Brownlee D. *et al.* (2006), *Science* **314**, 1711-1716.  
McKeegan K. D. *et al.* (2006) *Science* **314**, 1724-1728.  
Stadermann F. J. *et al.* (2007) *MAPS*, submitted.

## Mineral-melt trace element equilibria in plutonic rocks studied by Laser Ablation ICP-MS

K. HORCKMANS AND J. HERTOGEN

Geo-Instituut, K.U.Leuven, Celestijnenlaan 200E, B-3001  
Leuven, Belgium (karolien.horckmans@geo.kuleuven.be)

Magmatic intrusive systems often yield very complex cumulate rocks, consisting of different solid phases and interstitial residual liquid phases. It is an intrinsic difficulty of cumulate rocks to properly interpret whole rock contents of incompatible trace element data, because the amount of trapped interstitial residual liquid might be the controlling factor. Moreover, as early formed cumulates might have been permeated by later-stage evolved liquids, there is no guarantee that whole rock data represent 'equilibrium' compositions. In the late stages of differentiation accessory minerals often start to crystallize and have an important impact on the behavior of trace elements during differentiation. This raises an important issue since models of fractionation are usually largely based on whole rock geochemical trends.

Equilibria at the micro-scale can be studied in situ in standard, thick polished mounts with LA-ICP-MS. The most promising minerals for the study of REE melt/mineral distributions are clinopyroxenes and plagioclase. However, accurate results require rather meticulous standardisation. Several standard materials have been tested in the present study: the commonly used NIST612 glass, USGS BCR-2 fused glasses, and a natural, very homogeneous obsidian glass from the Krafla volcanic area, Iceland. The equipment consisted of a Cetac200 266 nm UV-light of a NdYAG laser, coupled to a quadrupole based HP4500 ICP-MS. The Krafla obsidian yielded the best analytical results.

Ongoing studies include the analysis of core samples from the oceanic gabbro section of Hole735B drilled during Ocean Drilling Program Legs 118 and 176, and a section from the Tron pluton from the Caledonide Trondheim Nappe Complex, Norway. The accuracy of the LA-ICP-MS could be checked against analysis of separated pure mineral fractions analyzed by other methods. The micro-analytical data allow to calculate the liquid compositions with which clinopyroxene and plagioclase equilibrated, and to estimate the stage of solification at which interstitial liquids were expelled. Mass balances further make it possible to estimate the amount of dispersed trapped late stage residual liquids.

## Development of *in situ* U-Pb analysis of uranium oxides using an ion microprobe

K. HORIE<sup>1</sup> AND H. HIDAKA<sup>2</sup>

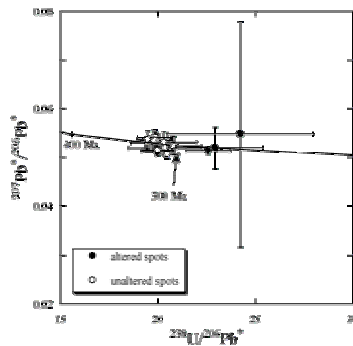
<sup>1</sup>Institute of Geology and Geoinformation, Geological Survey of Japan (JSPS fellow) (kenji-horie@aist.go.jp)

<sup>2</sup>Department of Earth and Planetary Systems Science, Hiroshima University, Japan (hidaka@hiroshima-u.ac.jp)

The chronological study of uranium minerals provides practical information on the formation of uranium deposits as well as elemental transportation in association with the alteration of uranium minerals. Moreover, the timing of uranium mineralization from the Archean to the Paleoproterozoic period is a good indicator of atmospheric oxygen evolution, because uranium is only mobilized as a uranyl ion (UO<sub>2</sub><sup>2+</sup>) under oxidizing conditions (e.g., Holland, 1984). However there are some issues to estimate the <sup>206</sup>Pb/<sup>238</sup>U age from SIMS analysis such as large variation of the ionization efficiency of secondary ions and standard material. In this study, we established a method for the *in situ* U-Pb isotopic analysis of uranium minerals in a similar manner to the conventional zircon analysis.

The Faraday mine uraninite from Bancroft, Canada was used as a standard material for the U-Pb calibration of three uranium minerals from Chardon, Ecarpière (the Armorica Massif, France) and Mistamisk (Labador, Canada). Quantitative analysis of major elements was carried out by EPMA. *In situ* U-Pb analyses of uranium minerals were performed by using a SHRIMP at Hiroshima Univ.

The calibrated SHRIMP <sup>206</sup>Pb\*/<sup>238</sup>U ratios of three uranium minerals from Chardon, Ecarpière and Mistamisk show a good correlation with Pb/U elemental ratios obtained from EPMA, which indicates the reliability of the SHRIMP calibration in this study. The SHRIMP <sup>206</sup>Pb\*/<sup>238</sup>U data of Ecarpière (285 Ma) and Mistamisk (1729 and 421 Ma) uraninite are consistent with previous chronological data obtained by TIMS. As shown in Figure, the selected SHRIMP data of the Chardon mine provide a <sup>206</sup>Pb\*/<sup>238</sup>U age of 313 Ma, which is older than the previously reported age of 264 Ma. Considering that the analytical spots were selected to avoid impure minerals and altered phases, which were probably formed by later processes, it is interpreted that the Chardon uraninite was crystallized by the remobilization of U during the cooling of the Mortagne granite (310-313 Ma).



### Reference

Holland H.D. (1984) *The Chemical Evolution of the Atmosphere and Oceans*. Princeton Univ. Press. pp. 582.

## Calcite-water oxygen isotope fractionation at elevated temperatures: Experimental and theoretical study on the effect of pressure and dissolved NaCl

J. HORITA<sup>1</sup>, V.B. POLYAKOV<sup>2</sup> AND D.R. COLE<sup>3</sup>

<sup>1</sup>Chemical Sciences Division, Oak Ridge National Laboratory, TN 37830-6110 (horitaj@ornl.gov)

<sup>2</sup>Institute of Experimental Mineralogy, RAS, Russia (polyakov@iem.ac.ru)

<sup>3</sup>Chemical Sciences Division, Oak Ridge National Laboratory, TN 37830-6110 (coledr@ornl.gov)

We have conducted an experimental and theoretical study for investigating the effect of pressure and dissolved NaCl on oxygen isotope fractionation in the system calcite – water at elevated temperatures. First, our novel corresponding state principles approach for calculating the effect of pressure (density) on the reduced partition function ratio (RPF) of H<sub>2</sub><sup>18</sup>O (Polyakov *et al.*, 2007) shows that the RPF increases up to 1.0 ‰ with increasing pressure to 1 kb at 273-523°C. The RPF of CaCO<sub>3</sub> increases only slightly, thus the oxygen isotope fractionation of the system CaCO<sub>3</sub>-water decreases up to 1.0 ‰ at 1 kb.

Our calculations of oxygen isotope fractionation factor between CaCO<sub>3</sub> and pure water are significantly (up to 2 ‰) lower than experimental values between CaCO<sub>3</sub> and calcite-saturated water at 300-750°C at 1 kb (this study) and 15 kb (Hu and Clayton, 2003). The cause of this discrepancy is due most likely to either errors in the calculation of ideal-gas RPF of H<sub>2</sub><sup>18</sup>O in the literature or the effect of dissolved CaCO<sub>3</sub> at elevated temperatures and pressures (Hu and Clayton, 2003). The effect of dissolved NaCl, ≤5m at 300-700°C and 1 kb (this study) and ≤37m at 300-750°C and 15 kb (Hu and Clayton, 2003), is found to be small (≤0.5 ‰).

It is very likely that pressure and dissolved CaCO<sub>3</sub> decrease and increase the calcite-water oxygen isotope fractionation at low and high pressures, respectively. In contrast, dissolved NaCl appears to have a small effect. However, the available data are still sketchy, and we have just begun to quantify the effects of these important variables for mineral-water isotope fractionation at elevated temperatures.

Research was sponsored by the Division of Chemical Sciences, Geosciences, and Biosciences, Office of Basic Energy Sciences, U.S. Department of Energy, under contract DE-AC05-00OR22725, Oak Ridge National Laboratory, managed by UT-Battelle, LLC.

### References

Hu G. and Clayton R.N., (2003), *Geochim. Cosmochim. Acta* **67**, 3227-3246.  
Polyakov V.B., Horita J., Cole D.R., and Chialvo A.A., (2007), *J. Phys. Chem.* **111**, 393-401.

## The late Eocene Chesapeake Bay impact structure – Status of research, insights, and implications

J. W. HORTON, JR., G. S. GOHN, AND D. S. POWARS

U.S. Geological Survey, 926A National Center, Reston, VA 20192, USA (whorton@usgs.gov)

This is an overview of studies since 2000 by the USGS Chesapeake Bay Impact Crater Project and the ICDP-USGS Chesapeake Bay Impact Structure Deep Drilling Project. The ~35.5 Ma Chesapeake Bay impact structure (CBIS), on the Atlantic margin of Virginia, USA, may be Earth's best preserved large impact structure formed in a siliciclastic, continental-shelf environment. The 85-km-wide structure formed in a layered target (seawater-sediments-rock), has an inverted-sombrero shape (deep central crater surrounded by a shallower annular trough), and is well preserved beneath postimpact sediments. Saline ground water in the CBIS affects water resources in an area of urban growth.

In 2000-2003, USGS drilled the Watkins School corehole just outside the structure, and the North, Langley, and Bayside coreholes in the annular trough, at 43, 39, 36, and 25 km from the center. These cores revealed (top to base) polymict sedimentary breccia interpreted as ocean-resurge deposits, target sediments modified by liquefaction, injection, and extensional structures, and unshocked Neoproterozoic basement. The sedimentary breccia contains shocked quartz and impact-damaged, mixed-age microfossils. In 2004, USGS drilled and partly cored the Cape Charles test hole on the central uplift, 1 km from the center. It revealed suevite, impact-melt clasts having a meteoritic component, a shock-induced TiO<sub>2</sub> polymorph, and hydrothermal alteration. Gravity, magnetic, seismic, and magnetotelluric surveys delineated the central uplift, moat, and outer margin. Numerical models simulated the inverted sombrero using strength contrasts of weak over strong layers.

In 2005-2006, the ICDP-USGS Eyreville coreholes were drilled to 1.77-km depth in the moat (deepest part) of the central crater, 9 km from the center. They cored (top to base) postimpact sediments, allogenic sedimentary breccia and sediment megablocks, granite megablock(s), sediment with lithic blocks, suevite and lithic impact breccias, and brecciated schist and pegmatite with breccia veins [1]. Studies by seven science teams will allow unprecedented understanding of a shallow-marine impact and its consequences. Topics include impactor type and relation to other late Eocene impacts (Popigai?), tektite formation, shock-pressure variations with depth and lithology, layered-target influence on cratering, resurge dynamics, unknown target basement, environmental consequences and hazard implications, hydrothermal conditions, source of contained ground-water brines, subsurface microbial diversity, and habitats unique to impact structures.

### Reference

[1] Gohn, G.S. *et al.*, (2006), *Eos* **87(35)**, 349, 355.

## Pre-Variscan Barrovian metamorphism in the eastern part of the Slavonian Mountains, Tisia Unit (NE Croatia): Application of quantitative phase diagrams and monazite age dating

PÉTER HORVÁTH<sup>1</sup>, DRAŽEN BALEN<sup>2</sup>, FRITZ FINGER<sup>3</sup>,  
BERNHARD HUMER<sup>3</sup>, BRUNO TOMLJENIĆ<sup>4</sup> AND  
PÉTER ÁRKAI<sup>1</sup>

<sup>1</sup>Institute for Geochemical Research, Hungarian Academy of Sciences, H-1112 Budapest, Budaörsi út 45., Hungary (phorvath@geochem.hu, arkai@geochem.hu)

<sup>2</sup>Faculty of Science, University of Zagreb, HR-1000 Zagreb, Horvatovac bb, Croatia (drbalen@geol.pmf.hr)

<sup>3</sup>Abteilung Mineralogie, Universität Salzburg, A-5020 Salzburg, Hellbrunnerstrasse 34, Austria (Friedrich.Finger@sbg.ac.at, Bernhard.Humer@sbg.ac.at)

<sup>4</sup>Faculty of Mining, Geology & Petroleum Engineering, University of Zagreb, Hr-1000 Pierottijeva 6, Croatia (bruntom@rgn.hr)

Petrological investigations, quantitative phase diagram modelling and monazite dating were carried out on medium-grade metamorphic rocks from the Kutjevačka Rijeka transect in the Slavonian Mts., Tisia Unit (NE Croatia). Micaschists contain complex zoned garnets with Mn-rich cores and Ca-rich rims. Mn decreases steadily from core to rim, but there is an abrupt increase in Ca between core and rim. This complex zoning was not observed in garnets from intercalated paragneisses and amphibolites. Quantitative phase diagrams and garnet composition isopleths using bulk rock compositions revealed that the garnet cores formed at 584-592°C and 6.4-7.8 kbar. For establishing the PT conditions responsible for garnet rim formation the composition of the garnet cores was removed from the bulk data and a new effective bulk composition was established. Using quantitative phase diagrams, mineral isopleths and thermobarometric methods we calculated peak PT conditions of 600-660 °C and 11-12 kbar for the garnet rim and the matrix assemblage of biotite, muscovite, plagioclase and quartz. Staurolite mentioned in the literature was not observed in this study and the application of quantitative phase diagrams contoured for H<sub>2</sub>O mode isopleths supports our opinion that during the retrograde PT path the rock did not pass staurolite-bearing fields. PT conditions for the intercalated paragneisses and amphibolites are the same as for the micaschists.

The Th, U and Pb contents of yttrium-rich accessory monazites indicate a pre-Variscan (428 ± 25 and 444 ± 19 Ma) age for the medium-grade metamorphism. These data are 70-100 Ma older than previously published mica Ar-Ar and K-Ar ages from the study area.

This study was financially supported by the Hungarian National Science Fund (OTKA, grant number F047322 to PH) and by the Croatian Ministry of Science, Education and Sports, Projects 119-1191155-1156 (DB) and 195-1951293-3155 (BT).

## Environmentally hazardous trace elements of Eocene coal deposits in the north Anatolia, Turkey

FATMA HOŞ ÇEBİ AND SADETTİN KORKMAZ

Karadeniz Technical University, Department of Geological Engineering, Trabzon/Turkey (hos@ktu.edu.tr, korkmaz@ktu.edu.tr)

Amasya, Bolu and Kastamonu in Northern Anatolian Region in Turkey host high-calorie lignite coals of Eocene age with reserve more than 1 million tones. In this study, distribution of environmental elements in coals, enrichment factors of these elements and total organic material-element relations were investigated.

The lignite coals in Amasya are found in 4 different fields within the Eocene clastic deposits. In these fields, concentrations of Cu, Zn and Se are generally higher than that of the Turkish coals. Considering the enrichment factor calculations with respect to world coals, Mo, Pb, Cd and Sb are depleted while Cu, Ni, Co, Mn, V, Cr, Hg, Se, Th and As elements are enriched.

Mo, V, B, Se and S% values of the Bolu field coals are higher than the average value of Turkey. Enrichment factor calculations on these coals reveal that Pb, Cd, Sb and Th are depleted and Se, Cr, Co, Zn and Cu are enriched while Mo, Ni, Mn, As, V, B, Hg, U and S are considerably enriched.

Lignites in Kastamonu are found within the Eocene marl-limestone sequence. It was determined that Cu, Pb, Zn, Ni, Co and S concentrations of this field are higher than the average value of Turkish coals. Enrichment factor calculations on the Kastamonu coals reveal that Cd, Sb and Se are depleted and Mo, Cu, Pb, Zn, Co, Mn, As, V, B, U, Th and S are enriched while Ni, Cr, and Hg are considerably enriched.

Using the environmentally sensitive elements and total organic matter values of coals from all the fields, statistical evaluation was made.

In the Amasya-Kastamonu coals, Cr-V and As-S element pairs show positive correlations while B-TOC, Th-TOC, Cu-TOC and B-Cu element pairs display negative correlations.

Except for S-Cu element correlation resembling to the Amasya field, the Bolu field does not display any similarity to any of the fields.

## Zeolite-calcite-silica formation in basalt during orogenic collapse, Washington Cascades

PAUL W.O. HOSKIN

Department of Geology & Geophysics, University of Calgary, Alberta, Canada (hoskin@ucalgary.ca)

Regional extension and collapse of the 96 to 45 Ma Cascade orogen during the Eocene is recorded by rapid basin subsidence, mafic to intermediate dike swarms, and exhumation of a partially migmatized gneiss complex (Miller *et al.*, 2007). Shallow hydrothermal systems developed as a response to high regional geothermal gradients (35–40 °C km<sup>-1</sup>) and local intrusions. The fossil hydrothermal system in the vicinity of the largest dike swarm (Teaway dikes) is recorded by calcite-gold veins in sandstone-shale and by zeolite-calcite-silica ± Fe-oxy/hydroxide assemblages in distal and stratigraphically higher basalt lavas and pyroclastics. Silica in distal assemblages occurs as α-quartz, chalcedony, and moganite, forming agate. Zeolite phases are heulandite and stilbite.

Oxygen-isotope ( $\delta^{18}\text{O}_{\text{SMOW}}$ ) values for silica phases range about 10–16 ‰ and 10–15 ‰ for calcite. Values of  $\delta^{13}\text{C}_{\text{PDB}}$  for calcite range -9 to -11 ‰. Calculated temperatures of formation based on calcite-quartz pairs, calcite-water, and quartz-water thermometry indicate precipitation at 50–60 °C in a meteoric water dominated system. Field-constrained 2D thermal models indicate that these temperatures are likely to have existed for about 10<sup>4</sup> years at subsurface depths of 50–100 m.

Compositional modeling using PTAX and the Geochemists Workbench indicate that zeolite-calcite-silica formation occurred at  $\log[a\text{Ca}^{2+}/a^2\text{H}^+] \approx 12\text{--}13$  and low  $\log[a\text{Al}^{3+}/a^3\text{H}^+]$  values that evolved up to 3–4 with time. Low Na activity in the fluid meant that mordenite or phillipsite were not stable zeolite phases in the CNKASH system. Based on phase relations in the albite-anorthite-quartz-H<sub>2</sub>O system (Liou *et al.*, 1991), heulandite + stilbite may coexist at 50–100 m depth at temperatures less than about 105 °C which is consistent with isotopic thermometry and inferences based on field observations.

Analytical and modeling results indicate that heated meteoric fluids reacted with basalt to produce an assemblage that at first was in equilibrium with basaltic glass, but later became more Al-rich indicating equilibrium with glass + plagioclase. It appears that as for the zeolite-calcite-silica occurrences of Iceland (Neuhoff *et al.*, 1999), porosity is an important factor in determining which zeolite precipitates during low-grade alteration-metamorphism of basalt.

### References

- Liou, J.G. *et al.* (1991) *N.Z. J. Geol. Geophys.* **34** 293-301.
- Miller, R.B. *et al.* (2007) *GSA Cordilleran Section Meeting*, Paper No. 5-1.
- Neuhoff, P.S. *et al.* (1999) *Am. J. Sci.* **299** 467-501.

## Chemical weathering, erosion, and CO<sub>2</sub> consumption in the southern Tibetan Plateau and Eastern Syntaxis of the Himalaya

MICHAEL T. HREN, C. PAGE CHAMBERLAIN,  
GEORGE E. HILLEY, PETER M. BLISNIUK AND  
BODO BOOKHAGEN

Stanford University, Dept. Geological and Env. Sciences,  
Stanford, CA 94305, USA (hren@stanford.edu,  
chamb@pangea.stanford.edu, hilley@stanford.edu,  
Blisniuk@stanford.edu, bodo@pangea.stanford.edu)

The Yarlung Tsangpo-Brahmaputra River drains a large portion of the Himalaya and southern Tibetan plateau, including the eastern Himalayan syntaxis, one of the most tectonically active regions on the globe. We measured the solute chemistry of 161 streams and major tributaries of the Tsangpo-Brahmaputra to examine the effect of tectonic, climatic, and geologic factors on chemical weathering rates. Specifically, we quantify chemical weathering fluxes and CO<sub>2</sub> consumption by silicate weathering in southern Tibet and the eastern syntaxis of the Himalaya, examine the major chemical weathering reactions in the tributaries of the Tsangpo-Brahmaputra, and determine the total weathering flux from carbonate and silicate weathering processes in this region. We show that high precipitation, rapid tectonic uplift, steep channel slopes, and high stream power generates high rates of chemical weathering in the eastern syntaxis. The total dissolved solids (TDS) flux from this area is greater than 520 t km<sup>-2</sup> yr<sup>-1</sup> and the silicate cation flux more than 34 tons km<sup>-2</sup> yr<sup>-1</sup>. In total, chemical weathering in this area consumes 15.2 x 10<sup>5</sup> mol CO<sub>2</sub> km<sup>-2</sup> yr<sup>-1</sup>, which is twice the Brahmaputra average. These data show that 15-20% of the total CO<sub>2</sub> consumption by silicate weathering in the Brahmaputra catchment is derived from only 4% of the total land area of the basin. Hot springs and evaporite weathering provide significant contributions to dissolved Na<sup>+</sup> and Cl<sup>-</sup> fluxes throughout southern Tibet, comprising more than 50% of all Na<sup>+</sup> in some stream systems. Carbonate weathering generates 80 to 90% of all dissolved Ca<sup>2+</sup> and Mg<sup>2+</sup> cations in much of the Yarlung Tsangpo catchment.

## Precipitation and aggregation of ZnS nanoparticles in the presence of low-molecular weight organic acids

HEILEEN HSU-KIM

Duke University, Civil & Environmental Engineering, Box  
90287, Durham, NC 27708 (hsukim@duke.edu)

### Introduction

ZnS and other metal-sulfide nanoparticles are known to exist as intermediates during precipitation and dissolution of their respective bulk mineral phases [1, 2]. However, the mechanisms that enable these nanoparticles to persist in surface waters and sediment porewaters are unknown. Humic substances and other hydrophilic organics can stabilize metal-oxide colloids in solution by adsorbing to particle surfaces and preventing aggregation [3]. This study seeks to identify whether similar processes occur for nanocolloidal ZnS.

### Experimental Methods

The stability of aqueous ZnS nanoparticles was investigated by assessing the role of low-molecular weight organic ligands (oxalate, serine, cysteine, thioglycolate, and glycolate) during precipitation of ZnS. Zn(NO<sub>3</sub>)<sub>2</sub> and Na<sub>2</sub>S were dissolved (2 uM each) in laboratory aqueous solutions buffered at pH 7.5 and containing one of the organic ligands. Particle formation and size was monitored over time by dynamic light scattering. Zn speciation was measured in filtered (<0.2 μm) ZnS solutions by anodic stripping voltammetry to confirm that Zn was coordinated to sulfide during the aggregation experiments and not in the form of dissolved Zn-organic complexes.

### Results and Discussion

Observed growth rates of ZnS aggregates varied by orders of magnitude, depending on the type and concentration of organic ligand in solution. Growth rates were slowest in the presence of thiol-containing ligands: cysteine and mercaptoacetate. In contrast, ZnS aggregation rates were generally not affected by oxalate, serine and glycolate. These compounds contain hydroxyl, carboxylate, and/or amine functional groups. Thermodynamic stability constants for the Zn-thiol complexes are greater than those for the other Zn-organic complexes. Thus, slow aggregation of ZnS nanoparticles may be caused by specific attachment of the thiol on surface Zn sites. These results demonstrate a possible mechanism that stabilizes nanocolloidal metal-sulfides in the aquatic environment.

### References

- [1] M. Labrenz *et al.*, *Science* **290**, 1744 (2000).
- [2] D. Rickard, G. W. Luther, in *Sulfide Mineralogy and Geochemistry* D. J. Vaughan, Ed. (2006), vol. 61, pp. 421-504.
- [3] E. Tipping, D. C. Higgins, *Colloids and Surfaces* **5**, 85 (1982).

## Distribution of Cesium sorption on micas and application on nuclear waste disposal

H. HU<sup>1</sup>, R.C. WANG<sup>1</sup>, A.C. ZHANG<sup>2</sup> AND S.J. XU<sup>1</sup>

<sup>1</sup>State Key Laboratory of Mineral Deposit Research, Department of Earth Sciences, Nanjing University, Nanjing 210093, China(huhuan@nju.edu.cn)

<sup>2</sup>Purple Mountain Observatory, Chinese academy of sciences, Nanjing 210008, China (aczhang@pmo.ac.cn)

**Introduction** Cs is an important radionuclide in nuclear waste. It not only <sup>135</sup>Cs is extremely long-lived ( $t_{1/2}=2.0\times 10^6$ ) and <sup>137</sup>Cs is a major radioactive contaminant in high-level nuclear waste (HLW), but also exhibits almost unlimited solubility, so it is very necessary to find highly insoluble phases able to fix radionuclide Cs and to have a long-term stability in geological repositories.

Natural micas are important constituents of geological formations and they also contain elevated contents of Cs, therefore we tried to make cesium sorption experiments on micas and to evaluate the ability of micas to incorporate and retard radionuclide cesium.

**Experiments** Four different micas, such as muscovite, lepidolite, biotite and phlogopite were hand-picked from the pegmatite and granite samples. Micas that had not been exposed to CsCl solution were analyzed by EMPA, average Cs content of muscovite and lepidolite are very lower and respectively are 0.02wt% and 0.09wt%, Cs content of biotite and phlogopite all below detectable limit.

All minerals were processed by ultrasonically washing in deionized water before absorption experiments. Cesium-absorption experiments were performed by 0.1g samples of the reaction vessels with 20ml 0.1M CsCl solution for 7 days, 14day and 21days. No additional buffer was used. Treated slab samples was simply removed from the reaction vessels, then ultrasonically washing in deionized water and allow to air dry. Treated slabs were observed and analyzed by the EMPA method.

**Conclusions** 1) Cs content of all treated micas became higher than untreated samples, even in the treated biotite for 21days, Cs content up to 2.05wt%. These show that the four micas are able to fix radionuclide Cs in their interlayer structure and may be the possible stable waste disposal phases in the near field of geological barrier; 2) The distribution of Cs in micas was variable, Cs was preferentially sorbed where individual sheet boundaries were crude steps and abundant on these areas; 3) The ability of bonding of cesium is different. Ferriferous micas, such as biotite and phlogopite, are likely to be higher than muscovite and lepidolite. It indicates that biotite and phlogopite are good candidates for the storage of Cs.

### Acknowledgements

This research was supported by National Natural Science Foundation of China (40302010)

## Biogeochemical investigations of the Zunyi sedimentary Ni-Mo-PGE ores in the Lower Cambrian black shale formation, South China

K. HU, S.P. YAO, J.Y. PAN, J. CAO AND J. ZHOU

Department of Earth Sciences, Nanjing University, Nanjing, 210093, China (kaihu@nju.edu.cn)

The metalliferous black shales and their Ni-Mo-PGE ores can be traced across a broad region of South China, mainly south of the Yangtze River, extending a 1600 km belt of main provinces. The Lower Cambrian black shales that host the ores are approximately 60 to 150 m thick and include the Niutitang Formation of Guizhou and Hunan and stratigraphic equivalents elsewhere. The Ni-Mo ore bed itself varies in thickness from a featheredge to ~30 cm and consists largely of pyrite, apatite, vaesite, gersdorffite (NiAsS), and an amorphous Mo-S-C mixed-layer phase. Lots of organic matter, including algae and bacteria are abundant and constitute up to 10% of the ores, which may have played an important role in their formation.

Combined organic petrography, elemental and stable isotope (S) analyses of samples from the Lower Cambrian shale Ni-Mo-PGE ores of Zunyi provide insight into the relationship of organic matter-ores, biogeochemical alteration of hydrocarbons, microbial sulfate reduction, and mineral deposition. In the absence of vitrinite, relative thermal maturity were determined from the reflectance of bitumen, and marine kerogen like algal remains, Ro basically in range from 2.0 to 4.1%. Elemental analyses suggest that organic matter has been oxidized throughout the study area. The sulfur isotopic composition of the metal sulfides correlates with the degree of biodegradation of hydrocarbons, with the base-metal content and with the proportion of aromatics in the organic extracts. Sulfur isotopes study shows that micro-organism took active part in the re-enriching processes of metal sulfide, barite and witherite during digenesis. Variation of conventionally determined  $\delta^{34}\text{S}$  values are great, ranging from +25% to -12% for samples from the study area in Zunyi. Individual nodules also show large variations in the drilled sulfide data of up to 15.7% between rims and cores of sulfide ore nodules. The high variation in isotopic fractionation of the ores may reflect the varying proportions of different sulfide minerals. On the other hand, Extreme variation of  $\delta^{34}\text{S}$  values during the formation of the Ni-Mo sulfide ores could have been caused by the effects of both biogeochemical and hydrothermal activity during the formation of these unusual ores.

Funding for this investigation was provided by NSF of China grants 40638042 and 40572056.

## Geological and geochemical constraints on the origin of the giant Lincang coal seam-hosted germanium deposit, Yunnan, SW China

RUIZHONG HU<sup>1</sup>, HUAWEN QI<sup>1</sup>, MEI-FU ZHOU<sup>2</sup>,  
WENCHAO SU<sup>1</sup>, XIANWU BI<sup>1</sup> AND JIANTANG PENG<sup>1</sup>

<sup>1</sup>The State Key Laboratory of Ore Deposit Geochemistry, Institute of Geochemistry, Chinese Academy of Sciences, Guiyang, China (huruihong@vip.gyig.ac.cn)

<sup>2</sup>Department of Earth Sciences, the University of Hong Kong, HK, China

The Lincang germanium deposit in Yunnan, SW China, contains at least 1000 tones of Ge at an average grade of ~850 ppm Ge, being one of the largest germanium deposits in the world. The deposit is hosted in coal seams of the Miocene Bangmai Formation deposited on a Ge-rich granitic batholith. The Bangmai Formation is divided into eight units among which three units are coal-bearing. The Ge-bearing coal seams are inter-layered with siliceous rocks and siliceous limestones in the basal coal-bearing unit. The coal seams of the other two coal-bearing units are not inter-bedded with siliceous rocks and siliceous limestones, and are barren. Equant or elongated germanium ore-bodies are mainly distributed at fault intersections, and are located at the top and bottom of coal seams where they mainly contact with the layered siliceous rocks or siliceous limestones. Ge is mainly associated with organic matters of coal seams. The major and trace elements, and O- and C-isotopes of the siliceous rocks and siliceous limestones are similar to those of hydrothermal sediments, indicating formation by hydrothermal sedimentation. Compared with barren coals, Ge-rich coals are notably rich in Nb, Li, Sb, W, Bi and U and show substantial enrichment of HREE which increase with Ge. Ge-rich coals have the vitrinite reflectance generally higher than barren coals. They contain disseminated pyrites with  $\delta^{34}\text{S}$  from 17.2‰ to 51.4‰, similar to the pyrites in barren coals, and thin vein-like pyrites with  $\delta^{34}\text{S}$  from 1.9‰ to -5.4‰, similar to the sulfides in granite-related quartz veins. We propose that circulating hydrothermal fluids leached abundant Ge and other elements from Ge-rich granite in the basement, and then discharged into the basin mainly along fault intersections to form layer-like siliceous rocks and siliceous limestones by depositing Si and Ca, and to form germanium deposit through interaction between germanium in the fluids and organic matters in coal seams.

### Acknowledgment

This study is supported by by Natural Science Foundation of China (grant 40634020 to Hu).

## Oxygen and carbon isotope composition and implication of Early Palaeozoic dolomites in Keping, Tarim Basin

WX HU, XM XIE, JT ZHANG AND XL WANG

Department of Earth Sciences, Nanjing University, Nanjing 210093, China (huwx@nju.edu.cn)

In order to approach to the formation environment and fluid condition, carbon and oxygen isotopes are analyzed of Early Palaeozoic dolomite sequences in Keping, northwest of Tarim Basin, for the dolomite sequences are important reservoir rocks in the basin.

104 field dolomite samples were collected from the outcrop of Early Palaeozoic in Keping. This outcrop is consisted of algal dolomite, bedding dolomite, calcareous dolomite, and some limestone. Evaporates and many siliceous aggregates were found in the middle Cambrian, which might be related to special environments. In order to figure out variations of the isotopes in the samples with different composition and texture, micro-area sampling was conducted by Hand Grinder with 1mm in diameter. The analysis was performed on CF-IRMS in Nanjing University.

The isotopic result is mainly consistent with ancient seawaters of that age. The  $\delta^{13}\text{C}$  of the samples ranges from -1.6‰ to 1.6‰, with an average of 0.515‰, and the  $\delta^{18}\text{O}$  from -12.7‰ to -5.7‰, with an average of -7.23‰. The  $\delta^{18}\text{O}$  varies larger in different samples than the  $\delta^{13}\text{C}$ , and the  $\delta^{18}\text{O}$  become depleted with increasing ages. The  $\delta^{13}\text{C}$  and  $\delta^{18}\text{O}$  have relatively lower values in middle Cambrian dolomites. But they rise to -1‰ and -7‰, respectively, and become relatively stable in upper Cambrian and Ordovician dolomites. In addition, the obvious variation of the isotopes can be found between different algal dolomite layers in middle Cambrian, but such a variation becomes small in the younger algal dolomites in upper Cambrian and Ordovician.

The depleted  $\delta^{18}\text{O}$  in middle Cambrian, most less than -10‰, is likely related to hydrothermal activity. On the other hand, evaporation process during middle Cambrian could make the  $^{13}\text{C}$  and  $^{18}\text{O}$  of the seawaters enriched, and the  $\delta^{13}\text{C}$  and  $\delta^{18}\text{O}$  rise in the related dolomites. Because the above two aspects had different constrains on the variation of the isotopes in the seawater, the  $\delta^{13}\text{C}$  and  $\delta^{18}\text{O}$  of middle Cambrian dolomites go up and down frequently. There was no effect of hydrothermal fluids and evaporation process in upper Cambrian and early Ordovician, and little variation of the  $\delta^{13}\text{C}$  and  $\delta^{18}\text{O}$  can be seen of the younger dolomites, just showing  $\delta^{13}\text{C}$  of about -1‰ and  $\delta^{18}\text{O}$  of about -7‰ consistent with the seawaters at that ages.

### Acknowledgement

This work is supported by the foundation of the State Key Basic Research 973 Program of China (Grant No. 2005CB422103)

## Effect of geologic and biologic cycling on Se variability in a soil ecosystem with high level of nonagenarians

BIAO HUANG, WEIXIA SUN AND YONGCUN ZHAO

State Key Laboratory of Soil and Sustainable Agriculture,  
Institute of Soil Science, Chinese Academy of Sciences,  
P.O. BOX 821, Nanjing, 210008, China  
(bhuang@issas.ac.cn)

### Introduction

The spatial variability of Se in soils is affected by geologic and biologic cycling and has the potential to induce human health problems through food chains. The objectives of this study were to determine the effect of sedimentation and pedogenesis on the spatial variability of Se in an agriculturally soil ecosystem with high level of centenarians in Rugao County, Jiangsu province, China and discuss the Se bioavailability to rice and human longevity.

### Materials and Methods

342 surface soil samples and 9 of soil profiles in the studied area with 1,450 km<sup>2</sup> of land area and 1.54 million populations were taken. Total and water soluble Se (H<sub>2</sub>O-Se) in surface soils and H<sub>2</sub>O-Se in profile soil samples were determined using atomic fluorescence spectrometer (AFS). 97 of rice grain and drinking water samples were taken for Se determination using AFS. The ratio of population of nonagenarians over total population (90-rate) was calculated using the data of the national census in 2002.

### Results and Discussion

The results showed that the total Se concentrations (0.127±0.021 mg kg<sup>-1</sup>, n=203) had a narrow variation in topsoils derived from paleo-alluvium, lacustrine deposits or neo-alluvium, while H<sub>2</sub>O-Se (2.42±1.09 µg kg<sup>-1</sup>, n=342) had a wide variation among the soils derived from different parent materials. The concentrations of H<sub>2</sub>O-Se in the soil series on lacustrine deposit with fine texture and long-term development were greater than those on paleo-alluvium with long-term development but coarse texture or neo-alluvium fine texture but short-term development. Increased H<sub>2</sub>O-Se in the topsoil of soil profiles was, in part, related to the changes of soil properties due to weathering, pedogenic processes, and human activities. Correlation analysis between Se in the soils and rice Se or 90-rate in the study area showed that H<sub>2</sub>O-Se in topsoil had a significant relationship with rice Se or the 90-rate at village level (p<0.01), but total Se had no any relationship between them (p>0.05). Similar variation of Se in drinking water to H<sub>2</sub>O-Se in soils was found as well.

### Conclusions

In conclusion, the geologic and biologic cycling in the studied area didn't cause the significant variation of total Se in soils, but significantly affected the variation of H<sub>2</sub>O-Se in soils, and further Se uptake by crops, Se in ground water, and human health. It suggested that H<sub>2</sub>O-Se in soils of the agricultural ecosystem might be one of the most important geochemical factors affecting human health or longevity.

## Mg and Fe isotopes as tracers of temperature gradient driven diffusive differentiation

F. HUANG, C.C. LUNDSTROM AND A.J. IANNO

Dept. of Geology, University of Illinois, Urbana-Champaign,  
Urbana, IL 61801, United States (fhuang1@uiuc.edu,  
lundstro@uiuc.edu, and ianno@uiuc.edu)

The development of high precision MC-ICP-MS has led to breakthrough observations which have fundamentally called into question our current understanding of melt-mineral equilibrium and chemical differentiation processes. Although the mafic terrestrial igneous earth appears to have a near constant Fe isotopic composition with  $\delta^{56}\text{Fe}_{\text{IRMM}}$  of ~ 0.07‰, a majority of granites and rhyolites with SiO<sub>2</sub> content > 71 wt.% have a significantly heavier Fe isotope signature than the mean mafic earth with  $\delta^{56}\text{Fe}_{\text{IRMM}}$  up to 0.4‰ (e.g. [1]). This has generated vigorous debate [2], since the origin of Fe isotope variation with differentiation remains unclear.

A thermal migration experiment using wet andesite (AGV-1) along a temperature gradient from 950°C to 350°C over 2 cm in a 3/4" piston cylinder apparatus for 66 days at 0.5 GPa produces silicic solid, melt + solid, and more mafic melt from the cold bottom to the upper top of the charge, respectively. Major-trace elements and mineralogy vary with temperature due to temperature gradient driven chemical differentiation (thermal migration). Most importantly, Fe-Mg isotopes of the experiment vary consistently as a function of position. The bottom solid portion does not deviate significantly from the starting material, AGV-1. However, the heavy isotopes of Mg and Fe are depleted in melt at the hot end and enriched in the middle melt + solid portion.  $\delta^{56}\text{Fe}_{\text{IRMM}}$  and  $\delta^{26}\text{Mg}_{\text{DSM-3}}$  vary by 2.8‰ and 9.9‰, respectively.

These total variations in Fe-Mg isotopes are much greater than those observed in the terrestrial igneous Earth. These variations are not caused by kinetic diffusion or equilibrium isotope fractionations. Instead, they appear to result from Soret diffusion, in which light isotopes are known to preferentially migrate up temperature gradient. Notably, this experiment shows isotopic variations despite essentially no concentration gradient in the melt. Thus, isotopic variations in natural samples could record soret effects that do not appear in melt compositions. Thus we speculate that compositions of high SiO<sub>2</sub> igneous rocks with long cooling histories may indeed reflect long time scale differentiation in a temperature gradient.

### References

- [1] Poitrasson, F. and Freydier, R. (2005) *Chem. Geol.* **222**, 132-147.
- [2] Beard, B.L., and John, C.M. (2006) *Chem. Geol.* **235**, 201-204.

## C and S isotope records in Doushantuo Formation: Implication for Redox Fluctuation of the Ediacaran Ocean

J. HUANG AND X. CHU

Institute of Geology and Geophysics, Chinese Academy of Sciences, Beijing 100029, China  
(jhuang@mail.iggcas.ac.cn; xlchu@mail.iggcas.ac.cn)

Carbon and sulfur isotope evidence from Oman and iron speciation data from Newfoundland suggested a stepwise oxidation of the Ediacaran ocean from ca. 635 Ma to ca. 542 Ma (Fike *et al.*, 2006; Canfield *et al.*, 2007). New isotope data obtained from the Ediacaran Doushantuo Formation, however, reveal alternative oxidation events from ca. 635 Ma to ca. 551 Ma that suggest stepwise oxidation of the Ediacaran ocean, with significant ocean anoxia following each oxidation event. No  $\Delta\delta^{34}\text{S}$  values exceed 46‰ in the Doushantuo Formation, indicating the absence of sulfur disproportionation before 551 Ma and a complete oxidation of deep oceans did not occur until the latest Ediacaran or early Cambrian. Our data of  $\delta^{13}\text{C}_{\text{carb}}$ ,  $\delta^{13}\text{C}_{\text{org}}$ ,  $\delta^{34}\text{S}_{\text{CAS}}$ , and  $\delta^{34}\text{S}_{\text{py}}$  provide an alternative environmental interpretation for the evolution of early animal life and subsequent Cambrian explosion.

Increases of  $\delta^{13}\text{C}_{\text{carb}}$  and  $\Delta\delta^{34}\text{S}$ , with occurrence and diversification of Doushantuo-Pertatataka acritarchs (DPA), in the lower and middle Doushantuo Formation after the Nantuo (or Marinoan) glaciation indicate the first oxidation event to cause oxic water column in the shelf. Constant  $\delta^{13}\text{C}_{\text{org}}$  values (about -29‰) with variable  $\delta^{13}\text{C}_{\text{carb}}$  (-6.93‰ ~ +6.17‰) are consistent with the existence of DOM (dissolved organic matter) rich deep-ocean. Following negative shifts in  $\delta^{13}\text{C}_{\text{carb}}$  (down to -9.62‰) and  $\delta^{34}\text{S}_{\text{CAS}}$  (down to +9.5‰), a temporary anoxia occurred between the middle and upper Doushantuo Formation that is concordant with DPA's extinction. Another oxidation in the upper Doushantuo Formation, where multicellular, macroscopic algae (the Miaohe biota) were found. The prominent negative  $\delta^{13}\text{C}_{\text{carb}}$  (down to -8.98‰) excursions and associated decline of  $\delta^{34}\text{S}_{\text{CAS}}$  (from +43.5‰ to +10.2‰) imply both oxidations of DOM and sulfide from anoxic water column of deep-ocean. Unusually low  $\delta^{13}\text{C}_{\text{org}}$  values (down to -38‰) and increasing  $\delta^{13}\text{C}_{\text{carb}}$  (from -8.16‰ to -2.00‰) in the uppermost Doushantuo Formation (ca. 551 Ma) suggest involvement of anaerobic methane oxidation, possibly associated with the upwelling of anoxic deep-ocean seawater. Eventually, another anoxia possibly occurred at the near Dengying-Doushantuo boundary.

### References

- Fike D.A., Crotzinger J.P., Pratt L.M. and Summons R.E., (2006), *Nature* **444**, 744-747.  
Canfield D.E., Poulton S.W. and Narbonne G.M., (2007), *Science* **315**, 92-95.

## Geochemical structure of the Hawaiian plume: Inferences from Mahukona volcano

S. HUANG<sup>1</sup>, W. ABOUCHAMI<sup>2</sup>, J. BLICHERT-TOFT<sup>3</sup>, D.A. CLAGUE<sup>4</sup>, B.L. COUSENS<sup>5</sup> AND F.A. FREY<sup>6</sup>

<sup>1</sup>Florida State University, USA (huang@magnet.fsu.edu)

<sup>2</sup>Max-Planck-Institut für Chemie, Germany

<sup>3</sup>Ecole Normale Supérieure de Lyon, France

<sup>4</sup>Monterey Bay Aquarium Research Institute, USA

<sup>5</sup>Carleton University, Canada

<sup>6</sup>Massachusetts Institute of Technology, USA

Young, <2Ma, Hawaiian volcanoes define two parallel spatial trends, Loa and Kea. Most Loa- and Kea-trend shield lavas are geochemically distinct in major and trace element compositions and radiogenic isotopic ratios. Lassiter *et al.* (1996), among others, proposed a radially concentrically zoned plume with Loa shields forming closer to the plume center than Kea shields. Abouchami *et al.* (2005) proposed that Pb isotopic ratios are the best Loa-Kea discriminant, e.g.,  $^{208}\text{Pb}^*/^{206}\text{Pb}^* > 0.95$  for Loa lavas; they proposed a bilaterally asymmetrically zoned plume with geochemical differences between the northeast and southwest halves of the plume. These models are oversimplified because they do not consider local (Ren *et al.*, 2005) or vertical heterogeneities (Blichert-Toft *et al.*, 2003) in the plume; nevertheless the alternative large-scale zonation models can be evaluated with geochemical data for shields formed at varying distances from the plume center; e.g., Bryce *et al.* (2005) suggested that when active the submarine Mahukona volcano was southwest of the current location of Mauna Loa, a Loa-trend volcano; hence Mahukona lavas should be Kea-like in the concentrically zoned model and Loa-like in the bilaterally zoned model.

We report major and trace element compositions, Pb and Hf isotopic ratios for 18 Mahukona lavas; these include three transitional to slightly alkalic basalts from the large 125–350 m cones that may represent preshield lavas based on their  $^3\text{He}/^4\text{He}$  ratios of ~20 R/Ra (Garcia *et al.*, 1990). Consistent with this inference, the cone samples overlap with the distinctive Pb isotopic field defined by preshield lavas from Loihi seamount. All other Mahukona lavas are tholeiitic basalt that define three groups based on CaO content at a given MgO content. The high CaO group, >12%, has unusually low  $^{206}\text{Pb}/^{204}\text{Pb}$  (<18.0) and may be derived from a peridotite source (Herzberg, 2006). All other tholeiitic lavas straddle the Loa-Kea boundary in Pb isotopic space with  $^{208}\text{Pb}^*/^{206}\text{Pb}^*$  between 0.940 and 0.951 compared to the range of 0.947 to 0.956 for Mauna Loa lavas. In a  $^{176}\text{Hf}/^{177}\text{Hf}$  vs  $^{208}\text{Pb}^*/^{206}\text{Pb}^*$  plot (Huang *et al.*, 2005), the inverse trend of Mahukona lavas also straddles the Loa-Kea boundary. Their Zr/Nb ratios (12.1–14.8), another Loa-Kea discriminant, are also at the Loa-Kea boundary. Clearly, Mahukona tholeiitic basalt has a weaker Loa geochemical signature than Mauna Loa lavas. This result may require modification of the simple large-scale zonation models.

## Inter-diffusion of Mg/Ca in synthetic polycrystalline carbonates at elevated temperature and pressure

WUU-LIANG HUANG

Department of Geosciences, National Taiwan University,  
Taiwan, R.O.C (wlhuang@ntu.edu.tw)

The transport rates of MgCO<sub>3</sub> from dolomite into calcite were measured within synthetic dry dolomite-calcite polycrystalline aggregate at 1.6 GPa and isothermally at 800, 850, and 900 °C over different run durations. Aragonite in the starting dolomite-aragonite aggregate was first transformed rapidly to calcite, which, then, reacted with dolomite to form Mg-calcite progressively rich in Mg at slower rates.

The average contents of Mg in calcites determined by XRD increase with run time, which can be described empirically by the first-order rate law. The temperature dependence of the overall transport rate of MgCO<sub>3</sub> from dolomite into calcite can be estimated by the kinetic parameters ( $E = 231$  kJ and  $A_0 = 22.7$  hr<sup>-1</sup>). The extrapolation using the Arrhenius equation to the prograde metamorphic conditions reveals that the formation of Mg-calcite saturated with Mg from dolomite-calcite aggregate in the absence of metamorphic fluid may not be completed at temperatures below medium-grade metamorphism (< 350 °C and < 10 my; Fig. 1). The extrapolation of the rate to the conditions during exhumation of UHPM rocks, at which the P-T path entered calcite stability field from dolomite-aragonite field, indicates that the reaction of dolomite with calcite can be completed in a geologically short period (< 1 my).

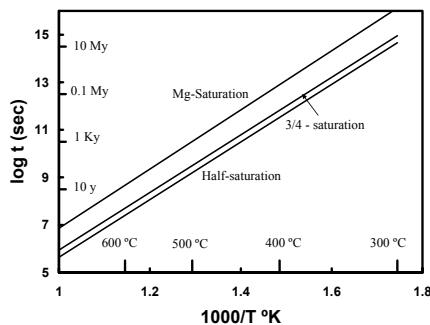


**Figure 1.**

T-t exposures for reacting calcite with dolomite to form Mg-calcite in poly-crystalline aggregate with grain size similar to those (around 10 μm) in experiments.

The SEM-EDS analysis of individual calcite grains shows that the Mg contents in calcite grains progressively decrease with increasing the distance from dolomite-calcite grain boundary, suggesting a diffusion control of the reaction. The Mg/Ca inter-diffusion coefficient at 850 °C calculated using the diffusion equation is around  $3 \times 10^{-16}$  m<sup>2</sup>/sec. The calculated closure temperatures for Mg/Ca inter-diffusion as a function of cooling rate and grain size in calcite reveal that the Ca/Mg resetting in calcite in dry polycrystalline carbonate aggregate may not occur at temperatures below 600 °C at geological cooling rate (> 100 °C/my), unless other processes were involved.

### Reference

Farver, J.R. and Yund, R.A. (1996) *Contrib. Mineral. Petrology* **123**, 77-91.

## Pressure dependence of viscosity of hydrous rhyolitic melts

HEJIU HUI, ZHENGJIU XU AND YOUXUE ZHANG

Department of Geological Sciences, The University of Michigan, Ann Arbor, MI 48109-1005, USA  
(huih@umich.edu; zhengjiu@umich.edu; youxue@umich.edu)

Knowledge of viscosity of silicate melts is critical to the understanding of igneous processes. Numerous viscosity measurements have been carried out on the natural and synthetic silicate melts under ambient pressure, but only a few investigations have examined the pressure dependence of viscosity of silicate melts. "Hydrous species reaction viscometer" (Zhang *et al.*, 2003) based on the concentrations of two hydrous species in the melts after a known cooling history is applied to investigate pressure dependence of viscosity of hydrous rhyolitic melts at near glass-transition temperatures.

The samples used here are natural obsidian glass with about 0.85 wt% water and hydrated natural obsidian glasses with higher water contents (2 wt% and 4 wt%). The experiments were conducted in piston cylinder apparatus at 1, 2 and 3 GPa. A prerequisite for viscosity inference with this "viscometer" is to know the temperature dependence of the equilibrium constant  $K$  of the interconversion reaction at a given pressure. Hence, pressure dependence of the speciation of dissolved water in these samples was investigated. Comparing with speciation model at ambient pressure (Ihinger *et al.*, 1999), equilibrium constant changes with pressure nonlinearly, decreasing from 0.1 MPa to 1 GPa and then increasing from 1 GPa to 3 GPa.

Cooling rates varied from ~ 100 K/s to 0.1 K/s in the cooling-rate experiments. Viscosity (in Pa·s) at the apparent equilibrium temperature of the hydrous species reaction (i.e., glass transition temperature) is obtained as  $10^{11.45/q}$  where  $q$  is cooling rate in K/s. So the total range of viscosity inferred from this method in this study is 3 orders of magnitude. Preliminary results show that viscosity of hydrous rhyolitic melts increases by about 1.4 log unit from 0.1 MPa to 3 GPa. The behavior of viscosity as a function of pressure for hydrous rhyolitic melts with water content of 0.8 wt% or more at low temperature range is similar to that of depolymerized melts.

### References

Ihinger P.D., Zhang Y. and Stolper E.M. (1999) *Geochim. Cosmochim. Acta* **63**, 3567-3578.  
Zhang Y., Xu Z. and Liu Y. (2003) *Am. Mineral.* **88**, 1741-1752.

## Nucleation, growth, and phase transformation of titanium oxides in hydrothermal solution

D.R. HUMMER<sup>1</sup>, P.J. HEANEY<sup>1</sup>, J.D. KUBICKI<sup>1</sup> AND J.E. POST<sup>2</sup>

<sup>1</sup>Department of Geosciences, The Pennsylvania State University (dhummer@geosc.psu.edu; heaney@geosc.psu.edu; kubicki@geosc.psu.edu)

<sup>2</sup>Department of Mineral Sciences, The Smithsonian Institution (postj@si.edu)

Fine grained titanium oxide minerals are environmentally important in soils, where they take part in a variety of geochemical processes. They are also industrially important as catalysts, pigments, food additives, and dielectrics. Recent research efforts have focused on an apparent reversal of thermodynamic stability between TiO<sub>2</sub> phases at the nanoscale that may be caused by the increased contribution of a surface energy term to the total free energy. We have performed time-resolved X-ray diffraction experiments at the National Synchrotron Light Source (NSLS) at Brookhaven National Labs (BNL) in which titanium oxides crystallize from aqueous TiCl<sub>4</sub> solutions between 100 and 200 °C, as diffraction patterns were collected at intervals of ~ 4 minutes. These experiments confirm that anatase is the first phase to nucleate from solution within the first ~ 20 minutes of heating, and then slowly begins converting to rutile. Whole pattern refinement of diffraction data reveals that lattice constants systematically change during particle growth for both phases throughout the crystallization process. The unit cell dimensions eventually converge to values close to those of the bulk phases.

Using the Vienna Ab-initio Package Simulation (VASP) with soft pseudopotentials, we modeled the energetics of bulk anatase and rutile using our refined structures of the evolving nanoparticles. The density functional theory (DFT) calculations indicate that the change in free energy between the incipient nanoparticles and bulk crystals was on the order of 0.5 kJ/mol for each phase, as compared to the 9 kJ/mol difference in free energy of formation between the two phases. To the extent that the structures of the nanoparticles that first nucleate in our experiments reflect the surface structures of bulk anatase and rutile, our results indicate that the energetics of the bare surface do not dictate the relative stabilities of nanoparticulate anatase and rutile.

## Predicting Raman spectra of aqueous silica and alumina species in solution from first principles

J.D. HUNT, E.A. SCHAUBLE AND C.E. MANNING

Dept of Earth and Space Sciences, UCLA, Los Angeles, California (jhunt@ess.ucla.edu)

Dissolved silica and alumina play an important role in lithospheric fluid chemistry. Silica concentrations in aqueous fluids vary over the range of crustal temperatures and pressures enough to allow for significant mass transport of silica via fluid-rock interaction. The polymerization of silica and alumina could afford crystal-like or melt-like sites to otherwise insoluble elements such as titanium, leading to enhanced mobility. Raman spectroscopy in a hydrothermal diamond anvil cell has been used to study silica polymerization at elevated pressure and temperature [1, 2], but Raman spectra of expected solutes are not fully understood. We calculated Raman spectra of H<sub>4</sub>SiO<sub>4</sub> monomers, H<sub>6</sub>Si<sub>2</sub>O<sub>7</sub> dimers, and H<sub>6</sub>SiAlO<sub>7</sub><sup>-</sup> dimers, from first principles using hybrid density functional theory (B3LYP). These spectra take the variation in Si-O-X bridging angle that the dimers will have at a given temperature into account, thereby broadening the main dimer peak. Solution effects are incorporated in two separate ways - by using a polarizable continuum model and adding explicit water molecules. Both methods are in excellent agreement with each other. However, the results are in contradiction with earlier results based on gas phase models, in which the bridging angle variation broadens the 630 cm<sup>-1</sup> silica dimer peak enough to explain the broad peak observed at high temperatures. In the solution phase, whether by a polarizable continuum model or adding explicit water molecules, the peak is not broadened enough to explain experimental results. The observed broadness, therefore, is most likely caused by additional, higher order polymers that have peaks within the broad observed peak. Ring polymers in particular may provide much of the observed broadness. The synthetic spectrum of the silica-alumina dimer suggests that there may be a higher ratio of complexed alumina to free alumina in solution at highly basic pH than previously estimated [3].

### References

- [1] Zotov, N. and Keppler, H., (2002) *Chem. Geol.*, **184**: 71.
- [2] Zotov, N. and Keppler, H., (2000) *Am. Min.*, **85**: 600.
- [3] Gout, R., *et al.*, (2000) *J. Sol. Chem.*, **29**: 1173.

## Paleoaltimetry from “clumped” <sup>13</sup>C-<sup>18</sup>O bonds in carbonates, Colorado Plateau

KATHARINE HUNTINGTON, BRIAN WERNICKE AND  
JOHN EILER

<sup>1</sup>California Institute of Technology, Pasadena CA, 91125  
(kateh@gps.caltech.edu; brian@gps.caltech.edu;  
eiler@gps.caltech.edu)

The elevation history of Earth’s surface is a key element linking tectonic, geodynamic, climatic, and surface processes, but remains difficult to reconstruct from the geologic record. In contrast to conventional stable isotope paleoaltimetry approaches, the new “clumped” <sup>13</sup>C-<sup>18</sup>O paleothermometer independently determines carbonate growth temperature and the  $\delta^{18}\text{O}$  of water from which the carbonate grew, potentially enabling the effects of altitude, climate, and seasonality to be distinguished. This approach has been successfully applied to paleosol nodules. Here, we examine what other materials may potentially access paleoelevation information using this technique, including gastropods, the bivalve *anomia*, oysters, barnacles, soil, marl, and limestone from Cretaceous to Pliocene deposits from and adjacent to the Colorado Plateau, southwestern USA.

The abundance of <sup>13</sup>C-<sup>18</sup>O bonds in diverse carbonate materials from related sediments records temperatures between 20-84°C and  $\delta^{18}\text{O}_{\text{snow}}$  water values of -2 to 12‰. Temperature estimates for independent preparations of the same sample are reproducible to within  $\pm 0.55$ -2.2°C (2 s.e.), and average temperatures determined for different materials from the same deposit exhibit negligible variations ( $\pm 0.05$ °C).

While samples at the lower end of the observed temperature range represent reasonable Earth surface conditions that may be interpreted in terms of paleoelevation, samples yielding temperatures in excess of ~33°C likely provide a record of carbonate recrystallization/replacement during burial metamorphism (‘resetting’). Clear examples of resetting include gastropod fossils in which original aragonite is completely replaced by calcite (yielding apparent temperatures of 76.5 $\pm$ 1.7°C) and a suite of more cryptically reset Pliocene molluscs from tidal flat facies that yield temperatures of >42°C. Most apparently unreset samples are fine-grained (impermeable) micrites, which consistently yield temperatures within the plausible Earth-surface range. This suggests that resistance to diagenesis is grain size dependent – a promising result given the abundance of well preserved fine-grained lacustrine and marine carbonates found throughout the geologic record. Results for micritic carbonates from Middle Miocene to Pliocene age record reasonable spring to summer depositional temperatures and oxygen isotopic values relative to modern lake waters on the Colorado Plateau.

## Simulations of dry-out and halite precipitation due to CO<sub>2</sub> injection

S. HURTER, D. LABREGERE AND J. BERGE

Schlumberger Carbon Services, La Defense, France  
(SHurter@slb.com, DLabregere@slb.com,  
JBerge@slb.com)

Although CO<sub>2</sub> is not very soluble in supercritical CO<sub>2</sub>, a continuous stream of CO<sub>2</sub> being injected into a formation, will result in a region around the injection well to dry out. As the water of the formation brine is continuously extracted, the irreducible water saturation may attain practically zero. Enhanced injectivity is the result in a low salinity brine environment. In formations saturated with highly saline brine (e.g. Northern German Basin) the outcome is opposite: injectivity is impaired. In this case, the brine becomes supersaturated as continuously H<sub>2</sub>O evaporates into the CO<sub>2</sub> phase and salt (halite) precipitates in the pores. The porosity and permeability diminish, which can lead to the loss of a injection well.

We present simulations of these processes as an example of pre-injection study for a CO<sub>2</sub> injection and storage site. The simulation tool consists of a commercial compositional code used extensively in the oil and gas industry to simulate the flow of multiple phases (oil, water, gas) in porous or fractured media. The mutual solubility of CO<sub>2</sub> and H<sub>2</sub>O with a correction for salinity is implemented as described in Spycher and Pruess (2005). The brine salinity is adjusted accordingly until the saturation threshold is reached and halite is precipitated. The severity of this process can be evaluated for a specific site and also remediation strategies (injection of dilute fluids) tested.

### Reference

Spycher N. and Pruess, K. (2005), CO<sub>2</sub>-H<sub>2</sub>O mixtures in the geological sequestration of CO<sub>2</sub>, II Partitioning in chloride brines at 12-100°C and up to 600 bar, *Geochim. Cosmochim. Acta* **69**, 13, 3309-3320.